NASA-CR-124402) DEVELOPMENT OF LIFE-TEST METHODOLOGY FOR LONG-LIFE MECHANICAL COMPONENTS. PHASE 1: DEVELOPMENT OF (Battelle Columbus Labs., Ohio.) 165 p
LIMIT GOVT.+NASA CONTR. CSCL 14D J3/15

X73-10493
Unclas
15524

RESEARCH REPORT

Battelle
Columbus Laboratories

BATTELLE'S COLUMBUS LABORATORIES comprises the original research center of an international organization devoted to research and development.

Battelle is frequently described as a "bridge" between science and industry — a role it has performed in more than 90 countries. It conducts research encompassing virtually all facets of science and its application. It also undertakes programs in fundamental research and education.

Battelle-Columbus — with its staff of 2500 — serves industry and government through contract research. It pursues:

- research embracing the physical and life sciences, engineering, and selected social sciences
- design and development of materials, products, processes, and systems
- information analysis, socioeconomic and technical economic studies, and management planning research.

505 KING AVENUE • COLUMBUS, OHIO 43201

INTERIM REPORT

on

DEVELOPMENT OF LIFE-TEST METHODOLOGY FOR LONG-LIFE MECHANICAL COMPONENTS PHASE I: DEVELOPMENT OF METHODOLOGY

(Contract NAS 8-27438)

July 31, 1973

by

D. B. Hamilton, Program Manager

and

D. K. Snediker, A. A. Mittenbergs, R. Lamonte,
B. G. Brand, W. Berry, and J. W. Kissel

(NASA-CR-155424) DEVELOPMENT OF LIFE-TEST METHODOLOGY FOR LONG-LIFE MECHANICAL COMPONENTS. PHASE 1: DEVELOPMENT OF METHODOLOGY Interim Report (Battelle Columbus Labs., Ohio.) 165 p

N78-72675

00/38

Unclas
57593

BATTELLE
Columbus Laboratories
505 King Avenue
Columbus, Ohio 43201

TABLE OF CONTENTS

TABLE OF CONTENTS
(Continued)

TABLE OF CONTENTS
(Continued)

X73-10463

INTERIM REPORT

on

DEVELOPMENT OF LIFE-TEST METHODOLOGY FOR LONG-LIFE MECHANICAL COMPONENTS PHASE I: DEVELOPMENT OF METHODOLOGY

(Contract NAS 8-27438)

by

D. B. Hamilton, Program Manager

and

D. K. Snediker, A. A. Mittenbergs, R. Lamonte,
B. G. Brand, W. Berry, and J. W. Kissel

SUMMARY

The purpose of this program is to develop short-term life tests for mechanical components whose intended lifetimes are as great as 10 years. The program is divided into two phases. Phase I covers the development of general life-test methodology. Phase II will involve subjecting a specific component to life testing. This report covers effort in Phase I.

The program has concentrated on valves and associated equipment. Three components were selected as representative by NASA project personnel:

- A four-inch electric-motor operated vent valve for air, gaseous nitrogen, and gaseous oxygen.
- A two-inch, pneumatically actuated, normally open recirculative valve for LOX and LH_2.
- A calibration gas supply module assembly to be used in the Metabolic Activity System of the Orbital Workshop. This system included solenoid valves, a pressure regulator and a gas bottle.

During the development of the life-test methodology, these components were considered representative of aerospace valves with respect to design, materials, service media, operating condition, duty cycle, failure modes and failure mechanisms. The life-test methodology developed, however, is considered valid for all long-term mechanical space components.

Effort in Phase I consisted of a literature study to determine the range of environments to which components may be exposed and to determine available life test techniques, analysis of detail drawings and specifications of the three representative components to determine possible failure mechanisms, and laboratory experiments of wear and creep to evaluate short term tests for wear and creep of nonmetallic materials.

From the literature, the range of environmental parameters were established for the various environments to which mechanical components for space applications are exposed.

The detail drawings and specifications associated with the three representative components were analyzed thoroughly to establish the potential failure mechanisms for each component. Critical failure mechanisms identified included structural fatigue, crevice, galvanic and stress corrosion of certain materials, fretting of bearing balls and races, metallic wear, and nonmetallic wear and creep of seats, bushings and seals. Of these, the mechanisms of nonmetallic wear and creep were judged to be the most critical with respect to performance. In addition, these mechanisms are those about which the least is known; consequently, appropriate accelerated life-test methodology had not been developed. Experimental studies of both wear and creep of nonmetallic materials were conducted to examine the validity of possible short-term tests.

The wear study involved cryogenic and room-temperature wear experiments of virgin polytetrafluoroethylene (PTFE), glass-filled PTFE, chlorotrifluoroethylene (KEL-F), and a polyester materiasl (Mylar). These nonmetallics represented the materials identified during the analysis of the three representative components. The wear study showed

(1) Initial creep during the wear process generally exceeds the total wear. Life tests for wear must, therefore, be conducted after the initial creep has occurred.

(2) Wear and wear rate at cryogenic temperatures is sufficiently different than that at room temperature that life tests for wear of cryogenic components must be conducted at cryogenic temperatures.

(3) Short-term life tests are best performed by increasing speeds up to a factor of 100. Life testing by extrapolation of short-term wear does not appear feasible.

The creep study involved a literature analysis and room temperature creep experiments with virgin PTFE (Halon G-700). The study showed

(1) Accelerated life tests for creep are feasible using temperature as the accelerating factor, provided that temperatures where material transitions occur are avoided during testing.

(2) Creep properties of polymers vary significantly from batch to batch and within batches. An initial short-term test should be performed on material samples to establish properties before performing life testing. A microhardness-type indentation test was evaluated as an initial short-term test; however, results were inadequate. A short-term creep test of, perhaps, two weeks duration is recommended instead.

As a result of the literature study, the experimental studies and BCL's general background, a general life-test methodology has been defined for mechanical components. The elements of this methodology are

(1) Establish life cycle of component

(2) Establish the possible failure mechanisms for the component and its elements or parts

(3) Conduct (separately, if necessary) life tests for each critical failure mechanism.

Specific short-term life test procedures have been developed for wear and creep of nonmetallic materials, and recommendations have been made for short-term life test procedures for the other failure mechanisms identified during the analysis of the three representative components. The life-test methodology is outlined in detail in the following separate section.

CONCLUSIONS

The problem of designing a life test for a mechanical component whose required lifetime is greatly in excess of the available test period has been studied by literature review and by experiment. Our principal conclusion is that it is, in general, possible at the present time to design a life test which will give a high degree of confidence that the component will function satisfactorily for a period at least as long as its intended lifetime. A general methodology for designing life tests is discussed in the next section.

In our opinion, if life tests are conducted for specific component prototypes according to the methodology given, the reliability of the production units can be at least as high as if the prototypes were life tested by running for the design lifetime under the intended duty cycle.

The development of accurate life tests is a difficult task, requiring the use of the highest state of art available in the areas of corrosion, nonmetallic material aging, wear, creep and fatigue. Further research is desirable in these areas in order to make the design of life tests less difficult for certain failure mechanisms.

RECOMMENDED LIFE-TEST METHODOLOGY

Introduction

The overall objective of this program is the development of short-term life-test methodology for mechanical components. Phase I has resulted in the development of a general methodology, together with specific short-term life tests for wear and creep of nonmetallic materials. The methodology is based on the following assumptions:

(1) The component to be life tested has been designed according to the current state of art.

(2) The component (or its prototype) has passed proof, qualification and acceptance tests and is capable of operating satisfactorily for at least a short period of time.

(3) The component design effort has been completed. Design modifications cannot, therefore, be made to facilitate life testing.

In general, short-term life testing of mechanical components is, at best, an extremely difficult task. During the development of our life-test methodology, it became apparent to us that life testing should actually begin during the design phase of the component. Our life-test methodology presumes that component design if completed (Assumption No. 3); however, we believe that the following recommendations are worth noting:

- Consideration of life testing should begin during the design phase as soon as the component configuration is established and materials are selected. At that time, possible failure mechanisms should be established.

- For those failure mechanisms which are not well understood, key laboratory experiments should be performed to assess their relevance.

- Considerations should be given to starting life tests on specific elements or parts (such as valve seats, bearings or gears) as soon as possible.

- Because of the difficult nature of life testing, the component should be designed, whenever feasible, around the need to be life tested. For example, sufficient information on proprietary processes or materials is sometimes not available to permit accurate life tests to be devised.

- It is important that parts and materials are used which are as well understood and well characterized as possible.

The next section discusses the general aspects of the life-test methodology. Subsequently, an outline is presented giving our specific recommendations for life tests.

General Discussion

Our recommended methodology involves first establishing the various failure mechanisms whereby the component parts or elements may fail, then performing life tests for each critical failure mechanism. Since quantitative accelerated tests are not available for most failure mechanisms, it will not usually be possible to predict the service life of the component. It is frequently possible, however, to conduct life tests which demonstrate that the component will last at least as long as its intended lifetime. Our recommended methodology is based on demonstrating that the component minimum life is at least as long as the required lifetime.

Theoretically, if the recommended sequence of determining the critical failure mechanisms and conducting separate life tests is correctly and successfully carried out, the component will be judged 100 percent reliable with respect to the failure mechanisms considered. That is, component failure would only be possible if a failure mechanism were overlooked, or if the duty cycle input information were inaccurate, or if the component were installed improperly. In practice, completely accurate life tests are not yet available for every failure mode. Nevertheless, it is our firm conviction that this is the most effective way to life test, and if the recommended methodology is applied to a component, the results will be at least as good as the present method of running a component for its intended lifetime under its intended duty cycle. It is important to bear in mind that the present method of life testing one or a few components of a production run does not guarantee that no failures will occur in space. Manufacturing tolerances on alignment, dimensions and materials are such that component failure in space is possible even though life tests have been successful.

Recommended Life-Test Sequence

The specific elements of the recommended life-test methodology are

(1) Establish Component Life Cycle

(2) Determine Possible Failure Mechanisms

(3) Conduct Life Tests for Each Failure Mechanism

Each is discussed separately below.

Establish Component Life Cycle

Establishing the component life cycle involves establishing the environments and operating conditions to which the component and its elements are exposed during the various phases of its existence. The various possible phases include:

- Construction. Practices during construction may affect the long-term performance of component elements. For example, insufficient cleaning of contaminants may prematurely corrode or age either metals or nonmetals. Residual contaminants from plating baths have been known to corrode materials in bearings, rings and brushes in slip-ring assemblies for despun antennas for communications satellites.

- Qualification and Acceptance Testing. If the individual component to be life tested has been subjected to such tests, then the conditions under which testing was performed and the test duty cycle should be defined.

- Transportation. Temperature extremes and environmental composition can vary widely throughout the United States. Vibrations on railcars have been known to brinell rolling bearing races.

- Storage. Components may be stored for several years. Corrosion of critical metals will depend on humidity and degree of salinity of the atmosphere. Nonmetals may also be deleteriously affected; for example, adsorption of salt-air humidity during the storage phase, followed by exposure to ultraviolet radiation during a subsequent phase could degrade polymers.

- Prelaunch. After withdrawing from storage, components may be exposed to uncontrolled environmental conditions either before or after installation.

- Launch. Shock and vibration are extremely important in this phase.

- Operational Phase. The component duty cycle must, of course, be established for this phase. For launch vehicles, of course, the launch phase is the operational phase.

- Reentry. High temperatures and other environmental extremes may occur.

- Parking Awaiting Reuse. Environmental control during this phase may be less than during storage or other phases.

The environmental parameters to be considered include

- Atmosphere: mist, fog, water, salt, sand, dust, corrosive gases, outgassed material
- Corrosive cleaning agents
- Ambient temperature: level and variation
- Vibration and shock
- Radiation type and exposure time: optical, ultraviolet, beta, gamma, alpha, protons, X-rays, neutrons
- Meteoroids.

After establishing the range of environments, the component duty cycle for the operational phases must be defined. Subsequently, the environmental and duty cycle information must be used to define the operating conditions of the elements in the component for each phase. It is essential to define the operating conditions of the elements in order to establish critical failure modes for each element. Important operating conditions include:

- Cycle rate
- Pressure
- Response time
- Temperatures – level and variation
- Flow rate (for valves, regulators, etc.)
- Tolerable leakage (for valve seats or seals)
- Power consumption and friction
- Loads (for bearings, gears, seals, etc.)
- Shock and vibration levels
- Environmental composition.

Determine Possible Failure Mechanisms

Using the life cycle information established previously, the critical failure mechanisms for each component element must be determined. This can be done in two ways: by a forecasting study in which specialists in various fields review

the component design, and by experimental operation of individual components followed by a thorough failure analysis of both failed and unfailed parts. Analysis of retrieved space hardware is also an attractive possibility; however, such hardware is not likely to be available.

Forecasting Study. This involves the following steps:

(1) Assemble a team of experts with experience with the specific component type in the following areas:

   (a) Structural failure

   (b) Wear

   (c) Metallic material corrosion and aging

   (d) Nonmetallic material aging, creep, and fracture

   (e) Radiation damage of materials

   (f) Lubricant degradation.

(2) This team should review detail drawings, specifications, qualification and proof tests, and other data relevant to the component

(3) Develop list of possible failure mechanisms on the basis of joint discussions.

(4) Laboratory experiments. In some cases, potential failure mechanisms may not be sufficiently well understood to assess their relevance. In these cases, key short-term laboratory experiments may be possible to establish criticality of the failure mechanisms.

Experimental Failure Analysis. An individual component should be run under the normal duty cycle and its elements disassembled and examined for incipient failure mechanisms. This, in itself, may be insufficient to identify latent failure mechanisms, since the single component may not be representative because of tolerances, misalignments, etc. In order to encourage such failure mechanisms to manifest themselves, we recommend running another individual component under slightly more rigorous operating conditions. Specifically, the following sequence is recommended:

(1) Operate a component under its normal duty cycle for a significant period (for example, one month)

(2) Operate another component under conditions somewhat more severe than the normal duty cycle: higher speeds, higher loads, higher flow rates, slightly higher temperatures, etc. These conditions should be selected such that as few as possible new failure mechanisms are introduced.

(3) For critical or poorly understood failure mechanisms identified in the forecasting study, elements such as seats or bearings may be withdrawn from the component and run individually. If time and funds permit, components or elements may be instrumented during operation to detect incipient failures. Material specimens should, in some cases, be exposed to environmental conditions if reactions are suspected, but not verified.

(4) If available, obtain retrieved hardware.

(5) Failure Analysis. The various elements should be disassembled and analyzed carefully. If failures occur, the causes (mechanisms) of failure should be clearly established. It is, perhaps, more likely that failures will not occur. Careful surface examination can, however, reveal incipient failures. Surface-analysis techniques which can be employed as warranted include

   (a) Optical microscopy

   (b) Scanning electron microscopy

   (c) X-ray or electron diffraction

   (d) Ion microanalysis

   (e) Ion scattering spectrometry

   (f) Metallographic sectioning

   (g) Infrared and mass spectrometry

   (h) Optical emission spectrometry

   (i) Atomic absorption spectrometry

   (j) Ellipsometry for identification of organic films.

   In addition, physical property measurements of elastomers and plastics may be performed to evaluate aging.

(6) On the basis of the forecasting study and the failure analyses, the list of critical failure mechanisms requiring life testing may be developed.

Conduct Short-Term Life Tests for Each Critical Failure Mechanism

A variety of types of life tests were identified in the literature study:

(1) Run component for intended lifetime. This is obviously not usually feasible.

(2) Statistical mechanical reliability analysis. Although popular at one time, this methodology is not now considered valid, since

a statistically significant sample is not usually available for mechanical components.

(3) Signature analysis. This includes sonic (acoustic), torque ripple, infrared, thermal contact resistance, electromagnetic emission and other signature techniques. In general, these have not progressed to the point where they are dependable. For some specific components (such as bearings), however, they hold future promise.

(4) Acceleration. This is the best possible short-term test technique, because a quantitative correlation is drawn between test time and real time. Unfortunately, accurate accelerated tests are not yet available for most failure mechanisms.

(5) Extrapolation. For cumulative damage failure mechanisms for which the damage rate is known either to remain constant or to decrease with time, it is possible to get an estimate of life by running for a short period, then extrapolating linearly to the desired lifetime.

(6) Time compression of duty cycle to reduce inoperative periods. Subject to equilibration of thermal or other processes, this is, perhaps, the simplest effective life test technique. For valves and other components which operate intermittently, the required number of cycles for cycle-dependent failure mechanisms (such as fatigue or wear) can sometimes be obtained in a short time. Time-dependent mechanisms, such as aging or corrosion must, however, be treated independently.

(7) Minimum-life testing. In this case, the component is run under a single set of conditions at least as severe as those in the normal duty cycle. The life test is then speeded up or accelerated in some manner, so that a successful component is determined to have a lifetime at least as long as the desired lifetime. Actual life is not determined. Most life testing involves using this technique in conjunction with one of the previous techniques.

Specific Recommended Short-Term Life Tests. Recommendations for specific failure modes are given below. Following life testing, the components or elements should be disassembled and examined carefully to make certain that new failure mechanisms were not introduced during testing.

(1) Low- and high-cycle metal fatigue. Fatigue life can frequently be estimated from published tensile data. If this is not possible, the following sequence should be carried out.

(a) Select test cycle. Examine duty cycle and select a test cycle (stress, temperature, time, rate) which is at

least as severe as duty cycle. If several factors enter in, such as both stress level and pressure cycling, or temperature level and temperature cycling, it may be necessary to select more than one test cycle.

(b) Accelerate tests by increasing cycling rate to accumulate total cycles; condense inoperative periods. For materials with strain aging properties (steel, titanium) cycle rate must be adjusted to the diffusion mechanisms involved. For other materials maximum cycle rates are limited by heat buildup from internal friction.

(c) Synergistic effects dealing with degradation in mechanical properties should be evaluated independently.

(2) Metallic wear. This can be divided into two cases: mild wear or severe wear. If severe wear is expected, the component should be redesigned. Mild wear is defined as not leading to progressive roughening of the surfaces.

(a) Wear life test should run for at least a week for equilibration.

(b) Testing rate should be raised by raising speed. Increasing load will change the wear mechanism. The specific component or part should be analyzed to determine maximum speed permissible. Heat transfer analysis based on frictional heat generation and contact conditions should be carried out to provide the following information.

- Maximum surface temperature should not exceed the yield point drop.
- Surface temperature should not exceed critical temperature for boundary lubrication (boundary film desorption or decomposition temperature).
- For fluid lubrication, the shear rate of the lubricant film should be controlled to provide the same lubrication regime the component will see (hydrodynamic boundary, mixed, EHD).

(c) Determine total wear by extrapolation assuming linear wear rate.

(d) Particle debris. In mild metallic wear, small particles are librated which would not be expected to foul the component.

(3) Metallic corrosion

(a) Fretting fatigue. Use established tests to examine material tendencies toward fretting fatigue.

(b) Corrosion fatigue. This mechanism does not appear relevant to space valves.

(c) Hydrogen embrittlement. Standard tests are available. These involve electrolytically charging a piece of material with hydrogen, then measuring fracture toughness.

(d) Galvanic corrosion. Standard tables are available, however, this should not be a problem in spacecraft valves.

(e) Corrosion products restricting movement. This does not appear to be a significant problem, so in order to evaluate it, life testing could be conducted by grossly overestimating the environment.

(4) Radiation damage. A great deal of data is already available in this area, including synergisms with mechanical effects. Specific life tests are not recommended.

(5) Nonmetallic aging

(a) Evaporation of materials and differential evaporation (such as departure of plasticizer). Conduct TGA (thermogravimetric analysis – vacuum microbalance) tests to determine evaporation rate as a function of temperature, then extrapolate to desired lifetime.

(b) Cross-linking aging. Accelerated testing is possible by raising concentration of the active component (such as ozone) in the environment.

(c) Autochemical and autocatalytic reactions. DTA (differential thermal analysis) can be used to identify the existence of such reactions. Life testing can then be speeded up by increasing temperatures.

(6) Creep of nonmetallic materials. Because of batch-to-batch variations in material properties, and because of the dependence of the mechanical properties of a polymer upon past history, the long-term creep of nonmetallic materials is difficult to predict in a general way. The general methodology recommended is to conduct some short-term creep tests in order to identify the particular piece or material batch with respect to its creep properties. On the basis of these tests, temperature and stress

acceleration factors can be determined for the particular material, and the long-term behavior predicted by temperature and/or stress superposition. Life tests for creep should be performed on the component elements withdrawn from the component.

The following sequence should be applied for the prediction of the long-term creep behavior of nonmetallic parts in the aerospace values under consideration.

(a) The parts should be identified and a failure criterion defined for each. That is, how much creep can be tolerated? Is permanent set more important than total creep?, etc.

(b) The use history and environment of each part should be established. This history should include

- stress
- atmosphere
- temperature

for each portion of the life cycle of a given part. For example, the stress profile might include several cycles of valve actuation where the part is alternately stressed and unstressed. Since the cumulative damage model is assumed to be operative here, the various cycles may be combined to provide an integrated, and simplified profile. For example, if a valve component is stressed 1000 times for 1 minute each, separated by 1-day dwell intervals at a lower stress, this profile may be simulated by 100 minutes at the high stress and 10 days at the low stress, but at a higher temperature.

(c) The component or a sample from the same materials batch and fabrication run should be subjected to a short-term room-temperature pressure creep test. This test will yield a creep-compliance under standard conditions that will uniquely identify the mechanical/creep properties of that batch, and will identify the set of creep compliance curves to be used.

(d) The material should now be subjected to an accelerated creep test based upon the principle of temperature-time, and/or stress-time, superposition. The stress profile described in Step 2 should be applied simultaneously with a temperature profile that yields the proper

degree of acceleration while avoiding the critical material transition temperature ranges for that material. The measurement of creep versus time in this test will yield data reflecting the creep behavior of this material for the requisite extended time period. The use of this method for Halon G-700 is described in detail on page 80.

(7) Nonmetallic wear; extent of wear. Prediction of the long-term wear behavior of the polymeric materials used in these valves is best carried out by a speed-accelerated test. In this type of test, the number of revolutions, oscillatory cycles, or total linear sliding distance for the expected life is determined. The material combination is then subjected to the equivalent number of cycles in a much shorter time period by increasing the rubbing or cycling rate. For example, if a steel/filled PTFE friction interface in, say, a valve stand, is determined to undergo 6000 meters of total sliding at a load of 3.45 MN/m^2 (500 psi) at 77 K in 10 years, this service may be accelerated by sliding at a rate of 0.50 m/sec for 200 minutes at 77 K under a load of 3.45 MN/m^2.

The following sequence should be applied in determining the long-term wear behavior of nonmetallic materials in the valves of interest.

(a) The parts should be identified and a failure criterion defined for each. The failure criterion should be based upon allowable wear and the possible specific wear mechanisms such as scoring or wear debris jamming.

(b) The use-history and environment should be established for each part. This history should include

- Load/stress
- Atmosphere
- Temperature
- Number of wear cycles
- Linear sliding distance
- Relative speed of wear surfaces during sliding

A profile should be constructed for each parameter.

(c) For the component or for a specimen from the same material batch and fabrication run, a wear test

should be carried out applying the stress, temperture profile defined in Step (2). The speed, or cycle rate, should be increased up to the upper limit defined for that material in order to achieve the requisite degree of acceleration. For example, if the filled PTFE gland just discussed spends 40 percent of its real-time life at 300 K under a load of 3.45 MN/m^2 (500 psi) and 60 percent of its real-time life at 77 K under a load of 13.8 MN/m^2 (2000 psi), then the 200 minute accelerated test should be run for 40 percent of 200 minutes (80 min) at 300 K and 3.45 MN/m^2 for 60 percent of 200 minutes (120 min) at 13.8 MN/m^2 and 77 K. The test should be carried out in such a way as to factor out initial creep effects (see page 85 for a preconditioning procedure to achieve this).

(d) The total wear should then be measured and observations made of the nature of the wear track and the quantity and morphology of the debris. These data and observations should be interpreted as though the specimen or component had been exposed for the extended real-time period. The effects of wear and debris on component function should be determined by the comparison of the posttest data with the failure criterion for this particular part.

(8) Nonmetallic wear; wear debris. The failure mode of interest is the fouling of clearances in valves.

(a) Run part for a significant period and collect and observe wear debris.

(b) Compare size of debris particles with clearances in the valve. Debris should be either clearly larger or clearly smaller than valve clearances. If debris particles are of the same order of size as the clearances, then it can be assumed that fouling is likely and alternative materials should be selected.

INTRODUCTION

Life testing of mechanical components for space applications has traditionally been performed by operating one or more individual components under the required duty cycle for the required lifetime. This method is obviously impractical for lifetimes in excess of, say, one year. Statistical mechanical reliability analysis, in which confidence limits and percentage reliability figures are used, is also impractical since sufficiently large samples of mechanical space components are not normally available.

The purpose of this program is to develop short-term life test methodology for mechanical components for space applications with lifetime requirements up to 10 years. The scope of the program was defined to cover specifically valves and associated equipment; however, the methodology developed is to be applicable to mechanical components in general.

The program is divided into two phases. Phase I covers the development of life test methodology. Phase II covers the life testing of a specific component, followed by modifications to the life test methodology, as warranted. This report covers Phase I activity.

Since the field of valves for space applications comprises hundreds of different functions and valve configurations, the program scope was defined by NASA project personnel by selecting three specific components and providing us with detailed drawings and specification for each. The components selected are a 2-inch recirculation valve, a 4-inch vent valve, and a calibration gas supply module assembly. A certain amount of general information has also been received for two other units. Those valves were considered representative of type and subsequent evaluation and development of specific life tests was based on these components.

The program plan for Phase I was first to perform a literature search to determine the state of the art of life testing of mechanical components and to establish the range of environments to which components will probably be subjected in space missions in the near future. The next step was to analyze the detailed drawings and specifications for the three representative components to determine the range of materials of interest, the relevant material aging processes, and the relevant component failure modes. The final step was to develop or specify appropriate life testing procedures for the various failure modes and aging processes. Since it is not possible in a limited program to cover all possible failure mechanisms and aging processes, the program ultimately focussed on nonmetallic wear and creep as the most critical and least understood failure mechanisms.

DISCUSSION OF MECHANICAL COMPONENT FAILURE

Introduction

The purpose of the program is to develop means for performing short-term tests to assess the lifetime capability of long-life (up to 10 years) mechanical components. A long-term capability of a mechanical component implies absence of failures in this component over the required life time. In other words, the component must operate satisfactorily, without failures, over the specified time period. What constitutes a failure is often determined by the application of the component and by the operational and environmental conditions imposed upon this component. In general, a failure is considered to be any damage, permanent distortion, deterioration, and nonconformance to specified requirements or change (degradation) in performance characteristics that prevents the component from meeting the specified requirements. Thus, a large number of various failures are possible, in principle, in any mechanical device. On the other hand, some failure modes and mechanisms might occur less likely than others. In some cases, for example, the occurrence of a certain degradation process may cause or constitute a failure in one mechanical component but not in another, depending on the application and on the specific requirements.

In developing a life-test methodology, which would permit the assessment of a mechanical component's long-life capability on the basis of short-term testing, the various potential modes of failure and their mechanisms must be sufficiently understood so that a prediction of the component's life could be made with certain confidence. Such predictions must be made with regard to each of the possible failure modes and mechanisms in a given component under the anticipated (or specified) service conditions. The most common types of mechanical-component failures are briefly reviewed in the next section.

Mechanical-Component Failures

This general review of mechanical-component failures is applicable to any mechanical component, except that most of the examples cited below are related to valves used in space applications. Generally speaking, the main reasons for failures in mechanical components are:

(1) Use of components under service and environmental conditions that are beyond those for which the components have been designed.

(2) Design weaknesses (faulty design) and limitations in material properties (short- and/or long-term).

(3) Factors that are beyond the control of a designer, such as human errors in manufacturing, faulty quality control, or service and maintenance abuse.

Within the framework of this program, it was assumed that the components will not be used under conditions that are beyond those for which they are designed, the components are properly designed in every respect, they have no manufacturing faults, and the components will not be abused. In other words, the components are "perfect" and are operating properly after they are produced. Only the long-term behavior of the components is uncertain and must be predicted either from available knowledge and information or on the basis of short-term tests.

Broadly speaking, any mechanical component, regardless of the above restrictions, can fail because of a failure in one or more of its structural or flexural parts or elements, a failure of surfaces (interfaces) of two or more contacting parts, a failure occurring in some critical (single) surface, and because of loss of degradation of its functional characteristics or performance. Material-property degradation, by itself, is usually not considered to be a failure, but it may cause or aggravate all of the other types of failure. There might be exceptions to the latter statement. For example, loss of permanent magnetism in a part of an electro-mechanical component will constitute a failure.

It should be pointed out that, in principle, all failure modes are time dependent. Even a properly protected unused piece-part stored for a long period of time may deteriorate because of gradual material aging, its property degradation, or because of some other reasons. In this discussion, the term "failure mode" is used as a macroscopic or broad-view descriptor of a failure. It usually describes something external and readily observable. "Failure mechanism" is the microscopic or fundamental descriptor of failure, relating to some basic physical or chemical phenomenon. For example, the breakage of a part is considered to be a failure mode. The failure mechanism in this case could be, e.g., tensile rupture, creep rupture, fatigue, or stress corrosion. Sticking of a valve stem is another failure mode. The failure mechanisms in this case could be cold welding between the stem and its guide, thermal distortions, accumulation of wear debris or other contaminants, or corrosion. Excessive leakage of a seal is still another mode of failure. The failure mechanisms here could be wear of sealing surfaces, some other damage to these surfaces (such as scratches), contaminant accumulation on the sealing surfaces, loss of seal seating force, etc. It should, perhaps, be noted that the use of the terms failure cause, mode, and mechanism sometimes depends on the system's level at which the failure is being considered. For example, in an entire "plumbing" system, with regard to a valve, the failure mode or cause may simply be an inoperative valve. For the valve itself, the failure mode could be, e.g., a functional failure of the valve's actuating device. With regard to the latter, the failure mode or cause could be a structural failure, e.g., such as breakage of the actuator gears. For the gears, the failure mode could then be tooth breakage and the failure mechanism, e.g., fatigue.

Structural- and Flexural-Element Failures

As was already stated, all failure modes are time dependent, including those of structural (and flexural) elements. However, in many engineering applications, involving steady loads and certain environments, the changes occurring in structural parts are relatively slow and, for all practical purposes, some of the structural-element failure modes can be considered as being time independent, i.e., failure occurs essentially instantaneously whenever certain critical load combinations are exceeded. These time independent or "basic" failure modes or mechanisms are:

(1) Deformation. Depending on the application, a structural part or element may be considered as failed or not performing its function properly if it exhibits excessive (beyond a permissible limit) elastic deformation, plastic deformation or yielding which causes a permanent set, or exceeds a permissible amount of plastic deformation. Deformations caused by thermal distortions, if they degrade the performance of a component, are also included here. Dimensional instability (loss of accuracy) caused by residual stress relaxation or by changes in the material, although belongs to the failure modes "by deformation", is usually time dependent.

(2) Fracture. Partial or complete separation of material which usually starts at some localized weak point or stress concentration. Fractures are customary classified as ductile or shear-type and brittle or cleavage-type.

(3) Instability. Elastic and plastic buckling.

Time- or cycle-dependent structural element failure modes (or mechanisms) are:

(1) Creep, creep rupture, and creep buckling. For metallic materials, these failures usually occur at elevated temperatures. For nonmetallic materials, such as plastic, creep or material flow may take place under load at room or even at low temperatures.

(2) Fatigue.

(3) Combined creep and fatigue.

(4) Failures occurring in one of the basic modes after the material has been subjected to creep and/or fatigue loading.

All structural-element modes of failure may be affected by various factors:

(1) Magnitude, direction, and manner of loading, e.g., tension, compression, shear, torsion, bending, or combined loadings; steady, intermittent, cyclic, vibratory, impact (including high-velocity projectile impact), or loadings imposed by thermal gradients.

(2) Environments, e.g., high and low temperatures, hard vacuum, high pressure, various atmospheres, exposure to radiation.

(3) Size and shape of the part and the conditions of its surfaces (in addition, any surface damage or surface failure may initiate or aggravate the structural-element failures).

(4) Material and its properties, including the effects of various material treatments, material aging, and material property degradation with time. The latter may be affected considerably by the environmental and loading histories of the part. (The subjects of material aging and its property degradation is discussed in somewhat more detail in several places throughout this report).

Interface and Surface Failures

All interface and surface failures are time dependent, except for surface damages that might be imposed by individual, accidental overloads, impacts, or rubbing action of hard, sharp objects on parts that have not been designed to sustain such an abuse. The latter are exceptions which are not included in the failure modes and mechanisms listed below. All these failure modes and mechanisms may be affected essentially by the same factors that were listed above for the structural-element failures, i.e., loading, environments, size and shape of the part, its surface conditions, and the material and its properties, including material aging and its property degradation. In many respects, the environmental effects can be more detrimental to interfaces and surfaces than to structural elements. For example, over-heating of a rolling-element bearing may cause an immediate bearing failure due to loss of clearances; any chemical attack, such as corrosion, starts at the surfaces whenever these are exposed to certain atmospheres.

The interface failure mechanisms are usually also more complex than the structural-failure mechanisms because they involve at least two parts or two surfaces with or without a lubricating medium. The most common interface failure modes or mechanisms are:

(1) Breakdown of sliding or rolling lubrication

(2) Wear (abrasive, adhesive, chemical)

(3) Fretting

(4) Galling

(5) Surface deformation

(6) Surface creep

(7) Surface fatigue (pitting, spalling)

(8) Seizure (self-welding, cold welding)

(9) Bond failures.

The major failure mechanisms for metallic surfaces that are not in contact with another solid surface (some of these may occur also in a gap between two solid surfaces) are:

(1) Corrosion

(2) Crevice corrosion

(3) Stress corrosion (and stress-corrosion cracking)

(4) Surface failures caused by chemical reactions other than corrosion

(5) Erosion

(6) Cavitation.

For nonmetallic materials and their surfaces there are, in general, many possible failure modes and mechanisms that are characteristic to the various types of these materials. These are covered elsewhere within this report.

Performance or Functional Failures Caused by Other Factors

Each structural- or surface-element failure or surface damage in a critical location may cause failure of a mechanical component (and of the system) or, at least, cause a performance degradation. However, there are frequent cases when a component fails to perform its function or its performance degrades below an acceptable level for reasons other than failures of structural and surface elements. In general, there is a large variety of factors that may affect the performance of various mechanical devices or make them inoperative. With regard to valves used in space applications, a few typical examples are listed below.

(1) Leakage, both internal and external, is one of the most common problems in all valves, including those used in space applications. Excessive leakage at valve seats and of the various seals that are parts of specific valve designs or of their connections with other components in a system is often caused by surface failures (such as wear or other types of surface deterioration) in the valving and sealing elements. However, in many cases, such leakage may occur due to causes external to these elements. For example, the loosening of threaded fasteners from vibrations during a launch may cause a loss in the sealing force of a seal and lead to leakage. Thermal distortions, particularly in the presence of high thermal gradients (sometimes a transient condition), can cause leakage. Icing (freezing moisture) at low temperatures may lead to a leaking or inoperative valve. Leakage at valve seals can be caused by improper action of the valving elements, such as binding in the guiding surfaces due to mechanical or thermal distortions or due to sticking between these surfaces. Leakage of valves often results also from contaminants in a system, discussed in somewhat more detail as the next item.

(2) Contamination in a system containing valves can cause various problems, in addition to leakage at the valve seals due to the contaminant particles collecting on the sealing interfaces and interfering with the normal valve-seal sealing ability. In general, contamination in a system may occur in several ways: it may be built-in at assembly, it may be introduced into the system, e.g., through seals and breather caps, and it may be self-generated within the system as a result of various processes such as wear, corrosion, fretting, and chemical reactions. For components operating in a hard vacuum, the products of outgassing may add to the contaminants. The contaminant particles (debris) may aggravate the wear process on all sliding or rolling surfaces, they may cause sticking of sliding interfaces, clogging of fluid passages and filters, and adversely affect the performance of valves.

(3) Degradation of valve performance is another problem encountered in space valves (and in other valves, in general). This includes increase in response time, sluggish behavior, unstable operation, regulated-pressure overshot or undershot, improper pressure or temperature control, etc., including inoperative valves. There may be many reasons for such performance failures, depending on the design of the specific valve, its function, and its application. Often such performance degradation is caused by the severe environments under which the space valves have to operate. These may include hard vacuum, high vibrational levels, high temperature excursions, extreme temperatures, various radiation effects, and certain atmospheres.

Material-Property Degradation

All materials change or age with time. These changes, in many instances, are imperceptibly slow and, as mentioned before, can be neglected in some practical engineering applications. On the other hand, there are many engineering applications in which aging of materials cannot be disregarded. Usually, the aging of materials leads to its property degradation. Cases in which material properties improve with time (e.g., coaxing effects in fatigue loading) are exceptions rather than the rule. Aging of materials with time is affected very strongly by the environment and by the loading conditions of the part. With regard to the environment, aging means permanent damage to the material and not, for example, a transient decrease in strength in a temporary environment, such as high temperature. The loading conditions here do not mean only loadings related to the creep and fatigue behavior of materials, but any loading that may cause or aggravate permanent changes in materials.

Although the fact of property degradation of materials with time is well known, there is generally not enough quantitative information available even on old and common engineering materials, and present technological needs, particularly in space applications, often require relatively new materials to be put in service before suitable aging data are available. Also, old materials are used in new space applications and environments for which the aging information might be missing. Nevertheless, material-property degradation due to aging is one of the most important factors for long-life mechanical components. It is particularly so in devices that have to operate for long periods of time, in one-shot devices that are stored (or are inactive) for long periods of time before use, and in all devices that are subjected to severe environmental conditions, such as space valves.

Changes in materials occur for several reasons and these changes can be of various natures. For example, many of the engineering materials are not really in thermal equilibrium. Therefore, more or less gradual changes in their properties do occur with time at any finite temperature, even in the absence of any external influences. Although such thermally induced changes may be imperceptibly slow at room and low temperatures, they are accelerated considerably by elevated temperatures. The phenomenon of so-called static fatigue ("catastropic" brittle failure) in some ceramic materials at room and low temperatures may be related to slow changes occurring in the material subjected to a steady load, such as lengthening of internal cracks by the stress produced by slight thermal fluctuations.

Many of the metallurgical changes that occur in metallic materials at elevated temperatures (and which may occur at lower temperatures also, but at a much lower rate) are a common cause of material-property degradation. These include such phenomena as recrystallization, diffusion of constituents, precipitation, phase transformation, diffusion through outer surfaces, and formation of intermetallic compounds. In addition to temperature, these changes may be affected by other environmental factors and loads. For example, in some metals the recrystallization temperature is lowered somewhat if they are subjected to loads.

Various environments may also cause changes that are detrimental to material properties. For example, gases with small atomic volume such as hydrogen and helium can penetrate many metals. Hydrogen embrittlement is a common detrimental effect occurring in some metals. Radiation damage is another. Nuclear radiation, for example, may cause loss of strength in some materials. In others, strength may be improved, but some other important property may deteriorate. It is known, for example, that in some metals the ultimate tensile strength and yield strength increase from exposure to nuclear radiation, but the ductility falls off considerably, making the materials unacceptably brittle. High pressures and hard vacuum can also be detrimental to some materials. High pressures may cause permeation of the surrounding matter into the material and hard vacuum, such as exists in the outer space, may cause some materials to sublimate.

Another category of material-property degradation is that caused by chemical reactions. These start, as a rule, at the exposed surfaces of parts and gradually penetrate (with or without diffusion) into the material. The most common of these is corrosion. Corrosion depends very much on the initial surface condition (protected or unprotected) of the part and the environment. It can be aggravated by elevated temperatures, and, in some instances, by loads. For example, stress corrosion is cracking of a metallic material at its surfaces due to corrosive atmosphere and mechanical stressing and/or residual stresses present in the material. Incompatibilities of two adjacent materials or of the environment with a material can cause various chemical reactions that may result in material-property degradation.

Some surface effects that actually represent failures of interfaces or surface elements and do not necessarily produce changes in the "bulk" material can also cause, from the viewpoint of structural integrity, material-property degradation over a period of time, either because of a significant decrease in load-carrying cross-sectional area or by aggravating the initiation of a structural-element failure. (These causes also apply, to a certain degree, to the chemical reactions mentioned in the previous paragraph.) These surface effects are, for example, mechanical wear, fretting or fretting corrosion, galling, self-welding under vacuum, cold welding, surface fatigue, and others.

Another effect of aging that does not produce changes in the material itself but which may be important from the viewpoint of structural integrity is the relaxation of internal or residual stresses over a period of time. Stress relaxation can cause slow dimensional changes that may not be acceptable in accurate devices. It can also lead to initiation of a failure in highly stressed parts, if the original residual stresses are of a beneficial nature.

Although the material property-degradation effects of the various aging phenomena are generally known, quantitative data on these effects is not always available, as was already mentioned. This discussion, although incomplete, does point out some of the problem areas associated with degradation of material properties with time and supports the previous statement that most of the failure modes, including those of structural elements, must be considered as time dependent,

unless the available information clearly indicates that no significant aging effects can be expected in a given structural part over the time period of interest.

Interactions of Failure Mechanisms and Modes

As has been mentioned on several occasions in the preceding discussion, one failure mechanism can aggravate or cause another. In general, material-property degradation and material aging can lead to structural, surface, and/or functional failures in any mechanical device. Surface deterioration mechanisms can initiate or cause structural and functional failures. Any structural failure of a critical part or element in a mechanical component renders this component immediately inoperative and may have catastrophic consequences. The latter is true also for severe cases of interface failures. The interrelationships among the various failure mechanisms are quite complex and cannot be readily generalized. This is particularly true for components, such as space valves, that must operate under severe encironments for prolonged periods of time and be subjected to transportation and, possibly, extended storage conditions prior to their use.

The environments to which space valves are subjected during both their inactive and active service lives may be quite varied and exist in various combinations. The effects of such combined environments which change periodically, and sometimes abruptly, during a required long-term lifetime are generally not understood quite as well as the effects of some single environments. There is less information available with regard to material aging and material-property degradation under the various environmental combinations, either simultaneous, or in some sequences, or both. It is, however, generally known that certain combinations or environments cause mutual interactions with regard to material-property deterioration and are synergetic. As was already mentioned, for example, elevated temperatures do accelerate the various chemical processes, including corrosion, in certain atmospheres, in addition to lowering the physical strength properties of most engineering materials.

The most common environments (and combinations of these) to which long-life space values might be subjected include various atmospheres, large temperature ranges, high and low (hard vacuum) pressures, various radiation effects, and vibrations, shocks, and acceleration forces, in addition the normal operating loads. The individual effects of most of these were briefly discussed in the preceding sections. Some problem areas typical to space values, not particularly emphasized previously, include the following.

(1) Loosening of joints, brinelling, fretting, and fatigue caused by vibrations and shocks.

(2) Thermal shocks and thermal cycling.

(3) Thermal distortions that may cause warpage and binding of moving parts.

(4) Outgassing and cold welding in a hard vacuum.

(5) Material embrittlement at cryogenic temperatures.

(6) Ineffectiveness of the usual lubricants under space conditions. Many lubricants solidify at low temperatures and outgas at high temperatures and in vacuum. Even though the use of dry or solid lubricants alleviates these problems, lubrication, friction, and wear are very critical items in all space applications.

(7) Explosion hazards in some individual applications.

The most severe problem areas in long-life space valves, however, are probably those of material aging and material-property degradation, for both metallic and nonmetallic materials, and the effects of interface and surface deterioration due to the severe environments. In most cases, a failure in a space valve, that is properly designed and manufactured, will not have a single cause. Rather, the failure will be caused by the interaction of several (failure) mechanisms.

Failure Modes in Space Valves

A failure is generally defined as inability to fulfill the specified function(s) of a device. The major functions (or categories) of the various space valves are:

(1) To start and stop flow. These valves are usually termed shut-off valves and they normally are in either closed or open position. Depending on their specific function, they may be called, e.g., fill, drain, dump, vent, or start valves.

(2) To regulate and throttle flow. These are usually called control, metering, or throttle valves and they may be in any position between and including the closed and open positions.

(3) To regulate pressure. These valves are usually called pressure regulators and they may be of various designs.

(4) To relieve excessive pressure. These are usually called relief valves or, less frequently, safety valves.

(5) To prevent backflow. These are check valves.

(6) Special purpose and multipurpose valves. There is a large variety of such valves used in space applications and they range from relatively simple to very complex valves consisting of many valving elements. Some examples of these are bipropellant mixing, temperature control, multiple-passage, servovalves and combined-purpose valves.

It should be noted that the valves used in space applications are usually custom designed for each specific application because of the variety of space missions and because of the stringent requirements imposed on these valves. For the same reasons, many of these valves contain or are integral with various auxiliary devices, actuating devices, position indicators, provisions for remote control, etc. Also, these valves are often integral parts of some other more complex space components. Because of the large variety and sometimes high complexity of space valves and because of the variety in their requirements and the environments to which they are subjected, valid generalizations with regard to the possible modes of failure in these valves are nearly impossible. Therefore each valve and each application has to be evaluated individually.

On a broad scale, however, the possible modes of failure in space valves can be divided into three general categories as follows.

(1) Loss of structural integrity. Any structural failure of a vital part or element leads to immediate failure of the valve and may have catastrophic consequences, as was already mentioned. Therefore, the structural modes of failure are usually considered to be the most critical. In principle, at the present state of the art, it is possible to design structurally sound valves, if weight, space (size), and cost were not restricted. Even within these constraints, it should be possible to develop valves that function properly and are structurally sound and capable of sustaining the loads and environments to be imposed upon them after they are manufactured, i.e., in the condition they are produced. Over a long service life, however, due to material aging and material property degradation, as well as due to interface and surface effects (deterioration), the structural integrity of such valves may be impaired. If these effects are taken into consideration during design by proper material selections and sufficiently high safety margins, the likelihood of structural failures in space valves can be minimized, but not completely eliminated.

(2) Loss of proper functioning. This failure-mode category may include a broad class of functional failures, depending on the application, requirements, and the criticality of the valve and depending on the consequences associated with these types of failures. These failures may range from inoperative valve (e.g., valve does not close or open) to degradation of some important performance aspect such as response time, improper flow or pressure control, excessive leakage in cases where such cannot be tolerated, etc.

(3) Loss of secondary functional characteristics. This failure-mode category is somewhat similar to the preceding one, except that these failures can be considered to be less critical than a loss of proper functioning of a valve. For example, leakage somewhat higher than the permissible specified level, sluggish response,

improper pressure or position indications in some cases may not affect adversely the success of a mission.

The latter two categories of functional modes of failures may be caused by various failure mechanisms discussed previously and combinations of them, including structural failure mechanisms such as excessive deformations and thermal distortions. These failure modes are much more difficult to predict and to control than those causing loss of structural integrity. As has been mentioned throughout this discussion, severe environments, material aging, and interface and surface deteriorations are often the major causes for these functional modes of failure in both short- and long-term applications.

RANGE OF ENVIRONMENTS

Introduction

It is clear that spacecraft applications impose a variety of environmental conditions on the mechanical components involved. Material degradation is therefore determined both by the operation of the component and by the environmental conditions. In order to determine relevant aging or deterioration mechanisms, a study was made of the possible environmental conditions to which mechanical components, such as valves, may be exposed for future space missions.

In general, the environments to which components will be exposed have been divided into the following categories: earth (storage, transportation, qualification testing, etc.), launch, and orbital. The latter also includes component environments induced by outgassing and decomposition of materials.

Earth Environments

Qualification Testing

Assembled mechanisms used in spacecraft and missiles are repeatedly tested on the ground prior to actual launch during the checking out of various components and entire systems. As a result, parts that will operate for less than a minute during the launch and ascent phases can accumulate as much as several hundred hours of test operation prior to the time of launching. Materials selected for use with component parts under the vacuum conditions in space will, therefore, have to operate for a considerable period under normal atmospheric conditions. (In some instances, mechanisms that are sensitive to prolonged ground operation must be replaced by fresh units prior to launch.)

Transportation

Necessary handling and transportation of delicate mechanisms involve an ever-present potential for damage from major shocks and vibration. Since such damage is not a time-dependent failure mode it is not a consideration here. Likewise, handling and transportation by rail which can cause shocks of as much as 30 g are not considered since damage from these sources should be avoided by design and special handling.

Storage

Exposure to the elements of parts during storage or while standing at launch sites can render them ineffective through corrosion, contamination, or changes in

the lubricants. Factors and conditions that contribute to this hazard, and which are generally found at launching sites, include high-humidity atmospheres, mist, fog, water, salt, sand, dust, corrosive gases, etc. Table 1 [1] lists surface-temperature extremes recorded for a number of NASA sites involved in testing, transportation, storage, and launch. From this listing it is concluded that the extreme high temperature to be anticipated is 46 C (115 F) and the extreme low temperature is -37 C (-35 F). In addition to these ambient temperature extremes, the long period storage requirements should be anticipated. For example, sea level solar radiation can cause compartment temperatures above 72 C (160 F) and skin temperatures above 100 C (212 F).

The Ascent Environment

The unique characteristics involved for the ascent/descent environment which will be imposed on spacecraft include (1) thermal energy arising from aerodynamic interaction or of mechanical energy sources such as aerodynamic pressure and shear forces, (2) acceleration loading, and (3) shock and vibration. Because the ascent environment is a consequence of spacecraft design and booster characteristics the thermal energy situation will vary considerably. In general, most of the heat generated will be absorbed by the shroud and consequently carried away when this is jettisoned. Maximum temperature of the inside of the forward cylindrical section of the shroud should be no more than 155 C (300 F), reached in 200 seconds. After shroud ejection, the spacecraft is subjected to free molecular heating as well as direct solar radiation. In one detailed analytical and experimental study of the boost phase heating to be expected for a particular satellite vehicle it was found that the maximum temperature rise possible on any portion of the spacecraft was 38 F (3.3 C) before heat shield ejection and about 240 F (116 C) after. It was determined that the latter temperature was localized so that the total heat input could be accommodated without significant overall temperature rise.

The spacecraft vibration environment depends also on its size and construction as well as on the characteristics of the boost rocket and the efficiency of energy coupling between the two. The various loads which might contribute to component fatigue damage appear at different places during different periods of its trajectory, and their intensity and excitation characteristics depend on both trajectory and geometric parameters. An estimate of these stresses is often the composite result of a theoretical computation, laboratory studies on models, and flight measurements on vehicles. Thus, it may be anticipated that these problems will be overcome by proper original design of components and of the whole structure. These stresses are not considered to be related to time-dependent failure modes.

(1) References will be found at the end of the report

TABLE 1. SURFACE AIR AND SKY RADIATION TEMPERATURE EXTREMES

Area		Surface Air Temperature Extremes[a]				Sky Radiation	
		Maximum		Minimum		Equivalent Temperature Minimum Extreme	Equivalent Radiation ($g\text{-}cal\ cm^{-2}\ min^{-1}$)
		Extreme	95%	Extreme	95%		
Huntsville	°C	43.9	41.7[b]	-23.3	-21.7[b]	-30.0	0.28
	°F	111	107[b]	-10	-7[b]	-22	
River Transporatation	°C	43.9	NA	-30.6	NA	-37.2	0.25
	°F	111	NA	-23	NA	-35	
New Orleans	°C	37.8	31.7[c]	-12.8	7.8[c]	-17.8	0.35
	°F	100	89[c]	9	46[c]	0	
Gulf Transportation	°C	40.6	NA	-12.8	NA	-17.8	0.35
	°F	105	NA	9	NA	0	
Eastern Test Range	°C	37.2	30.0[c]	-3.9	12.2[c]	-15.0	0.36
	°F	99	86[c]	25	54[c]	5	
	°C	37.2	31.7[d]	-3.9	6.7[d]		
	°F	99	89[d]	25	44[d]		
Panama Canal Transportation	°C	41.7	NA	-12.8	NA	15.0	0.36
	°F	107	NA	9	NA	5	
Space and Missile Test Center	°C	41.7	31.1[c]	-2.2	3.9[c]	-15.0	0.36
	°F	107	88[c]	28	39[c]	5	
West Coast Transportation	°C	46.1	NA	-6.1	NA	-17.8	0.35
	°F	115	NA	21	NA	0	
Sacramento	°C	46.1	e	-6.1	e	-17.8	0.35
	°F	115	e	21	e	0	
White Sands Missile Range	°C	41.1	e	-21.1	e	-30.0	0.28
	°F	106	e	-6	e	-22	
Wallops Test Range	°C	39.4	e	-11.7	e	-17.8	0.35
	°F	103	e	11	e	0	
Edwards AFB	°C	43.3	39.4[d]	-15.0	-3.9	-30.0	0.28
	°F	110	103[d]	5	25[d]	-22	

a. The extreme maximum and minimum temperatures will be encountered during periods of wind speeds less than about 1 meter per second.

b. Based on worst month extreme

c. Based on hourly observations

d. Based on daily extreme (maximum or minimum) observations.

e. To be determined

Orbital Environments

Introduction

The altitude of 56 miles (90 Km) constitutes the limit for viscous gas phenomena; above this, molecular flow phenomena dominate. The primary atmospheric properties to be considered in this region are temperature, pressure, density, and mean molecular mass (composition). To account for variations in these characteristics the following factors must be considered.

(1) Time (hour, day, sun-rotation period, season, year, sunspot cycle)

(2) Location (altitude, latitude, longitude)

(3) Solar activity (ultraviolet radiation, X-rays, solar plasma, and associated magnetic storms)

(4) Processes (condition, diffusion, mass transport, photoionization, dissociation, recombination, particle escape into space).

The problem of describing upper atmospheric behavior is difficult because many of these phenomena are interrelated. The rarification of the gaseous constituents leads to several new concepts.

(1) There will be a static distribution of gas constituents (stratification) due to gravitational attraction.

(2) Neutral hydrogen atom escape will significantly skew the Maxwellian velocity distribution above a certain threshold altitude, and this is dependent on sunspot activity.

(3) The thermal conductivity is very large compared with the heat capacity; hence, the kinetic temperature is nearly constant with altitude for many thousands of miles.

Since upper atmosphere measurements are not made on a routine basis, it is necessary to predict a model for deriving the atmospheric properties. Data obtained from such a procedure are presented in Tables 2 and 3 [9].

TABLE 2. NEUTRAL PROPERTIES OF UPPER ATMOSPHERE AT SUNSPOT MAXIMUM FOR VARIOUS ALTITUDES

Altitude		Pressure[a] (dynes/cm^2)	Pressure[a] (Torr)	Temperature (°K)	Molecular Weight	Scale Height (km)	Density[a] (g/cm^3)	Concentration[a]						
								Total (cm^{-3})	Constituent (cm^{-3})					
(km)	(sm)								n(N_2)	n(O_2)	n(A)	n(O)	n(He)	n(H)
100	62.1	3.3 (-1)	2.48 (-4)	223	27.76	7.0	5.00 (-10)	1.09 (13)	8.15 (12)	1.76 (12)	7.42 (10)	8.81 (11)	4.10 (8)	1.11 (6)
120	74.6	3.8 (-2)	2.85 (-5)	348	24.41	12.6	3.18 (-11)	7.83 (11)	4.54 (11)	6.89 (10)	1.92 (9)	2.59 (11)	1.18 (8)	3.53 (6)
140	87.0	1.1 (-2)	8.25 (-6)	569	22.44	22.5	5.42 (-12)	1.45 (11)	6.68 (10)	8.27 (9)	1.53 (8)	7.01 (10)	5.91 (7)	2.06 (6)
160	99.4	5.5 (-3)	4.13 (-6)	758	21.12	32.0	1.84 (-12)	5.24 (10)	1.95 (10)	2.11 (9)	2.99 (7)	3.07 (10)	3.88 (7)	1.49 (6)
180	111.9	3.1 (-3)	2.33 (-6)	826	20.09	36.9	9.00 (-13)	2.70 (10)	8.15 (9)	7.89 (8)	8.90 (6)	1.80 (10)	3.18 (7)	1.33 (6)
200	124.3	1.8 (-3)	1.35 (-6)	882	19.24	41.4	4.84 (-13)	1.51 (10)	3.68 (9)	3.21 (8)	2.94 (6)	1.11 (10)	2.68 (7)	1.22 (6)
220	149.1	7.7 (-4)	5.78 (-7)	984	18.01	49.9	1.69 (-13)	5.64 (9)	8.81 (8)	6.36 (7)	4.00 (5)	4.68 (9)	1.99 (7)	1.04 (6)
300	186.4	2.6 (-4)	1.95 (-7)	1,085	16.94	59.6	4.83 (-14)	1.72 (9)	1.38 (8)	7.77 (6)	2.96 (4)	1.56 (9)	1.41 (7)	8.85 (5)
340	211.3	1.3 (-4)	9.75 (-8)	1,108	16.50	63.2	2.41 (-14)	8.78 (8)	4.56 (7)	2.19 (6)	6.12 (3)	8.19 (8)	1.18 (7)	8.34 (5)
400	249	5.3 (-5)	3.98 (-8)	1,109	16.01	66.4	9.24 (-15)	3.48 (8)	9.24 (6)	3.54 (5)	6.26 (2)	3.29 (8)	9.38 (6)	7.87 (5)
500	311	1.2 (-5)	9.00 (-9)	1,109	15.15	72.2	2.06 (-15)	8.17 (7)	6.89 (5)	1.82 (4)	1.53 (1)	7.45 (7)	6.47 (6)	7.17 (5)
600	373	3.4 (-6)	2.55 (-9)	1,109	13.59	82.9	5.01 (-16)	2.22 (7)	5.53 (4)	1.02 (3)		1.76 (7)	4.51 (6)	6.51 (5)
700	435	1.2 (-6)	9.00 (-10)	1,109	10.93	106	1.37 (-16)	7.54 (6)	4.77 (3)	6.19 (1)		4.35 (6)	3.18 (6)	5.96 (5)
800	497	5.2 (-7)	3.90 (-10)	1,109	7.95	150	4.46 (-17)	3.38 (6)	4.40 (2)	4.06 (0)		1.11 (6)	2.26 (6)	5.48 (5)
900	559	2.9 (-7)	2.18 (-10)	1,109	5.84	210	1.87 (-17)	1.93 (6)	4.34 (1)			2.96 (5)	1.62 (6)	5.04 (5)
1,000	621	1.9 (-7)	1.42 (-10)	1,109	4.76	264	1.00 (-17)	1.26 (6)	4.55 (0)			8.17 (4)	1.18 (6)	4.64 (5)
1,200	746	9.9 (-8)	7.43 (-11)	1,109	4.11	323	4.40 (-18)	6.45 (5)				6.88 (3)	6.34 (5)	3.97 (5)
1,400	870	5.5 (-8)	4.13 (-11)	1,109	3.99	350	2.37 (-18)	3.57 (5)				6.58 (2)	3.53 (5)	3.43 (5)
1,600	994	3.1 (-8)	2.33 (-11)	1,109	3.96	372	1.35 (-18)	2.05 (5)				7.08 (1)	2.02 (5)	2.98 (5)
1,800	1,119	1.9 (-8)	1.42 (-11)	1,109	3.94	393	7.94 (-19)	1.22 (5)				8.50 (0)	1.19 (5)	2.60 (5)
2,000	1,243	1.1 (-8)	8.25 (-12)	1,109	3.91	416	4.81 (-19)	7.41 (4)				1.13 (0)	7.18 (4)	2.29 (5)
2,500	1,553	3.7 (-9)	2.78 (-12)	1,109	3.79	481	1.52 (-19)	2.42 (4)					2.24 (4)	1.70 (5)
3,000	1,864	1.4 (-9)	1.05 (-12)	1,109	3.58	569	5.49 (-20)	9.26 (3)					7.95 (3)	1.31 (5)
3,500	2,175	6.4 (-10)	4.80 (-13)	1,109	3.26	693	2.25 (-20)	4.15 (3)					3.12 (3)	1.03 (5)
4,000	2,486	3.3 (-10)	2.48 (-13)	1,109	2.86	872	1.03 (-20)	2.17 (3)					1.34 (3)	8.27 (4)
4,500	2,796	2.0 (-10)	1.50 (-13)	1,109	2.44	1,122	5.28 (-21)	1.30 (3)					6.25 (2)	6.78 (4)
5,000	3,107	1.3 (-10)	9.75 (-14)	1,109	2.07	1,450	3.00 (-21)	8.75 (2)					3.11 (2)	5.64 (4)
6,000	3,728	7.6 (-11)	5.70 (-14)	1,109	1.55	2,290	1.28 (-21)	4.99 (2)					9.11 (1)	4.08 (4)
7,000	4,350	5.2 (-11)	3.90 (-14)	1,109	1.28	3,226	7.23 (-22)	3.40 (2)					3.21 (1)	3.08 (4)
8,000	4,971	3.9 (-11)	2.93 (-14)	1,109	1.15	4,142	4.86 (-22)	2.53 (2)					1.30 (1)	2.40 (4)
9,000	5,592	3.0 (-11)	2.25 (-14)	1,109	1.09	5,019	3.00 (-22)	1.99 (2)					5.97 (0)	1.93 (4)
10,000	6,214	2.5 (-11)	1.88 (-14)	1,109	1.06	5,878	2.83 (-22)	1.62 (2)					3.00 (0)	1.59 (4)

(a) Numbers in parentheses denote powers of 10. Thus, 3.3 (-1) means 3.3×10^{-1}.

TABLE 3. NEUTRAL PROPERTIES OF UPPER ATMOSPHERE AT SUNSPOT MINIMUM FOR VARIOUS ALTITUDES

Altitude		Pressure [a] (dynes/cm^2)	Pressure [a] (Torr)	Temperature (°K)	Molecular Weight	Scale Height (km)	Density [a] (g/cm^3)	Concentration [a]						
								Total (cm^{-3})	Constituent (cm^{-3})					
(km)	(sm)								n(N_2)	n(O_2)	n(A)	n(O)	n(He)	n(H)
100	62.1	2.9 (-1)	2.18 (-4)	204	28.11	6.4	4.83 (-10)	1.04 (13)	8.14 (12)	1.74 (12)	6.65 (10)	4.80 (11)	1.44 (8)	1.83 (6)
120	74.6	2.1 (-2)	1.58 (-5)	287	26.77	9.4	2.40 (-11)	5.41 (11)	4.07 (11)	5.86 (10)	1.39 (9)	7.49 (10)	1.57 (7)	1.06 (5)
140	87.0	3.9 (-3)	2.92 (-6)	420	25.08	14.8	2.79 (-12)	6.71 (10)	4.43 (10)	4.90 (9)	6.86 (7)	1.79 (10)	8.28 (6)	6.77 (4)
160	99.4	1.3 (-3)	9.75 (-7)	588	23.53	22.3	6.23 (-13)	1.60 (10)	8.91 (9)	8.23 (8)	7.97 (6)	6.20 (9)	4.93 (6)	4.62 (4)
180	111.9	6.0 (-4)	4.50 (-7)	730	22.24	29.4	2.19 (-13)	5.93 (9)	2.79 (9)	2.25 (8)	1.63 (6)	2.91 (9)	3.47 (6)	3.60 (4)
200	124.3	3.2 (-4)	2.40 (-7)	824	21.15	35.1	9.91 (-14)	2.82 (9)	1.11 (9)	7.98 (7)	4.64 (5)	1.63 (9)	2.74 (6)	3.10 (4)
220	149.1	1.2 (-4)	9.00 (-8)	948	19.44	44.6	2.91 (-14)	9.01 (8)	2.41 (8)	1.43 (7)	6.06 (4)	6.43 (8)	1.95 (6)	2.56 (4)
240	186.4	3.4 (-5)	2.55 (-8)	996	17.75	52.2	7.39 (-15)	2.51 (8)	3.59 (7)	1.62 (6)	4.24 (3)	2.12 (8)	1.43 (6)	2.28 (4)
260	211.3	1.6 (-5)	1.20 (-8)	997	17.02	55.1	3.36 (-15)	1.19 (8)	1.08 (7)	4.12 (5)	7.74 (2)	1.07 (8)	1.20 (6)	2.18 (4)
280	219	5.7 (-6)	4.28 (-9)	997	16.27	58.7	1.12 (-15)	4.15 (7)	1.83 (6)	5.42 (4)	6.30 (1)	3.87 (7)	9.32 (5)	2.05 (4)
300	311	1.1 (-6)	8.25 (-10)	997	15.21	64.7	2.06 (-16)	8.16 (6)	1.02 (5)	1.99 (3)	1.06 (0)	7.42 (6)	6.17 (5)	1.85 (4)
320	373	2.6 (-7)	1.95 (-10)	997	13.24	75.9	4.27 (-17)	1.93 (6)	6.15 (3)	8.07 (1)		1.49 (6)	4.13 (5)	1.67 (4)
340	435	8.4 (-8)	6.30 (-11)	997	10.13	103	1.02 (-17)	6.10 (5)	4.02 (2)	3.58 (0)		3.14 (5)	2.80 (5)	1.51 (4)
360	497	3.8 (-8)	2.85 (-11)	997	6.67	156	3.13 (-18)	2.74 (5)	2.84 (1)			6.91 (4)	1.92 (5)	1.38 (4)
380	559	2.2 (-8)	1.65 (-11)	997	4.95	223	1.32 (-18)	1.61 (5)	2.16 (0)			1.58 (4)	1.33 (5)	1.25 (4)
1,000	621	1.5 (-8)	1.13 (-11)	997	4.10	276	7.35 (-19)	1.08 (5)				3.78 (3)	9.27 (4)	1.15 (4)
1,200	746	7.8 (-9)	5.86 (-12)	997	3.54	337	3.32 (-19)	5.65 (4)				2.41 (2)	4.66 (4)	9.64 (3)
1,400	870	4.5 (-9)	3.38 (-12)	997	3.25	397	1.75 (-19)	3.24 (4)				1.77 (1)	2.42 (4)	8.19 (3)
1,600	994	2.8 (-9)	2.10 (-12)	997	2.95	418	9.83 (-20)	2.00 (4)				1.48 (0)	1.30 (4)	7.00 (3)
1,800	1,119	1.8 (-9)	1.35 (-12)	997	2.64	528	5.80 (-20)	1.33 (4)					7.23 (3)	6.04 (3)
2,000	1,243	1.3 (-9)	9.75 (-13)	997	2.32	629	3.61 (-20)	9.36 (3)					4.12 (3)	5.24 (3)
2,200	1,553	6.8 (-10)	5.10 (-13)	997	1.69	969	1.38 (-20)	4.91 (3)					1.13 (3)	3.78 (3)
3,000	1,864	4.4 (-10)	3.30 (-13)	997	1.34	1,368	7.05 (-21)	3.16 (3)					3.56 (2)	2.82 (3)
3,500	2,175	3.2 (-10)	2.40 (-13)	997	1.17	1,741	4.43 (-21)	2.29 (3)					1.26 (2)	2.17 (3)
4,000	2,486	2.4 (-10)	1.80 (-13)	997	1.08	2,065	3.16 (-21)	1.75 (3)					4.94 (1)	1.70 (3)
4,500	2,796	1.9 (-10)	1.43 (-13)	997	1.05	2,354	2.41 (-21)	1.39 (3)					2.11 (1)	1.37 (3)
5,000	3,107	1.6 (-10)	1.20 (-13)	997	1.03	2,624	1.92 (-21)	1.13 (3)					9.68 (0)	1.12 (3)
6,000	3,728	1.1 (-10)	8.26 (-14)	997	1.01	3,156	1.32 (-21)	7.88 (2)					2.47 (0)	7.85 (2)
7,000	4,350	8.0 (-11)	6.00 (-14)	997	1.00	3,707	9.65 (-22)	5.78 (2)						5.78 (2)
8,000	4,971	6.1 (-11)	4.58 (-14)	997	1.00	4,290	7.36 (-22)	4.42 (2)						4.42 (2)
9,000	5,592	4.8 (-11)	3.60 (-14)	997	1.00	4,912	5.80 (-22)	3.49 (2)						3.49 (2)
10,000	6,214	3.9 (-11)	2.93 (-14)	997	1.00	5,574	4.70 (-22)	2.83 (2)						2.83 (2)

(a) Numbers in parentheses denote powers of 10. Thus, 2.9 (-1) means 2.9×10^{-1}.

Nonpenetrating Radiations

The temperature of artificial satellites or spacecraft orbiting about a planet (or a moon) in the solar system are determined mainly by (1) the direct solar radiation, (2) the reflected solar radiation, or albedo of the planet (moon), (3) the emitted radiation of the planet (moon), and (4) the surface radiation characteristics of the artificial satellite or spacecraft, which depend on its composition, shape, and orientation. This relationship is illustrated in Figure 1.

The total amount of electromagnetic radiation emitted from the sun is equivalent to that emitted from a 5800 K black body. About 99 percent of the solar energy has wavelengths between 0.3 and 4.0 microns. In the region between 0.095 and 7.0 microns, the solar spectral irradiance data shown in Figure 2 are considered the best available. The values shown represent the distribution of energy in the solar radiation incident on the earth's upper atmosphere when the earth is at its mean distance from the sun. The sum total of solar irradiance at the earth's mean distance is called the solar constant, and has the value 0.140 W/cm^2. Variations in the energy distribution occur, primarily at the shorter wavelengths, during the solar sunspot cycles. The curves shown illustrate the extent of this change [2].

Penetrating Radiation

Because the components of the penetrating radiation environment arise from various sources and are characterized by quite different spatial distributions and time variations, the assessment of accumulated fluxes encountered by a space vehicle over any length of time is a complex problem. These components, from natural and man-made sources, are discussed below.

Charged Particles. From this standpoint of damage to materials the charged particles are the most important; however, only electrons, protons, and helium nuclei exist in sufficient numbers to cause damage.

For spacecraft orbits out to approximately 23,000 statute miles (37,000 Km) geomagnetically trapped, or Van Allen radiation is of great importance, a charged particle trapped on a magnetic field line follows a helical path around the field line. At some point the particle "mirrors" or reverses its motion parallel to the field, then bounces back and forth between mirror points of equal field strength. The motion is stable unless changed by collision with atoms or electrons or unless the field line become distorted. Because of the symmetrics involved the spatial distribution of trapped particles may be easily visualized as a toroid surrounding the earth. Both protons and electrons are included in this pattern; however, their respective maxima do not coincide. Protons produce by far the most severe damage; Figure 3 illustrates the distribution of the most energetic ones. Note that the > 34 MeV protons are separated into essentially two belts: one at about 2000 miles (3220 Km) altitude, and one at about 8000 miles (12870 Km) altitude. The energy level variation with numbers of protons per cm^2 per second (flux level) is illustrated

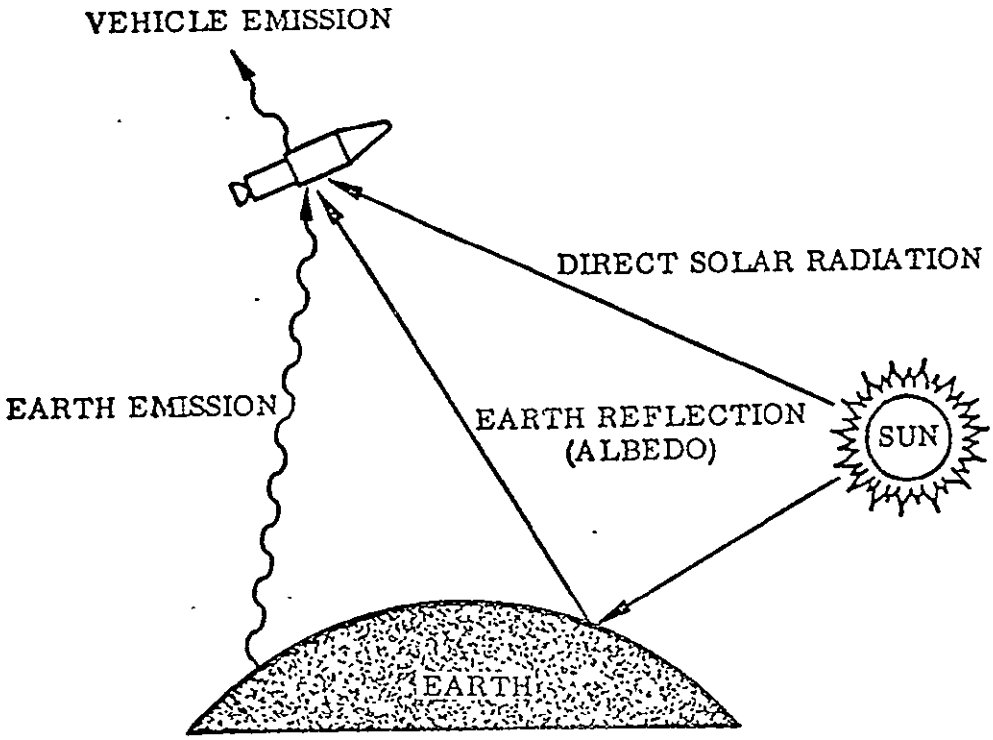

FIGURE 1. SPACECRAFT HEAT BALANCE

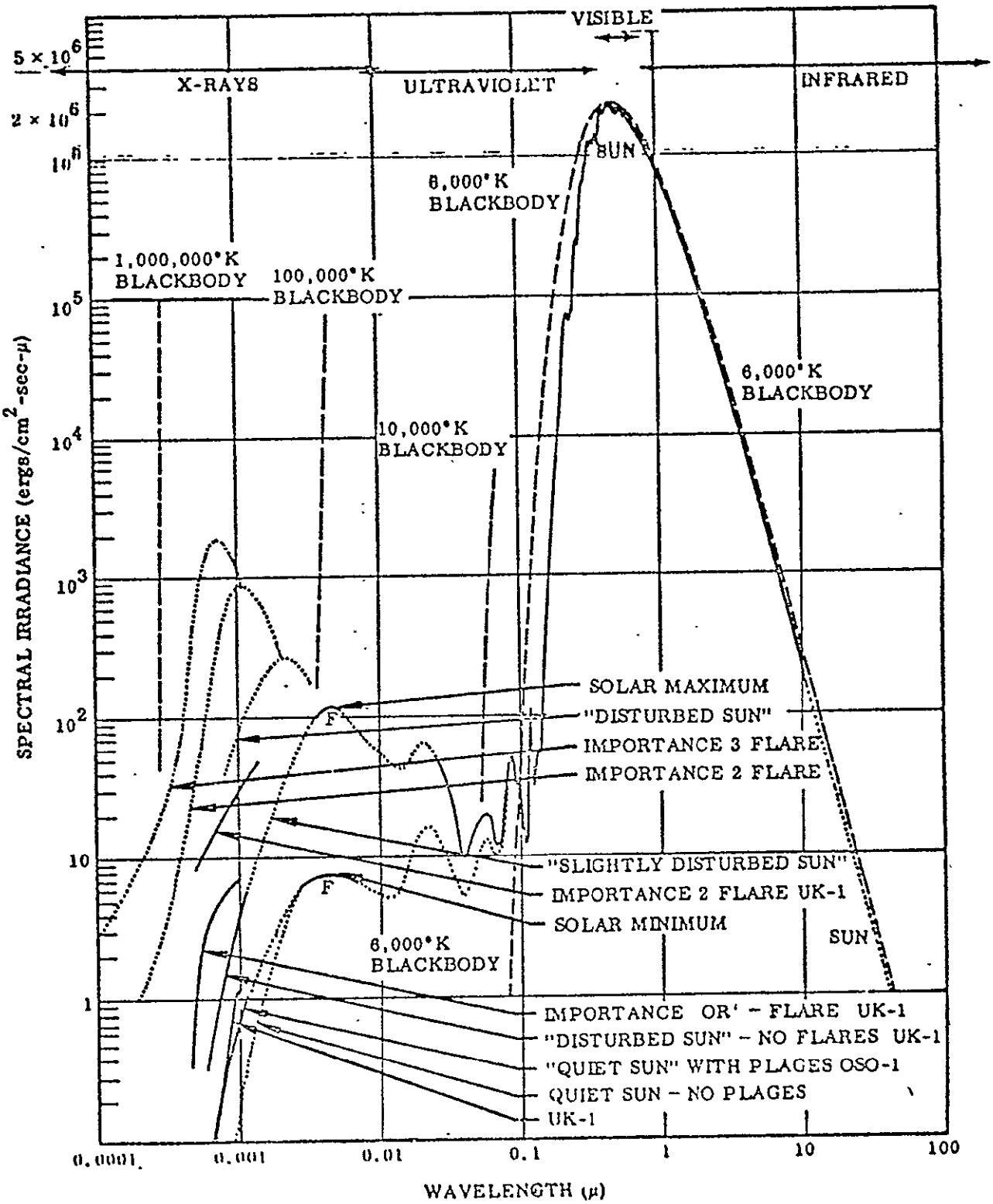

FIGURE 2. THE SOLAR ELECTROMAGNETIC RADIATION SPECTRUM. SOLID LINES REPRESENT MEASUREMENTS; DOTTED LINES, ESTIMATES

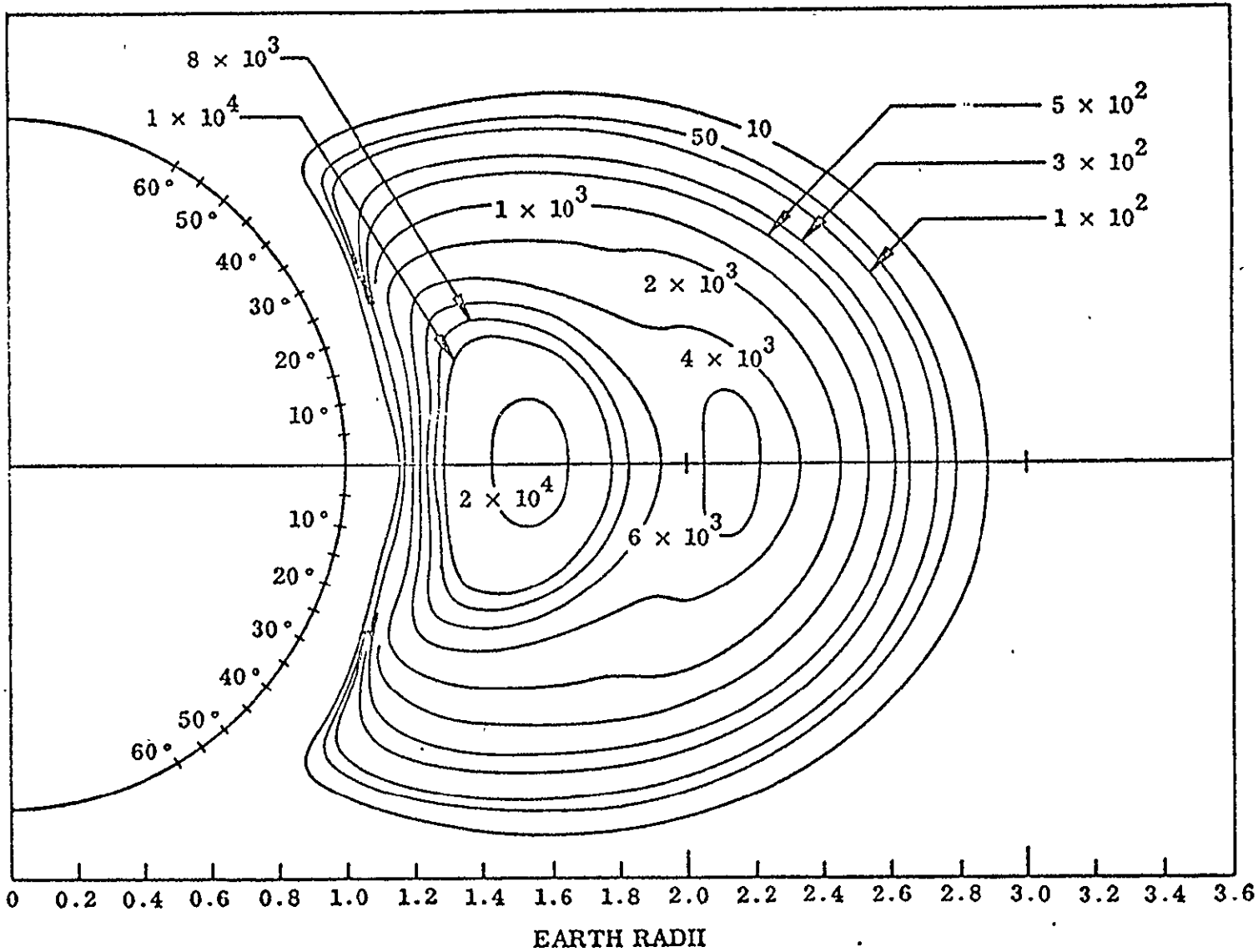

FIGURE 3. PROTON ISOFLUX CONTOURS (E > 34 MeV). (CONTOURS ARE LABELED IN UNITS OF PROTONS/CM^2-SEC.)

for the most energic zones in Figure 4. It is noted that the intensities and energy spectra of protons for $L \leq 2$ in the inner zone are the most stable, this is due to the greater magnetic rigidity (and, consequently, less distortion) in this region. The solar-cycle related variation influxes for altitudes up to ~300 miles (483 Km) is not included in the plotted data – the flux is reduced to ~1/2 during solar maxima.

The trapped electrons belt coincides spatially with the proton belt but has different configurations in its intensity and energy spectrum distributions. Although electron densities are high (2×10^6 electrons/cm^2/sec-max), the maximum kinetic energy they can transfer upon impact is much less than for the proton fluxes descrbied above. For this reason, any detailed description of electron flux distribution seems unnecessary.

Although alpha particles trapped in the geomagnetic field have been observed, their peak flux level is extremely sparse; also there are almost no alpha particles with energy levels above 10 MeV. Thus, as far as damage to structural materials is concerned, their presence may be ignored.

Intense fluxes of protons and electrons have been observed in the auroral regions – 60 to 70 degrees geomagnetic latitudes and up to ~500 miles (805 Km) altitude. The origin and storage mechanism for these particles is not well understood; however, based on very limited data, proton energies of 10 to 20 KeV and peak fluxes greater than 10^6 protons/cm^2/sec/steradian are present. A rough estimate for accumulated exposure rate gives ~10^{10} protons/cm^2/day with an average energy of 15 KeV.

Within the solar system the cosmic rays consist mostly of protons (~90 percent). Energies range as high as 10^{10} GeV; however, the integral flux above 40 MeV is ~2 protons/cm^2/sec during solar maximum and about 5 protons/cm^2/sec during solar minimum.

Neutral Particles. The upper limit average neutron flux from the sun is estimated at 10^{-2} neutron/cm^2/sec. This is negligible as is also the neutron flux accompanying solar flares. Other solar radiations, X-rays, gamma, and photons, because of the insignificant damage they can cause, are neglected.

High-altitude nuclear explosions (e.g., "Star-Fish") have contributed (1) charged and neutral particles and electromagnetic radiations from the detonation itself and from the fission debris, and (2) charged particles injected into trapped orbits. A large portion of the detonation energy is at X-ray frequencies; some of the remainder is fission products. The estimation is complex, and since the probability for future detonations is becoming remote it is being neglected here. At least six detonations have occurred and the most powerful was 1.4 MT of TNT equivalent. Following this detonation, electron fluxes of the order of 10^9/cm^2/sec were recorded. Thus, the injection of electrons by this method can present a serious hazard for years (during decay processes), to many satellite programs designed to take advantage of the normally low radiation levels at altitudes of ~150 miles (241 Km).

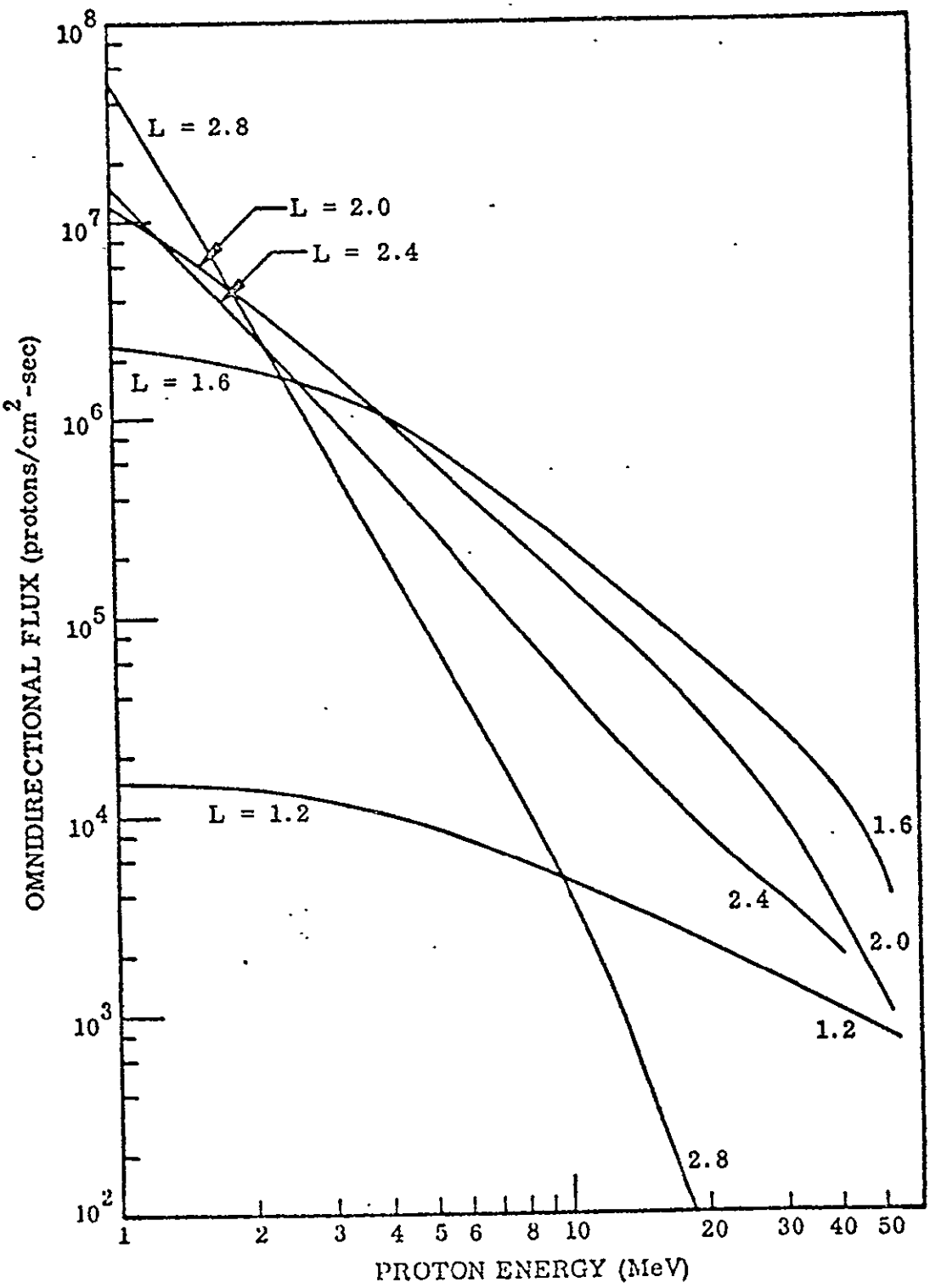

FIGURE 4. INNER ZONE PROTON SPECTRA

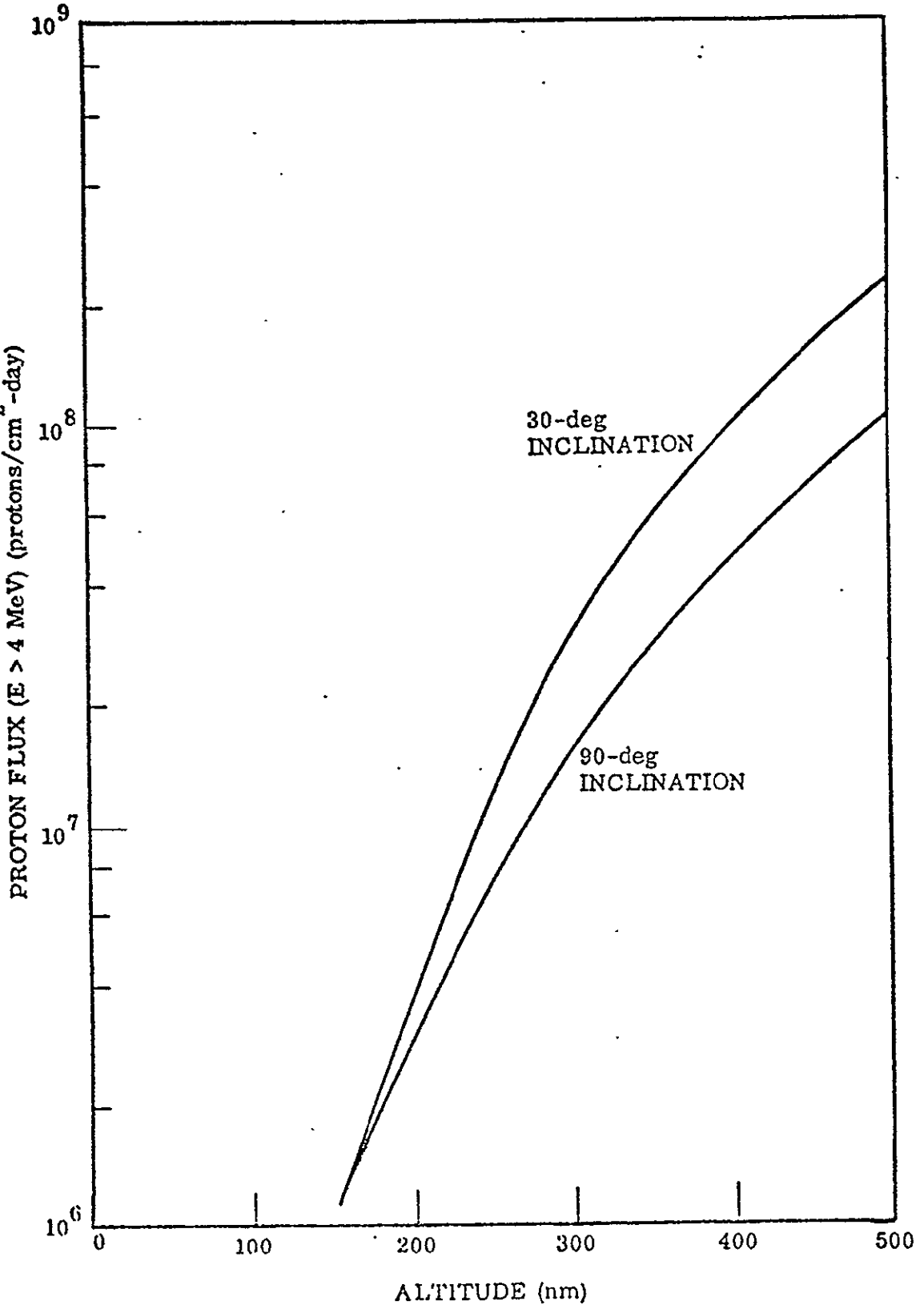

FIGURE 5. PROTON FLUX PER DAY ENCOUNTERED IN CIRCULAR ORBITS

Calculation of Accumulated Fluxes. Computer programs are available for calculating accumulated particle fluxes for a particular spacecraft at a given time. Figure 5 shows the results of a proton flux calculation made for two orbital inclination angles, 30 and 90 degrees, at various altitudes. The proton fluxes intercepted per day for particles having energies greater than 4 MeV are plotted. These values are believed to represent the upper limites to be expected (for later dates). Obviously, spacecraft with highly eccentric or unusual orbital configurations must be treated individually [2].

The geomagnetic field deflects charged particles incident on it from the interplanetary space and thereby provides very effective shielding to the region of space between ~60 degrees north and south magnetic latitudes. Near the magnetic poles and in interplanetary space outside the influence of the magnetosphere, the direct charged-particle radiation from the sun can be observed. This radiation consists of two components: high-energy particles that occur sporadically (originating from solar flares), and low-energy protons and electrons, which are present more continuously.

The solar flare radiation consists of electrons, protons, alpha particles or helium nuclei, and very small number of higher mass nuclei. Once again, the proton flux is the most damaging component; however, since the events occur sporadically and vary widely in intensity, a statistical treatment is necessary. Plots of the probability of encountering a total flux of protons with energies greater than 30 MeV for mission durations of two weeks and one year are shown in Figure 6. As a representative calculation of the proton intensity – in a 52-week mission there would be a 0.8 probability for having a 30 MeV proton flux of 3×10^8 protons/cm^2. The numbers of alpha and heavier particles present varies from ~0.1 to ~0.001 of the numbers of protons [2].

The solar wind is a plasma consisting of protons, electrons, and alpha particles which continuously streams radially outward from the sun. The particle velocity in the vicinity of the earth varies between about 350 and 700 Km/sec, which corresponds to energies of ~0.6 to 2.6 KeV for protons. The flux intensity varies between ~3×10^7 and $1 \times 10^9/cm^2/sec$. Although these are large fluxes, the energies are small and consequently damage to materials will be confined to surfaces.

Meteoroids

This natural "space debris" (meteoroids) is believed to originate primarily in the solar system – comentary degradation probably contribues more than 90 percent of the total. Mass density of the meteoroid material is ~0.5 gm/cm^3; however, those originating from the asteroid belt (between Mars and Jupiter) range in density from 3 to 9 gm/cm^3. Actual velocities of meteoroids vary from ~11 to 42 Km/sec, relative impact velocities can be at least twice as great.

Although meteoroid interception by the earth exhibits a fairly continuous sparadic background, increases in the average hourly rate of influx are observed

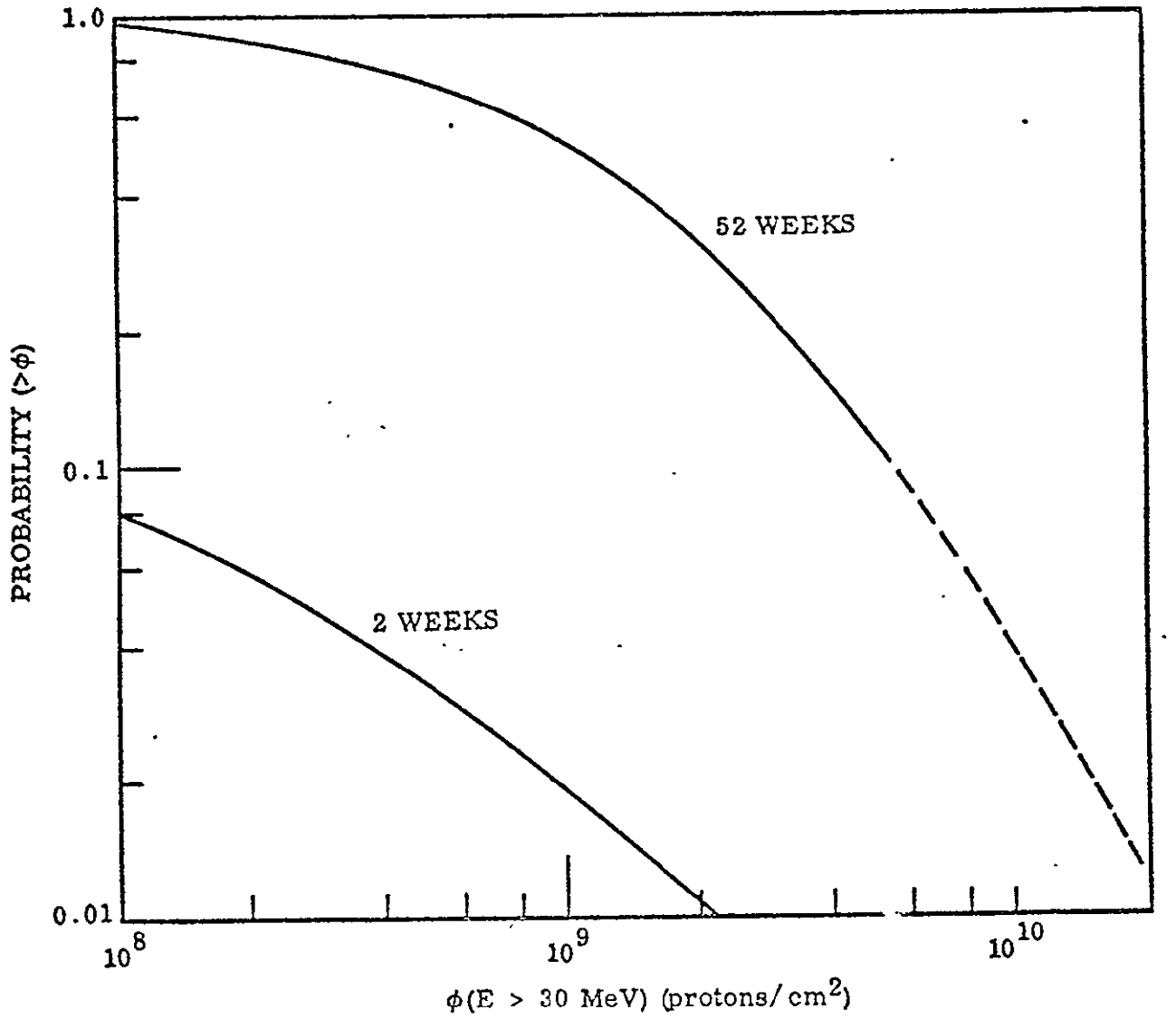

FIGURE 6. FREE-SPACE SOLAR FLARE PROTON ENVIRONMENT FOR A 2-WEEK AND A 52-WEEK MISSION

at regular intervals during the calendar year. These are caused by passage of the earth in its orbit through the oribt of a stream of particles, probably of cometary origin, that are traveling in similar helioecentric orbits. The meteoroids stream influx can increase over background by as much as 20 times for periods of several hours.

The impingement of high-velocity particles on thin-skinned pressurized structures can cause small punctures that could result in a gradual loss of pressure of the space vehicle or actual rupture by explosive decompression. The kinetic energy of the impinging particle is absorbed by the particle and the skin to cause fragmentation and vaporization of both. Interaction of these fragments with the spacecraft atmosphere can result in oxidative explosions to produce high-temperature and high-pressure fluctuations. In addition, penetration, impingement, or erosion by the particles could result in nonstandard operation, malfunction, or failure. To estimate the penetration hazard to spacecraft the flux-mass relationship for meteoroids has been converted to a flux-penetration-probability model as shown in Figure 7 (2).

It is noted that to design a single-wall spacecraft for a high probability of no perforations for a large area-duration product would impose a possibly unacceptable weight penalty. To avoid this the spaced armour principle has been investigated. Equations for this have been developed and were employed for designing a double-wall configuration for the Apollo program.

Temperature

Thermal effects associated with gases in space environments are negligible. This is true even though the kinetic energy of individual gas molecules may be several thousands of degrees. Because of the extremely low density, the heating from convection even at satellite velocities is some three orders of magnitude less than incident solar radiation. The equilibrium vehicle temperature as a result of the latter will depend on the absorptance/emittance ratio of the vehicle surface. Figure 1 displayed the factors which contribute to a spacecraft's heat balance. Apart from the importance of the lower wavelengths present in solar radiation in space, the primary thermal effects are those associated with changes in temperature occasioned by a vehicle or parts of a vehicle being periodically exposed directly to the sun and periodically in shadow. In general, temperature effects in induced environments are much more severe than those resulting from natural space environments.

Induced Environments

Induced environments include those conditions unique to specific vehicles and mission requirements; thus, they represent design parameters and are outside the scope of this program. Examples of some of the requirements which go beyond those normally encountered on earth will be given.

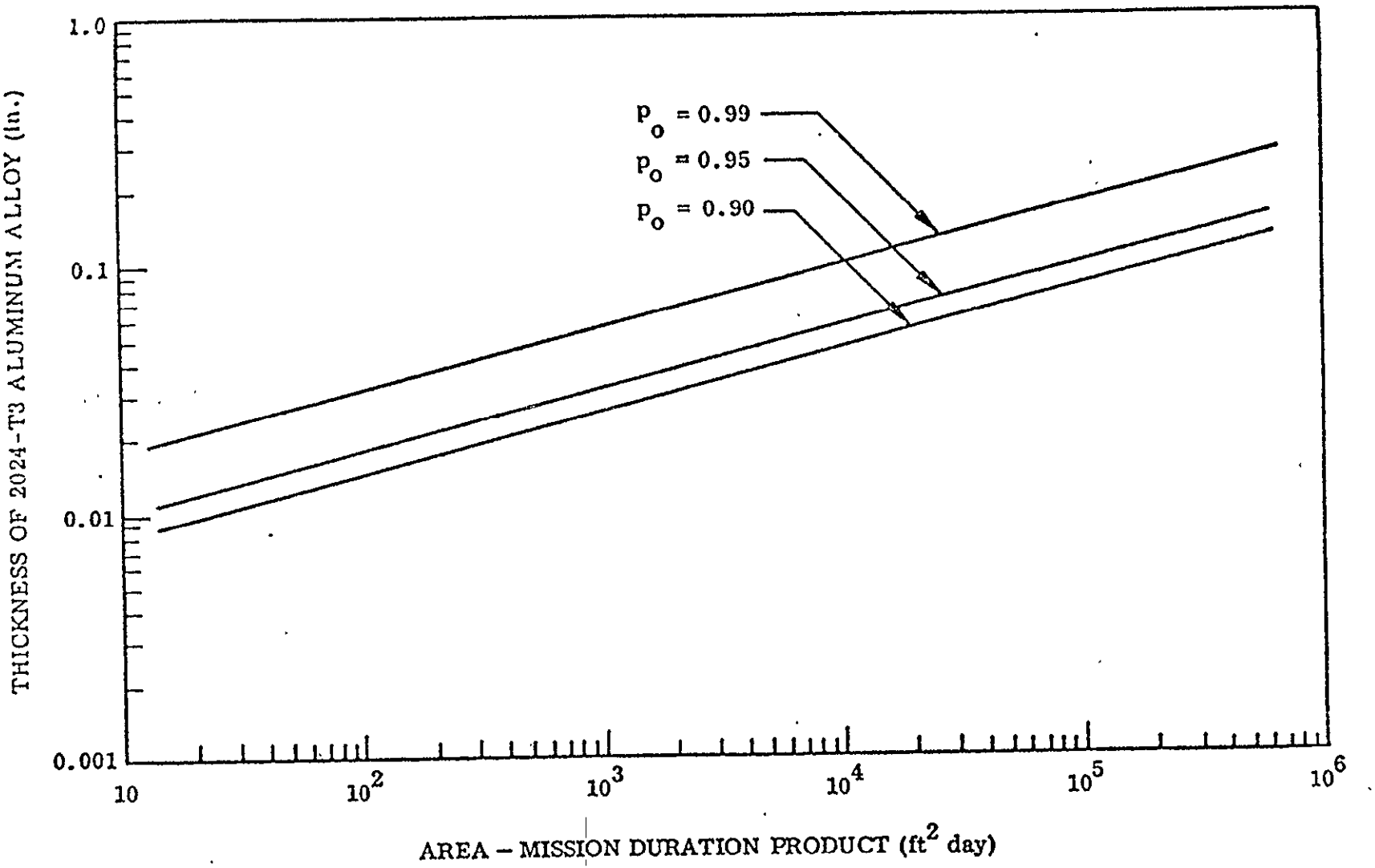

FIGURE 7. PROBABILITY, p_o, OF NO METEOROID PENETRATIONS THROUGH A SINGLE SHEET OF 2024-T3 ALUMINUM ALLOY

Radiation. Due to the presence of shielding provided by the spacecraft structure and the possible existence of an on-board nuclear reactor or radioactive isotopes, the internal radiation environment may be quite different from the external radiation environments discussed above.

In general, radiations lose energy by a variety of interactions, some leading to secondary radiations. Computer programs have been developed for estimating the exposure levels for rather complex enclosures. Damage which involves perturbation of atoms in a crystal lattice by particle radiations may best be predicted by application of damage coefficients; for other types of damage it is convenient to convert the radiation environment incident on the material to the energy deposited per unit mass; i.e., the dose in the material. This applies where the main damage is from breakage of chemical bonds. The currently used unit of dose is the rad, defined as 100 ergs of energy absorbed per gram of material. The damage per unit energy transfer becomes greater as the particle slows down and its ionization rate becomes greater.

On-board radioisotope sources have a relatively low damage potential; however, leakage fluxes from nuclear reactions can present serious problems of material damage. The unshielded radiation rates 100 feet (30.5 m) from a 1000 MW reactor might be as high as 10^{11} neutrons/cm^2/sec and 10^6 rad/hr from gamma rays. Thus serious damage to many components would occur in a short time unless very effective shielding were provided.

Temperature. It is difficult to say which of the induced environments poses the most severe problem for future aerospace components. Certainly, temperature extremes must be included near the top of the list. Consider, for example, the requirements for the hinge bearing on the aerodynamic control surfaces of maneuvering reentry vehicles. The exact thermal environment of such a bearing will depend not only on trajectory and configuration, but also on the location of the bearing and the heat-transfer characteristics of the surrounding structure. For a typical configuration the control bearings must withstand temperatures of 1500 to 2500 F (816 to 1371 C) for periods of 15 to 30 minutes. Peak temperatures of 3000 F (1649 C) may be reached. Since the temperatures attained may be at least partly dependent upon the spacecraft heat balance situation they should be considered a time-dependent factor. Consideration of in-flight temperature data suggests that the thermal control design has been adequately handled; consequently, thermal degradation, in these parts at least need not be further considered.

Shock and Vibration. Vibration of enclosed components will undoubtedly be isolated to some extent from the severe levels associated with ground transportation and during the ascent phase. Also, some constant or intermittent loading may be expected during long period flight operations associated with a given satellite. No specific information is available at present; however, the source and mode of in-orbit vibration must be defined and evaluated in order to predict the long-term effects on component materials and function.

IDENTIFICATION OF CRITICAL FAILURE MECHANISMS FOR THE THREE REPRESENTATIVE COMPONENTS

In order to establish a life test methodology for mechanical components, it was necessary to determine the probable failure mechanisms to be dealt with. This was accomplished by examining the three representative components in detail to determine the most critical failure mechanisms associated with each. Specialists in the areas of aging, corrosion, machine design and tribology analyzed detail drawings and specifications in order to identify the life-critical components and the most probable failure mechanisms. The results of these analyses are summarized below.

Each component is first identified, then a summary is given of the most critical areas and their possible time-dependent modes of failure under the specified operating conditions and environmental conditions with respect to structural and flexural parts, nonmetallic aging, metallic corrosion and aging, and friction and wear interfaces.

With regard to the three representative components being considered in this program, it has been assumed (within the framework of the program) that they are designed and manufactured correctly and are functioning properly for short-term operation. Only the long-term behavior of these items is uncertain and must be evaluated on the basis of short-term testing.

Four-Inch Vent Valve

This valve is covered by MSFC Design Procurement Drawing (Specification) 20M32043. It is shown on Amatek/Calmec Drawing 1079. The actuator assembly (electric motor) was excluded from consideration.

Structural and Flexural Components

The most critical structural parts and their postulated possible time-dependent structural modes of failure are as follows.

(1) The valve body is made of 6061-T6 aluminum alloy. Possible (but not necessarily likely) modes of failure include fatigue due to fluctuating pressure differentials and due to vibrations.

(2) The blade is mode of 6061-T6 aluminum alloy. Internal serrations are probably the most critical location. They are subjected to repeated (cyclic) torsional loading and may fail, in principle, over a period of time because of fatigue, fretting, wear, or a combination of these.

(3) The blade driver shaft is made of A-286 alloy. This shaft transmits oscillating (cyclic) torque; hence, in principle, it could fail in torsional fatigue or in serrations, as in (2) above.

(4) The coupling is made of 17-4PH alloy. This is an oscillating part that is subjected to cyclic torsion. Its arms are subjected to cyclic bending. Thus, fatigue failures are conceivable, in addition to failures in the serrations.

(5) The actuators are made of Inconel 718. The tabs of these actuators act as springs and are subjected to repeated bending. Hence, they are subject to bending fatigue.

(6) The blade seal spring, made of beryllium copper, is another flexural part that is subjected to cyclic loading and might be suspect for fatigue failures, even though the likelihood of such failures here is rather remote.

Nonmetallic Materials

The 4-inch vent valve contains 5 nonmetallic parts which are identified in Table 4. Fluoropolymers, in general, when used under the expected conditions can give rise to two major problems – cold flow and radiation damage in the presence of oxygen. A survey of the applications of the above parts indicates that the most critical situation exists with Part Number 8. This part can be subjected to pressure when the valve is closed. The magnitude of the pressure exerted on the seal cannot be determined from the available information. If this pressure is sufficiently high, permanent deformation due to cold flow might result giving rise to valve leakage. This seal is also exposed to air or oxygen during certain phases of operation. Combined exposure to oxygen and radiation can cause deterioration of TFE if the dose is above the threshold value.

As a matter of note, the threshold dose for radiation deterioration of FEP is higher than that of TFE (see Table 5). FEP is also easier to mold into usable shape than is TFE. Therefore, it appears that advantages might accrue from changing Part Number 8 from Halon G-700 (TFE) to an FEP molding-grade Teflon.

The other four parts appear to be adequately shielded from radiation and cold flow so as to not present serious problems.

It is suggested the cold flow properties (permanent set) of Part Number 8 be explored, as well as the possibilities of exposure to combined radiation and and oxygen.

TABLE 4. NONMETALLIC PARTS IN 4-INCH VENT VALVE

Part Number	Name	Material	Identity
8	Seal	Halon G-700	TFE[a]
12	Gasket	Chlorotrifluoro-ethylene	KEL-F
27	Seal	Teflon	TFE
29	Sleeve	Teflon	TFE
44	Grommett	Teflon	TFE

(a) Tetrafluoroethylene.

TABLE 5. RADIATION REQUIRED TO DAMAGE FLUOROPOLYMERS IN AIR

Polymer	Threshold of Damage, rads	25 Percent Level of Damage, rads
TFE	1.7×10^4	3.4×10^4
FEP[a]	1×10^6	6.5×10^6
KEL-F	6.5×10^5	6.0×10^6

(a) Fluoroethylene-propylene.

Metallic Materials

The metallic materials in the 4-inch vent valve are made from corrosion-resistant materials that will perform well in the gases that they are designed to handle. In addition, these materials are also resistant to the normal cabin atmosphere. The most likely cause of failure is prolonged exposure to a marine atmosphere prior to launch. Corrosion initiated under these conditions could be propagated by the moist-oxygen cabin atmosphere.

Of particular concern are crevice and galvanic corrosion of aluminum alloys and the intergranular corrosion of sensitized stainless steel. Both of these failure modes are time dependent. The possible failure modes are as follows:

(1) Most critical failure modes.

a. Crevice corrosion of 6061-T6 aluminum blade where it seals against the Teflon plastic (corrosion products could prevent complete closing of the valve).

b. Galvanic corrosion between 6061-T6 aluminum and the Ni + Ag plated Berylco 25 spring that holds the Teflon plastic seal. The corrosion products could prevent complete sealing of the valve.

(2) Other failure modes.

a. Intergranular attack of sensitized 18-8 stainless steel, particularly of thin washers.

b. Possible stress-corrosion cracking of the 17-4 PH in the indicator portion (residual and operating stresses are probably low, thereby, minimizing this problem).

c. Galvanic corrosion of the 6061-T6 plate beneath the tin-plated phosphor bronze terminal to produce loss of electrical continuity and lack of indication of valve position.

d. Crevice corrosion between actuator set screw and aluminum housing with resultant buildup of corrosion product and possible failure of indicator switch to operate properly.

e. Crevice corrosion of aluminum at stainless steel bolts that hold the motor housing to the aluminum valve body. May enlarge the bolt holes and produce wobble.

f. Crevice corrosion between the Stellite bearing race and the aluminum housing. This could cause the race to rotate, but may not cause failure.

Friction and Wear Interfaces

(1) Primary failure mode

Leakage of Gate Valve Seal.

a. Combined aging and wear of Halon G-700 seal lip.

b. Fouling of seal lip by corrosion and/or wear debris.

c. Distortion of Halon G-700 seal lip.

d. Indentation of Be-Cu spring into back of Halon G-700 seal member by creep loss of spring force and thinning of seal material with eventual wear-through.

(2) Secondary failure modes

Gate Valve Pivot Bearings.

a. Wear of Teflon retainer such that the retainer becomes structurally weak, breaks, and fouls bearing.

b. Loosening of bearing races on shaft and in housing from cyclic heating and cooling (differential expansion between Stellite and aluminum, Stellite and stainless steel). Fretting of loosened bearing races produces damaging debris and further loosening of axle bearing and loss of precision in locating gate seal face with Halon G-700 lip.

c. Fretting of balls in races from vibration resulting in higher friction, rough running bearings.

Spline Coupling.

a. Fretting of spline coupling leads to loosening of coupling and backlash in driving the gate valve.

Calibration Gas Supply Module

This module is covered by MSFC Design Procurement Drawing (Specification) 20M32245. It is shown on Amatec? Calmec Drawing 1179. The module contains a gas bottle, four solenoid valves, a pressure regulator, a pressure transducer, and several auxiliary elements. No details are available on the pressure transducer.

Structural and Flexural Components

Although the module consists of many parts, there are only a few structurally critical parts:

(1) The pressure bottle with its body made of Cryostretch 301 alloy and a welded neck made of 304L alloy. This bottle is subjected to a rather high (1500 psi or 10.3 MN/m^2) internal operating pressure, and it might be repressurized a number of times. Thus, it might be subject to bursting due to overpressure and due to low-cycle fatigue. In addition, it is subjected to vehicle vibrations.

(2) The body assembly made of 304L alloy. Certain portions of the body are subjected to the same internal pressures as is the bottle. However, because of the relatively small cavities and small-diameter gas passages within the body, the latter appears to be less critical than does the bottle. For large numbers of pressurization cycles, it is conceivable that fatigue cracks might be initiated at stress concentrations within the body.

(3) The tubing made of 321 alloy, particularly the fill tube and the pressure-transducer tube. These are subjected to the same pressure regimes as is the bottle and the same modes of failure could apply, except that these tubings which have a higher wall thickness-to-diameter ratio should be somewhat safer, in general.

(4) The regulator diaphragm made of 0.001 inch (0.025 mm) thick annealed 321 alloy. This diaphragm is subjected to slight flexural motions and is critical for proper functioning of the pressure regulator. Any surface damage may lead to cracks in the diaphragm that might propagate by fatigue.

(5) Various welds. The module assembly contains a number of various welds. Any cracks in these welds caused either by pressurization cycles or vibrations, or both, could result in a leaking module.

Nonmetallic Materials

There are 12 nonmetallic parts (see Table 6) in this assembly that must receive careful attention. Past experience with the materials specified indicate two potential areas for failure.

RTV-type potting compounds are usually two-component systems that require mixing of the catalyst with the resin just prior to application. Some of these compositions employ components that are corrosive to metals. For example, RTV-602 potting compound contains a catalyst that corrodes freshly cleaned copper metal. RTV-601 has not been examined in detail in this laboratory. In view of the corrosion potential of RTV-602, the RTV-601 potting compound should be carefully explored for similar effects. Uniformity of mixing before application is also a determinant in the performance of the potting compound. Careful instructions as to its use should be a part of the specifications.

The second area of concern is the Teflon valve seat, Part Number 1179-7. Teflon is subject to "creep", or "cold flow", the amount depending on the temperature and pressure involved. The possibility exists that the Teflon seat could be subjected to combinations of heat and pressure during its life that

TABLE 6. NONMETALLIC PARTS IN CALIBRATION GAS SUPPLY MODULE

Part Number	Name	Identity
3	Potting	RTV-601
11	Gasket	KEL-F[a]
15	Seal	Teflon
37	Gasket	KEL-F
40	Gasket	KEL-F
56	Jacket	NBG elastomer
71	Retainer	Fluorogreen
72	Clamp	Nylon
73	Nut	Nylon insert
82	Sleeve	KEL-F
85	Tube	Teflon
86	Primer	DC-1200

(a) Chlorotrifluoroethylene.

could result in enough deformation of the seat to cause the valve to leak. This is especially true if the armature (Part Number 1179-6) can rotate with respect to the seat.

A word of precaution should be made regarding application to metal surfaces of the silicone primer Number DC-1200. Proper performance of this primer depends on application to clean, grease-free, dry, rust-free surfaces. The metal during application of DC-1200 should be at a temperature of at least 50 F (10 C), and preferably below 100 F (38 C). Film thickness should be controlled to the recommended value, since poor performance can result from either a film that is too thick or too thin. Primer coatings are not formulated to furnish good protection alone, and should be coated with a proper topcoat designed to perform satisfactorily under the specified conditions.

Metallic Materials

The comments made with respect to the metallic materials in the 4-inch vent valve are also applicable to the calibration gas supply module. The possible failure modes are as follows.

(1) The gas in the tank is presumed to be dry and all materials are presumed to be excluded from the external atmosphere by closed valves during prelaunch activities. The only possible failure modes are at welds where the sensitized heat-affected zones may be attacked intergranularly by a marine or an

industrial atmosphere. (The performance of solder under these conditions is not well documented.)

(2) However, if an external marine atmosphere penetrates the solenoids and the pressure regulator, the following areas could be a problem.

(a) Intergranular corrosion at the heat-affected zone of the weld on the 1-mil-thick Type 302 diaphragm.

(b) Corrosion products blocking passages or preventing seating because of

- Crevice corrosion at A-286 (36) or Type 304 (12) seats
- Crevice corrosion that plugs the small hole in the Type 304 leak plate (43)
- Crevice corrosion or attack of sensitized Type 304 screens in Items 42, 74 to 76, or 77 to 79
- Crevice corrosion of the Type 430 armature (16) where it contacts the Teflon seal (15).

Friction and Wear Interfaces

Two types of problems are possible in the solenoid and poppet regulator

(1) Cold flow of the Teflon seal seat resulting in leakage of solenoid valve

(2) Seizure of the armature or the poppet regulator owing to fouling from self-generated wear debris. The principal source of debris would be fretting of the 430 stainless armature against the 304 stainless sleeve.

Two-Inch Recirculation Valve

This valve is covered by NAR Procurement Specification MC284-0284. Unfortunately, this specification was unavailable. For review purposes with regard to external environments and exposures, the NAR Procurement Specification MC284-0158 was used. The latter specification is for another valve employed in the same recirculation system. Most of the relevant information on the recirculation valve was obtained from a report entitled "Saturn Component Evaluation for Extended Life - Saturn S-II 2-Inch Normally Open Recirculation

Valve P/N V7-480328-91, S/N 06361-A002086", prepared by E. D. Storms, Space Division, NAR. This valve is shown on NAR Space Division Drawing V7-480328 (-91). It consists of a gate (butterfly) valve, an integral internal relief valve, a pneumatically operated actuator assembly, a rack and pinion drive, an external vent (relief) valve, and a position indicator. The latter was excluded from consideration.

Structural and Flexural Components

Similarly to the preceding two items, most of the structurally critical parts are those subjected to pressures and/or cyclic loadings with the possible failure modes being typical of such loadings (predominantly low- and high-cycle fatigue). These parts include, but are not limited to the following.

(1) The housing made of permanent-mold aluminum alloy casting

(2) The cap made of 6061-T351 aluminum alloy

(3) The gate made of A-286 alloy

(4) The gate drive shaft made of beryllium copper, including the teeth of the pinion

(5) The piston shaft made of beryllium copper, including the teeth of the rack

(6) The piston return springs made of Elgiloy (two sizes)

(7) The relief valve spring made of Elgiloy

(8) The vent valve spring made of 302 alloy.

Nonmetallic Materials

This valve contains 17 separate nonmetallic parts. For the most part, these parts are seals, gaskets, and bearing surfaces. Three of these parts are deemed to be very critical to the satisfactory performance of the valve, as noted in the partial parts list given in Table 7. Probably the most critical are the Teflon bearings, Part Numbers 480563 and 480564. Part Number 480563 is a combined bearing and seal for the operating rack gear, fabricated from Teflon (type not specified). Similarly, Part Number 480564 is a combined bearing and seal for the piston that operates the rack gear. The tendency of Teflon to "creep" or cold flow has been discussed before. Any distortion of shape of these spacer-seals can cause misalignment of the piston-rack assembly and result in malfunction due to binding. Similarly, it can lead to leakage of the actuating

gas (N_2), causing improper operation. A critical study of the temperature-cold flow relationships of the grade of Teflon being used should be made, and compared to the operating conditions.

TABLE 7. NONMETALLIC PARTS IN 2-INCH RECIRCULATION VALVE

Part Number	Name	Material	Criticality
480357	Spring guide	Teflon	Not critical
480555	Bearing	Teflon	Critical
480556	Bearing	Teflon	Critical
480557-3	Spacer	Teflon and asbestos	Critical
480557-5	Spacer	Teflon and asbestos	Critical
480558-3	Seal (seat)	KEL - F	Very critical
480563	Bearing rack	Teflon	Very critical
480564	Bearing piston	Teflon	Very critical
480565	Seal	Mylar	Critical
480568	Retainer assembly	Nylon	Not critical
480570	Seal (gasket)	Mylar	Critical
480588	Seal (gasket)	Mylar	Critical
RD170-2028-0002	Name plate	Mylar	Not critical
MS29512-04	Packing	--	Not critical
MS29512-06	Packing	--	Not critical
ME261-0003	Seal	Black Teflon coating	Not critical
ME261-0028	Seal	Black Teflon coating	Not critical

Another very critical item is the valve seat. This seat is made of KEL-F instead of Teflon. KEL-F has somewhat less of a tendency to cold flow than does Teflon. Hence, this seal might be expected to deform less under pressure than did the previously examined Teflon seats. In addition, this valve is normally open and can be expected to be in the closed position for shorter time periods than it is open. This can be expected to minimize cold flow. Similarly, it can be expected to close only when it is at low temperature (filled with either LOX or LH_2), which should decrease the tendency to deform. Therefore, this seat is expected to be less critical than other valve seats that have been analyzed.

Other Teflon applications are far less critical than are the three discussed above; therefore, they might be expected to present fewer problems.

One area where inadequate knowledge exists is the performance of Mylar under cryogenic conditions. Part Numbers 480565, 480570, and 450588 are seals that rely on the flexibility of the Mylar film to maintain a gas-tight seal. Not enough information is available on the flexibility, elasticity, and recovery properties of Mylar at low temperatures to predict its performance under as wide

a range of conditions as it is subjected to in this particular design. A study of the relationships between the above properties and low temperatures should be made. This should also include fatigue studies of Mylar.

The black Teflon coating applied to metal surfaces (seals, washers, etc.) is applied to improve the sealing characteristics of the joint. Once the seal is established, no problems should be expected, since the purpose of the Teflon is to cold flow, to fill voids, etc. Once the flow has been accomplished, the pressure is relieved, and no further flow should be experienced. If repair is necessary, it should be standard practice to discard these parts on dismantling, and to use new seals on reassembly.

Metallic Materials

As in the 4-inch vent valve and the calibration gas supply module, the potential failure in the 2-inch recirculating valve is from exposure to the earth environment prior to operation rather than from exposure to the liquid oxygen or post-launch environment.

The primary failure mode appears to be seizing or corrosion product build-up that would prevent the movement of the shaft (-749) or affect the seal (E). The corrosion could occur on the aluminum housing in the crevice between the housing and the chromium-plated Be-Cu shaft. Moist air would have to enter via the inlet or outlet ports of the valve.

Similar crevice attack could occur between the piston cylinder and the housing if moist air entered this area. However, the seal at E and a plug at the helium entrance port would prevent ingress of air.

Friction and Wear Interfaces

Wear probably constitutes a major factor in controlling service life of this component. Fretting of dry surfaces and the fouling of nearby seals by debris probably is the most probable failure process. The report on wear analysis of recirculation valves from Saturn tests proved of great value in analysis of used parts. These analyses indicated possible sites for failure not anticipated from examination of the drawings (for instance, fretting of the spring against the ID of the piston – the drawing shows ample clearance between these parts). The most critical areas are as follows:

(1) Main Gate Lip Seal (Kel-F). Wear and scratching of the sealing surface by the A286 gate material will eventually result in leakage. Under dry conditions, wear will occur as transfer of Kel-F to metal-mating surfaces – causing localized build up on the originally smooth surface.

(2) Actuator Piston Seal – Mylar Versus Chromium Plate. Scoring, fouling, and wear by debris generated from other dry sliding surfaces can destroy the sealing capacity of this thin seal. This seal was tagged in the Saturn report as being the one component that was well on the way to failure during tests. Leakage has almost exceeded the maximum allowable value – the same holds for the piston-shaft seal mylar versus chromium plate.

(3) Shaft Bearings (piston-shaft bearings, piston bearing, idler-shaft bearings). All of these bearings are pure Teflon-split sleeves. Wear of pure Teflon is quite high – (wear under cyrogenic conditions is not well established) and it is possible that the bearing would wear away, allowing metal-to-metal contact and seizure, galling, or considerable metal particle generation.

Of note is that the Saturn wear analysis indicates that Teflon bearings appear capable of collecting and holding a good deal of debris generated elsewhere.

(4) Piston Stops. The surfaces, against which the ends of the piston slam home are metal. The surface for the fully open position is aluminum. These are ready-made sources of fretting and spatting – releasing debris which can foul the Mylar seals. Fretting was observed on the piston end and aluminum surface contacted in the Saturn analysis.

Another source of fretting debris is the outer spring in the piston. It can contact the sides of the piston ID during vibration and produce debris which can get into the Mylar seal. Aluminum wear debris is particularly detrimental because of the Al_2O_3 coating on each particle.

(5) Relief Poppet Valve. The valve seat consisting of a ring of pure Teflon attached to the under side of the valve, can cold flow and eventually distort to allow leakage. There is also a possibility of failure of the Teflon-metal bond under continual impact.

The poppet valve stem can hang up in the valve guide because of a bad material combination (303 stainless steel versus 303 stainless steel). Failure would be unexpected and unpredictable – but final.

AVAILABLE LIFE TEST METHODS

The literature search has indicated that the state-of-the-art of life-test methodology for long-life space components is not highly developed. Because of relatively short required lifetimes, most components have been life-tested by operating for a period which approximates their intended lifetime. Attempts to accelerate component tests have not been notably successful. It appears that this lack of success is due to the failure to consider each one of the possible failure modes for the component. To many engineers, a "life-test" for a complicated component, such as a valve, is a single test in which the component is run under a more severe duty cycle for a shorter period. Such a single test may simulate some of the possible failure modes, but not all of them.

The approach which we recommend is to perform a life test for each critical failure mechanism. The success of this approach depends on the extent to which life tests are available for the various failure mechanisms of interest. On the basis of the literature search and our past experience, the failure mechanisms identified for the three components were examined with respect to available short-term test techniques.

Structural and Flexural Failure Mechanisms

The examples of structurally critical parts and their time-dependent modes of failure discussed in the foregoing section, although incomplete, indicate that in the majority of cases low- and high-cycle fatigue due to pressurization cycles, vibrations, and repeated loading are potentially the predominant modes of structural failure, even though the likelihood of such failures should be small in correctly designed and manufactured valves. Since fatigue is cycle-dependent, and most of space valves operate only periodically and infrequently, it is entirely possible to condense the testing within a relatively short time period even without increasing the operating speed. Such tests are available within the present technology and they are being employed already throughout the space-valve industry. For example, repeated pressurization tests, in addition to proof and burst testing, are being conducted routinely whenever they are applicable. A certain number of samples from each space-valve design is subjected to vibration tests at vibration levels at least as severe as those expected in service. For long-life valves, which might be used during several launches, the duration of these tests would have to be increased accordingly, but they still could be performed within a reasonably short time period. Also, samples of space-valves are being routinely cycled (operated) under some established duty regime that may involve simulated operating conditions and more severe requirements than are those expected in actual service.

There are other mechanical tests available to ascertain the structural integrity and proper functioning of space valves in a relatively short period on samples that are newly produced. These include impact tests, acceleration tests, and

various mechanical functional tests such as tests for leakage, flow, pressure drop, crack and reseat pressure, response, pressure regulation, force or power requirement, thermal shock, etc. These tests are often combined with some environmental tests and performed in various sequences, depending on the application and the specific requirements. Unfortunately, all these tests provide indications on what are the valve's capabilities at the present time, i.e., at the time of testing, but not on the valve's behavior over a long-life period.

The available testing methods briefly mentioned above should also be valid for ascertaining long-life structural integrity in cases where there is no material property degradation and no surface deterioration that may affect the structural integrity. In these cases, there is no need for new life-test methods from a purely structural-integrity point of view. However, these available testing methods would not assure the long-life functional or operational reliability of the valves.

In cases where material aging, material-property degradation, and surface-deterioration processes occur that may affect the structural integrity of value elements, as well as in those cases where a valve has to operate continuously for extended period of time, the presently available structural testing methods cannot provide, in general, the necessary answers with regard to long-term structural integrity of valve elements on the basis of short-term testing. In these cases, it is necessary to determine those aging and deterioration mechanisms that may cause or aggravate the structural failures and to devise test methods specifically tailored to each individual set of conditions.

Nonmetallic Materials

Deterioration of nonmetallic materials is frequently the result of several possible deteriorative mechanisms operating simultaneously and synergistically.

Many investigators active in the study of material deterioration have called attention to the complexity of the relationship that exists. Provided a single failure force or stress can be related to a single failure mode, simple relationships can be developed. For example, Langmuir [3], many years ago, developed a basic relationship between vapor pressure, temperature, and the rate of weight loss per unit area of exposed surface. The relationship works well for metals and other materials, but is not valid for polymers or other organic materials of high molecular weight. For the latter cases, studies by the National Bureau of Standards[4] show that direct experimental data must be collected for each material in question. In correlating the data, some success has been realized by applying a derivation from the classic Clausius-Clapyron equation of thermodynamics, i.e.,

$$\log p = C - \frac{B}{T} \quad ,$$

where p = vapor pressure, C and B are constants, and T = temperature. This relationship is similar to the Arrhenius and Eyring methods of analyzing data, as discussed later in this report.

It should be emphasized at this point that the relationships established to date involve very simple relationships, where one measurable force results in one measurable mode of degradation.

Thomas [5] and Thomas and Gorton [6] have used the Arrhenius relationship to determine the authenticity of an accelerated test to predict the service life of such electronic components as resistors, diodes, transistors, etc. They point out that the Arrhenius relationship can be considered as a first approximation to the more complicated Eyring relationship. The Arrhenius relationship states that "if a true accelerated test is performed at an elevated thermal stress for t' hours, then this is equivalent to t hours of operation at normal stress", and the relationship is given by

$$t = \tau t' \quad .$$

Here

$$\tau = e^{-B(1/T' - \frac{1}{T})}$$

where,

B = a constant
T = thermal stress at t time
T ' = thermal stress at t' time.

In practice, a graph of the logarithm of the rate of degradation versus the reciprocal of temperature ($\frac{1}{T}$) is drawn. If a straight line through the data is obtained, it may be extropolated to an expected service life under any temperature condition.

Many writers have pointed out that this relationship is valid only where a single deterioration mode is present, and is valid for only one deterioration force. If the above conditions are not met, the Arrhenius plot deviates from a straight line, and extrapolation becomes difficult to make. However, if the Arrhenius plot is "true", it is possible to accurately determine the rate of acceleration (τ) from experimental data.

If more than one stress is present, the Arrhenius relationship can be modified to the Eyring relationship by the insertion of appropriate factors into the equation. The rate of acceleration for a deteriorating process involving T and S as two deteriorating forces now becomes

$$\tau = \left(\frac{T'}{T}\right)^{E} \quad ,$$

where,

$$E = \left\{ -\frac{B}{k}\left(\frac{1}{T'} - \frac{1}{T}\right) + \frac{C}{k}\left(\frac{S'}{T'} - \frac{S}{T}\right) + \frac{D}{k}\left(\frac{S'}{T'} - \frac{S}{T}\right) \right\} ,$$

and B, C, D, and k are constants.

The Eyring model is best solved by a graphical process which is described in detail by Thomas and Gorton and several other authors, and is not repeated here.

Lohr, et al., [7] have used the Arrhenius relationship in conjunction with TGA and RGA data to determine the thermal integrity of such polymeric materials as Delrin, P.V.C., and P.M.M.A. Good straight line failure-stress (Arrhenius) curves were obtained, where temperature was the only stress applied, and the results were used to accurately preduct thermal stability of these materials over a period of weeks from a test requireing approximately four hours.

Similarly, the Arrhenius relationship has been used for many years to determine the maximum temperature for which an expected service life of 20,000 hours exposure can be obtained.

Hahn and Nelson [8] have used the Arrhenius relationship to solve regression problems where the observations result in data that are known to lie above or else below some value. Plotting the data on lognormal probability paper results in straight line relationships that can be interpreted. The authors claim that the method can be applied to any regression relationship between an independent variable and a performance function, whether or not the procedure results in data have a normal distribution curve. However, they point out that the method cannot be readily applied when there are more than two independent variables in the regression. In such cases, use of the complicated inverse power law relationship is recommended.

At this point, it is necessary to emphasize that in the exposure of any nonmetallic material to a degrading environment, the usual situation presents more than one deteriorating force, and usually more than one failure mode is present. As pointed out earlier in this report, although the relationship of force or stress to rate of deterioration can be determined individually for each pair of dependent and independent variables, the problem becomes extremely complicated when combinations of these variables are simulataneously present.

It must be recognized that interdependence of stresses and of deterioration mechanisms exist. The presence of synergistic relationships is also well established. For example, degradation of polymeric materials under the combined action of ultraviolet light and presence of moisture exceeds many fold the rate of degradation caused by the presence of either stress alone. If we now introduce thermal variations, the rate changes as some high exponential function – greater than that predicted by the Arrhenius relationship.

In short, the performance of nonmetallic materials under a given set of conditions is determined by a number of stresses operating both independent and interdependently to cause deterioration modes which may or may not be interrelated. The entire process exists in a close balance. If attempts are made to accelerate the failure in order to obtain results in a shorter time period, by intensifying one or more of the stresses, chances are the balance of stresses and modes will be altered, and the results will be undependable. A careful study of all of the stresses and modes must be made for each material, and the relationships must be carefully

established by laboratory data before a method for establishing an expected service life can be selected.

With respect to the three representative components studied, the most critical failure mechanisms for nonmetallic materials appear to be wear and creep of seal lips, valve seats and bearing bushings. Insufficient information was found in the literature for the nonmetallic materials encountered in the representative components to enable accurate life tests to be specified.

Metallic Materials

It does not appear that tests are needed to predict corrosion performance in oxygen, hydrogen, or the space environment because of the low rates of attack under these conditions. The main problem is the corrosion due to the earth environment that the components encounter during storage and preoperation on the launch pad. The high-humidity marine environments are expected to be the most corrosive, and in these cases, the available test methods are not very good for evaluating long-term performance. For example, the ASTM salt spray test (B-117-64) is used extensively to rate materials; however, this test has not been too successful in correlating with in-service performance. The specifications for the 4-inch vent valve contain a combination salt fog plus high humidity-oxygen test (Paragraph 4.3.4.1) that is a modification of Method 509, Procedure 1, MIL-STD-810B. The test consists of one hour exposure to the salt fog from a 1 percent NaCl solution followed by 4 cycles of a heat up to 125 F (52 C) – hold 6 hours – and cool down to 60 F (16 C) in a 95 percent relative humidity, 95 percent oxygen environment. This test appears to be too mild to simulate what might happen in service.

Battelle's own experience at the Long Beach, California, site with fully exposed specimens of sensitized Type 304 stainless steel showed intergranular attack of the material to a depth of 10 mils (0.25 mm) in 6 months' exposure. This material was sensitized at 1200 F (650 C). We have no data for weld sensitized stainless steel under comparable conditions.

Thus, it can be concluded that there is no test available at this time that is capable of evaluating long-term performance under the proposed conditions. In fact, there is no accelerated test to predict performance for, say, one year in a marine atmosphere. It may be possible to design such a test by increasing the temperature, and substituting oxygen for air to take into account the lower solubility of oxygen in aqueous films at the higher temperatures.

Friction and Wear Interfaces

Life tests for mild metal wear, have, in the past, been successfully conducted by assuming that a constant wear rate exists after the surfaces have been worn

in. For nonmetallic materials, however, wear mechanisms are less well understood, and wear rate data relatively scarce. There is no information available on the wear rates of Teflon, Mylar, Halon G-700, etc., in cryogenic environments.

Fouling from wear debris is difficult to predict. If solid debris is generated from metal or ceramic surfaces, knowledge of the distribution of particle size will aid in estimating the probability of fouling of close fitting parts. If the size distribution is such that all particles generated are larger in diameter then is the diametral clearance of a moving part, the particles cannot enter the clearance space and foul it. On the other hand, if all of the particles are much smaller than the clearance, fouling will not occur, unless there is a mechanism for accumulation of debris in the clearance (e.g., imbedding in a soft surface). As the clearance of a close fitting part increases owing to wear, it may reach a critical size for fouling by wear debris from another surface contact. Knowledge of the probable size distribution of wear debris for various sliding material combinations operating in the anticipated environments would be of help in determining critical conditions for fouling.

Discussion

The study of the three representative components indicated the following:

(1) In the majority of cases, low- and high-cycle fatigue due to pressurization cycles, vibrations, and repeated loading are potentially the predominant modes of structural failure; however, the likelihood of such failures is small. Relatively good life test techniques exist for these failure mechanisms.

(2) Prolonged exposure to the space-flight conditions will not cause corrosion failure of the metallic materials specified thus far. The most probable cause of corrosion is a high-humidity marine environment that the component may encounter during handling, transportation, storage, and the period of attachment to the vehicle prior to launch. In this respect, corrosion can be minimized by materials selection during the design phase.

(3) The principal time-dependent failure modes resulting from contacting surfaces in the mechanical components studied appear to be wear-induced leakage of seal lips, fouling and seizure of close fitting moving parts by wear-generated debris, and creep or cold flow of elastomeric materials used as valve seats, bearings, and seals. Adequate life test techniques for wear and creep of nonmetallic materials do not exist in the literature.

Careful weighing of the various design, materials, and environmental factors along with the performance requirements, indicates that the major life critical components in these valves are the nonmetallic materials. Furthermore it appears that creep and wear of these components represent the most probable degradative mechanisms. Laboratory investigations were, therefore, undertaken to develop life test techniques for nonmetallic wear and creep.

In order to determine the long-term effects of creep and wear, and to determine the best configuration for accellerated tests, it is necessary to study the two processes in detail for the actual materials involved and to carry out experiments and tests designed to determine long-term behavior and the stress limits for a particular degradative mechanism. Long-term behavior may be determined by the extrapolation of short-term data, by the increase in level of a specific variable to effect acceleration, or by some combination of the two. The creep and wear studies were undertaken to determine which of the two methods is appropriate.

CREEP OF NONMETALLIC MATERIALS

Summary of Creep Literature

A brief literature survey was conducted on the cryogenic properties of polytetrafluoroethylene (PTFE) (e.g., Teflon) and of polyethylene terephthalate (PET) (e.g., Mylar) to determine if the type of rheological data needed for accelerated tests are readily available. The literature on these materials is fairly extensive; however, the data presented are not of a directly applicable nature. Rather, the data are useful in more accurately defining the nature of the problems that are likely to be encountered in making valid service-life predictions.

The low-temperature properties of both PTFE and PET are very complex. At certain temperature levels, the rheological properties of these materials go through transitions, and the rheological properties of the materials change dramatically with temperature (or equivalent time). Several of the factors affecting the intensity of the transition are crystallinity of the material, structural anisotropy, and molecular weight. No systematic study of the effect of molecular weight on the transitions appears to exist. At extremely low temperatures (<100 K) the effects of crystallinity and orientation almost disappear. At room temperature, however, these effects are pronounced and must be considered.

Cryogenic Properties of PTFE

The rheological properties of PTFE have been measured at temperatures as low as 4.2 K (liquid He). The data in the literature are mostly isochronal measurements, i.e., fixed deformation conditions with varying temperature. Usually, the measurements were performed in a torsional pendulum-type apparatus at a fixed frequency.

McCrum[9] examined the properties of PTFE over wide ranges of temperature (4.2-600 K). He found that the logarithmic decrement undergoes marked changes at about 176 K, 300 K, and 400 K. The logarithmic decrement is related to the ratio of viscous to elastic deformation in the material. The lower the decrement, the more elastic the response. The type of response being observed is sketched in Figure 8.

While the decrement changes about ninefold in the 176 K transition, the transitions are generally not so large at the other temperatures. The transition at 400 K is far above any anticipated operating conditions. The transition at 300 K (23 C) is at approximately room temperature and may pose some problems in superimposing data for extrapolation.

Other experimenters [10-16] have observed the same or similar transitions. In the literature examined, the transitions identified are in the neighborhood of

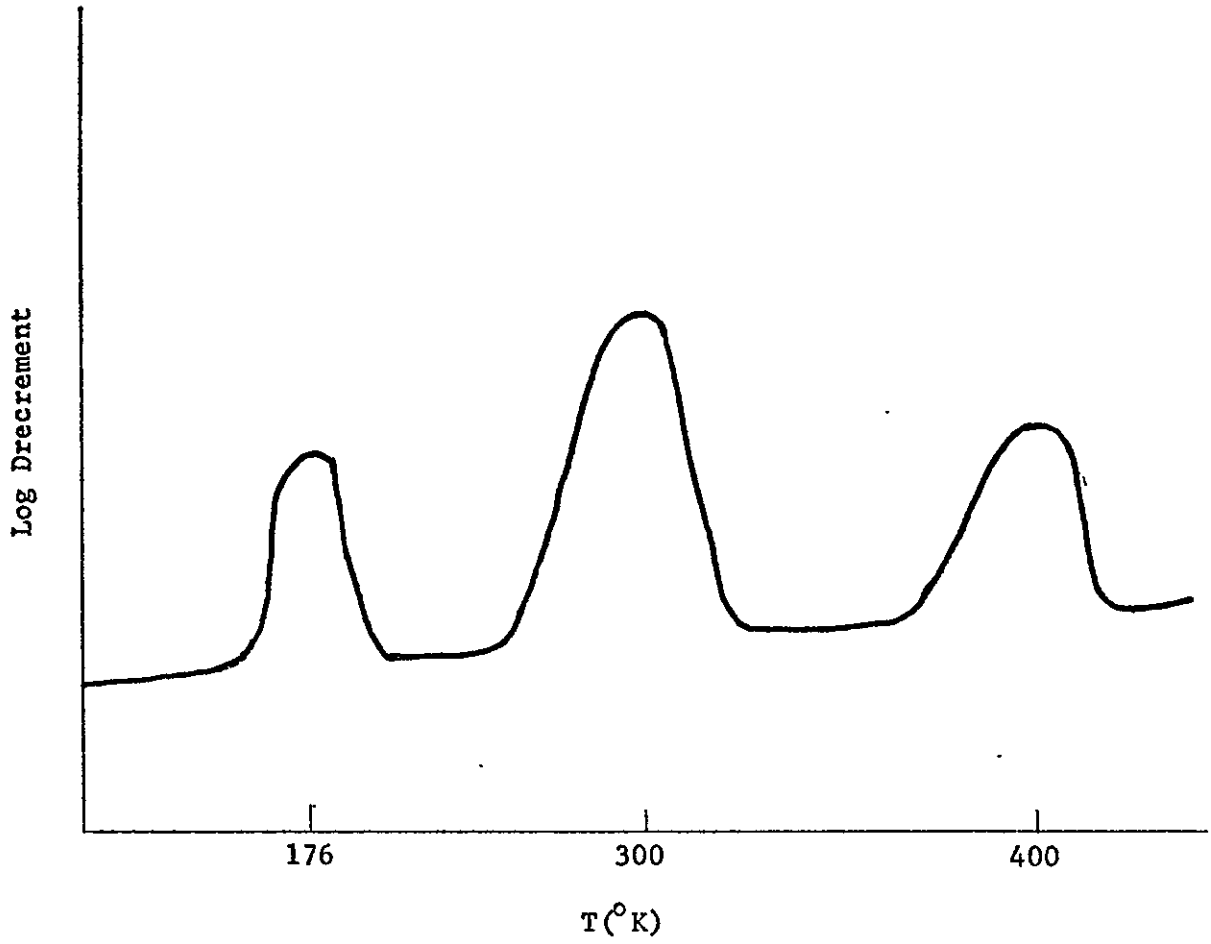

FIGURE 8. LOG DRECREMENT AS A FUNCTION OF TEMPERATURE FOR TEFLON

400-360 K, 310-290 K, and 182-176 K. The temperatures are not exact due to slight differences in material properties from one test to another. Also, it has been reported [14] that each observed transition is actually a closely-spaced series of transitions smeared out by the measurement methods. These transitions have been associated with changes in the solid structure at the specific temperatures.

The degree of crystallinity affects the rheological response of the material. Several authors [9, 12] have found increased crystallinity intensifies the transition at room temperature and depresses the transition at 176 K. More important, however, is the observation that the modulus and logarithmic decrement appear to be fairly independent of crystallinity [9, 14] at temperatures below ≈100 K (in the range of interest). This is beneficial for this study, since it appears that the effect of crystallinity is of concern only at the room-temperature conditions, and not under the use conditions (<100 K).

There are wide variations in the rheological properties of PTFE. In the literature examined, approximately 12 different domestic and foreign PTFE compounds are identified. The literature lists 4 different Teflons made by Du Pont, Nos. 1, 5, 6, and 7. It is presumed that Nos. 2, 3, and 4 also exist, but this has not been verified with Du Pont. The differences in the Du Pont Teflons listed by Tobolsky, et al. [16], are in the molcular weights. The crystalline structure of any given PTFE can be altered by the heat treatment. Quenching from the melt leads to an amorphous polymer, while annealing leads to varying degrees of crystallinity.

Some authors [10, 13, 14, 16] Have studied the rheological properties at constant temperature over wide frequency or time scales and attempted time-temperature superposition to extend the range of their data. In some of the studies [10, 15], temperature anomalies were observed around room temperature. That is, the data were not monatonic with regard to temperature, and the superposition failed. The data could only be superimposed over more limited temperature ranges. Nagamatsu, et al. [10], for example, found that superposition worked for stress-relaxation data up to about 293 K, but they could not include the data above that temperature. In fact, they used the breakpoint to locate the transition. In other studies [9, 12, 13], no such anomalies were observed, and the data could be extended over a wide time scale (>>10 years). There is no general agreement on the presence of the anomalies, however, we should be aware of their possible presence.

Cryogenic Properties of PET

The literature for PET is as equally extensive as is that for PTFE. Transitions have been identified [17, 23] at approximately 340 K, 200-230 K, 180-195 K, and 25-60 K. The primary trnasitions are the first two, the one at 340 K being the glass-transition temperature of the material. The remaining ones are secondary transitions of greatly reduced intensity.

In the literature, only one sample was clearly identified [18], a Du Pont PET having an average molecular weight of 15,000. As with PTFE, most of the experimental studies have been isochromal in nature. The transitions are similar to those of PTFE in that the logarithmic decrement goes through a maximum.

Several studies [13, 20, 22] have shown that intensity of the transitions decreases as the crystallinity increases, but the location of the peak on the temperature scale is roughly unchanged. The presence of solvents, such as water, benzene, nitrobenzene, and dioxane, remaining in the PET caused the transition to broaden and shift in temperature.

Orientation [18] can affect the properties of PET, shifting the transition to slightly higher temperatures and broadening the temperature range over which the transition occurs. The viscoelastic properties were measured for samples taken at different angles to the prevailing orientation. It was found that samples cut at 45 degrees to the orientation axis had substantially different transition amplitude than those either parallel or normal to the orientation axis.

The effects of orientation and crystallinity on the rheological properties appear to be negligible at temperatures below ≈100 K. The effect of the angle on the orientation direction at which the sample is cut also diminishes as the temperature is reduced.

Tajiri, et al. [21], studied the isothermal frequency response of several PET samples with various degrees of crystallinity. They tried time-temperature superposition to construct master curves at 213 K and observed that there was considerable scatter in the data at high frequencies, indicating that simple time-temperature superposition did not strictly apply. Data determined as low as about 100 K were presented.

Other Materials

The behavior described above for PTFE and PET, i.e., transitions in rheological properties at certain temperatures is common in many materials. Of the other materials of interest to the program, polyethylene [14, 24] show relaxation effects at cryogenic temperatures. Polychlorotrifluoroethylene has a transition at about 150 K.

CREEP TESTS AND THE PREDICTION OF LONG-TERM CREEP BEHAVIOR

Experimental Procedures

Two sets of experiments were conducted. In one set, compressive creep tests were performed to establish the creep properties of PTFE relative to space valve applications. In the other set, microhardness indenter-type tests were evaluated as a possible short-term method of determining creep properties of materials.

Creep Measurements. A relatively short-term program was carried out at BCL to evaluate the creep properties of polytetrafluoroethylene (PTFE), one of the materials used in the valves. A series of six compressive creep tests were performed to evaluate the effects of temperature and stress on the creep properties of PTFE. Halon G-700, a polytetrafluoroethylene, manufactured by Allied Chemicals, was used for these tests, which were conducted at four temperatures and three stress levels. The experimental conditions are described in Table 8.

TABLE 8. EXPERIMENTAL CONDITIONS FOR COMPRESSIVE CREEP TESTS (a)

Sample	Temp	Stress (b)
1	73	300
2	73	600
3	85	600
4	100	600
5	125	600
6	73	1200

(a) Samples were 0.25 inch (6.35 mm) diameter x 0.75 inch (19.05 mm) long circular cylinders.
(b) Initial stress in psi.

The compressive creep tests were carried out in a compressive cage type apparatus, shown schematically in Figure 9. By applying the weights as shown, plate A is pulled downward, while plate B is rigidly supported. This arrangement applies a compressive stress to the sample. The magnitude of the stress is determined by the amount of weight used and the cross-sectional area of the sample. The separation between plates A and B at time (t) is the height of the sample at that time. The plate separation was monitored by a moving slide. The zero position of the slide was marked prior to the application of the stress. The movement of the slide, which corresponds to the movement of plate A, was measured optically.

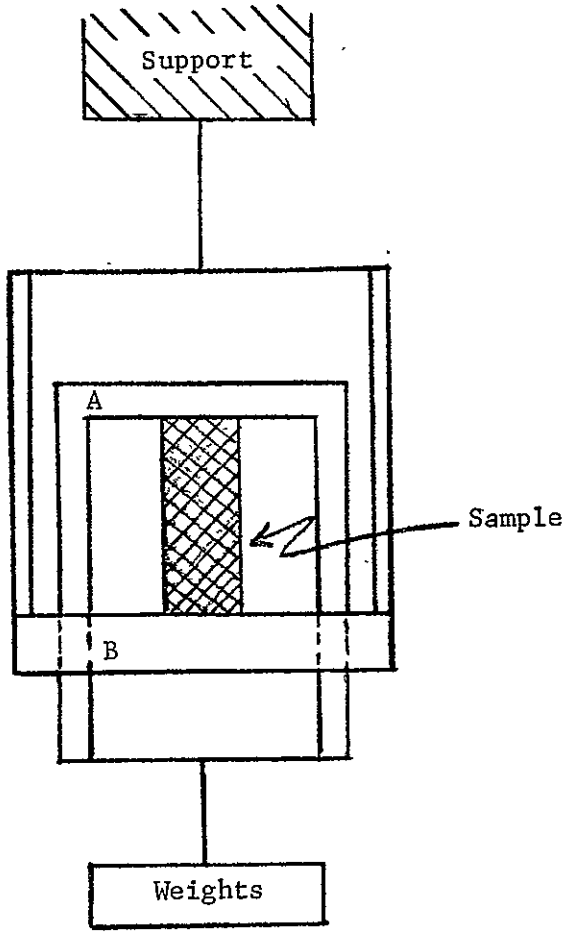

FIGURE 9. SCHEMATIC OF COMPRESSIVE CREEP APPARATUS

The data can be translated into a term known as creep compliance, which is determined from measurements of the change in height with time of a sample under load and is the ratio of the strain to the stress.

The strain is defined by

$$\epsilon = \ln\left[H/H_0\right] \quad \text{or} \quad \epsilon = \ln\left[1 - \Delta H/H_0\right] \tag{1}$$

where H is the height at time t, H_0 is the initial height, and ΔH is H_0-H.

The stress decreases slightly with time due to the change in radius caused by the strain. The instantaneous stress (assuming constant density) is expressed by

$$\sigma = \sigma_0 \left[1 - \frac{\Delta H}{H_0}\right] \tag{2}$$

where σ_0 is the initial stress. The compressive creep compliance as a function of time ($D_{(t)}$) can then be calculated from Equations (1) and (2) and is given by

$$D(t) = \epsilon/\sigma_0 \left[1 - \frac{\Delta H}{H_0}\right] . \tag{3}$$

The results of the creep tests are given in Appendix A. The stresses and strains listed in the tables are negative. By convention a stress acting in compression is given a negative sign, and the negative strains come from the fact that the length of the sample decreases with time.

Microhardness Tests. In the microhardness test, the indentation steel ball into a surface is measured (Wallace Microhardness Tester). If the indentation over a period of time is monitored, the creep compliance can be determined. The ball is first brought into contact with the surface to be tested. The desired load is then applied to the indentor and the indentation is monitored by the displacement of a capacitor element.

Two indentors were used in these tests. The first was a standard steel ball indentor, 1/64-inch (0.397 mm) diameter, supplied with the equipment. The second indentor was constructed at BCL and was a 1/64-inch diameter rod with ≈0.1-inch (2.54 mm) radius crown on the end. The second indentor was used to examine the effect of a different radius of curvature on the indentation tests. The microhardness tests were carried out at several different loads, from 35 to 315 grams, and the results are given in Appendix B.

Results and Discussion

Strain Versus Time. When a compliant polymeric material is subjected to a constant stress, the material will continue to deform with time. In the case of

creep, the deformation proceeds relatively rapidly at first and then at progressively slower rates. Figure 10 shows a typical representation of the creep behavior of an uncrosslinked polymer subjected to a constant stress. At time t = 0, a stress σ is applied to the specimen and the stress remains constant up to time $t = t_1$, when the load is removed.

When the stress σ is applied at t = 0, the strain increases instantly (or almost so) to a level ϵ_0 shown in Figure 10. This initial deformation is purely elastic and is recovered instantly when the stress is removed at time t_1. As the time under load increases, the strain increases, but the rate of increase (i.e., slope of the line) decreases with time until a steady state is reached (i.e., the slope of the line is constant). When the slope of the strain versus time curve is constant, the deformation is primarily nonrecoverable viscous flow.

When the applied stress σ is removed at time t_1, the sample instantly recovers the initial elastic deformation ϵ_0. Following the initial elastic recovery, a time-dependent recovery takes place and the strain in the sample approaches a limiting value ϵ_{NR} at time t_2. The value of t_2 may, however, be very large, depending on the memory characteristics of the material. The limiting strain ϵ_{NR} is the nonrecoverable deformation of the material or "permanent set", and for purely viscoelastic materials is related to the properties of the material by

$$\epsilon_{NR} = \sigma t_1 / \eta \tag{4}$$

where σ is the stress, t_1 is the time under stress, and η is the viscosity. The nonrecoverable deformation at any time ti is given by

$$\epsilon_{NR}(t) = \sigma t/\eta \tag{5}$$

where t can vary from 0 and t_1.

The strain, therefore, contains three basic components: an initial elastic strain ϵ_0; a time-dependent viscoelastic strain ϵ_{VE}; and a viscous nonrecoverable strain $\epsilon_{NR} = \sigma t/\eta$,

$$\epsilon(t) = \epsilon_0 + \epsilon_{VE}(t) + \sigma t/\eta \quad . \tag{6}$$

The strain, $\epsilon(t)$, versus time data obtained during the creep tests are presented in Figures 11 and 12. Only data up to the removal of the stress have been included. These strain-time curves show the same general trend as that depicted in Figure 10, although there is some scatter in the data.

The data in Figure 11 show that, in general, as the temperature increases, the strain at a given time t increases. Also, the slope of the curve increases as the temperature increases. The increasing slope reflects the decrease in viscosity as the temperature rises. The data presented at 73 F (23 C) are anomalously high, i.e., the strain is greater at 73 F than it is at 85 F (29 C). Several authors[10,26] have reported that at approximately room temperature, PTFE can go through a transition. The properties at the transition temperature can be

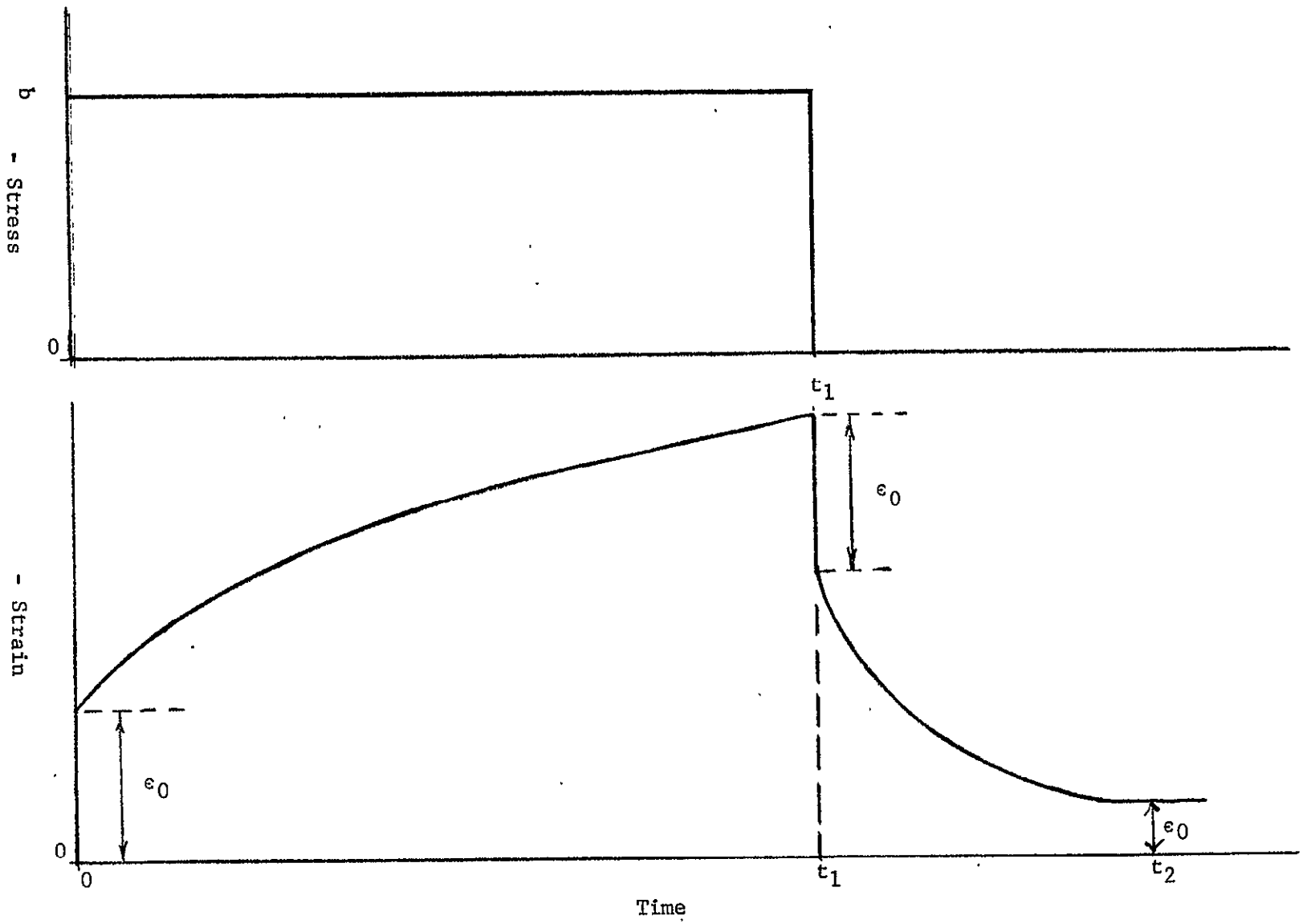

FIGURE 10. TYPICAL CREEP BEHAVIOR OF AN UNCROSSLINKED POLYMER (COMPRESSION)

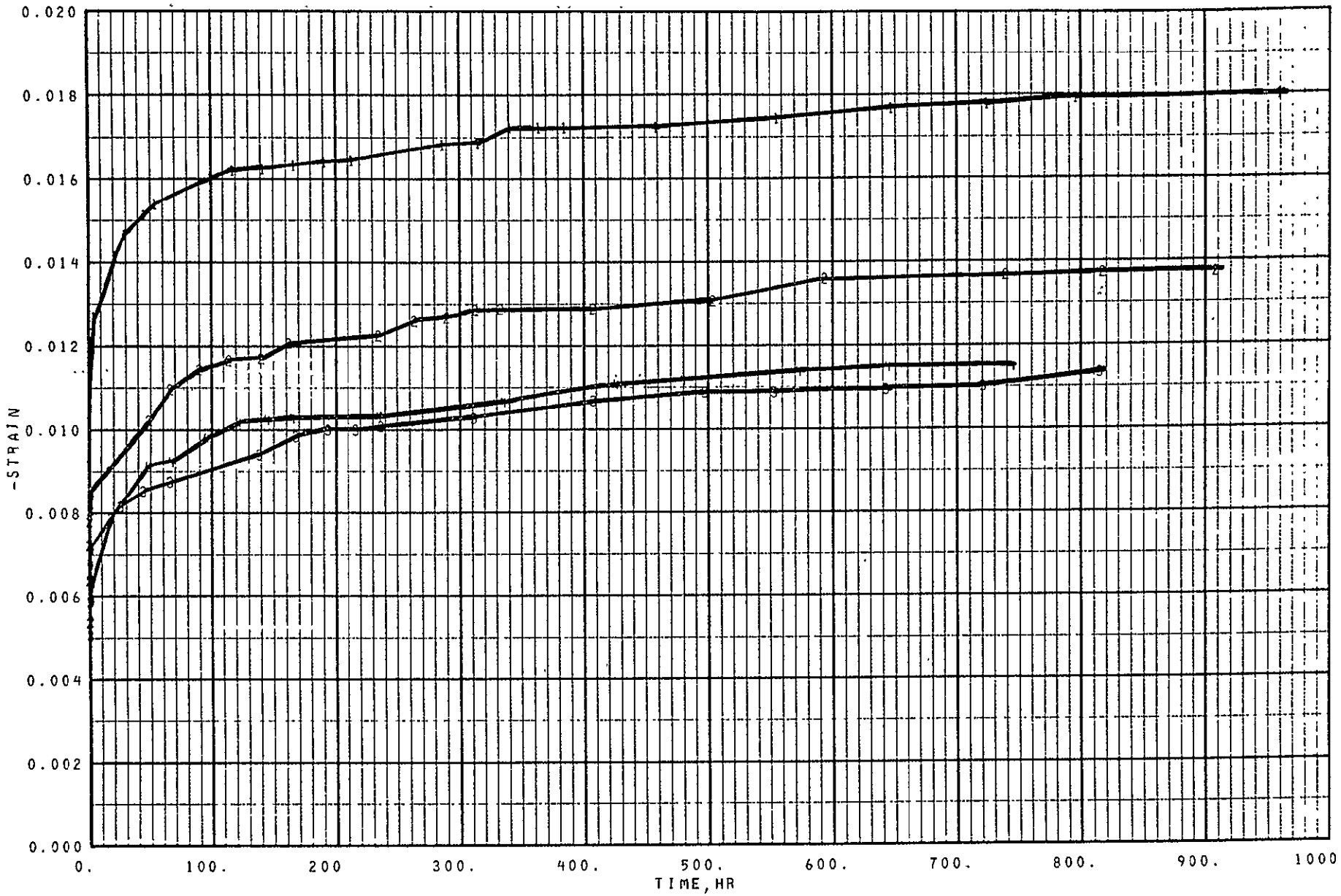

FIGURE 11. STRAIN DEPENDENCE OF HALON® G-700, AS A FUNCTION OF TIME AND TEMPERATURE, 600 PSI STRESS

(1) Temp = 128 F
(2) Temp = 100 F
(3) Temp = 85 F
(4) Temp = 73 F

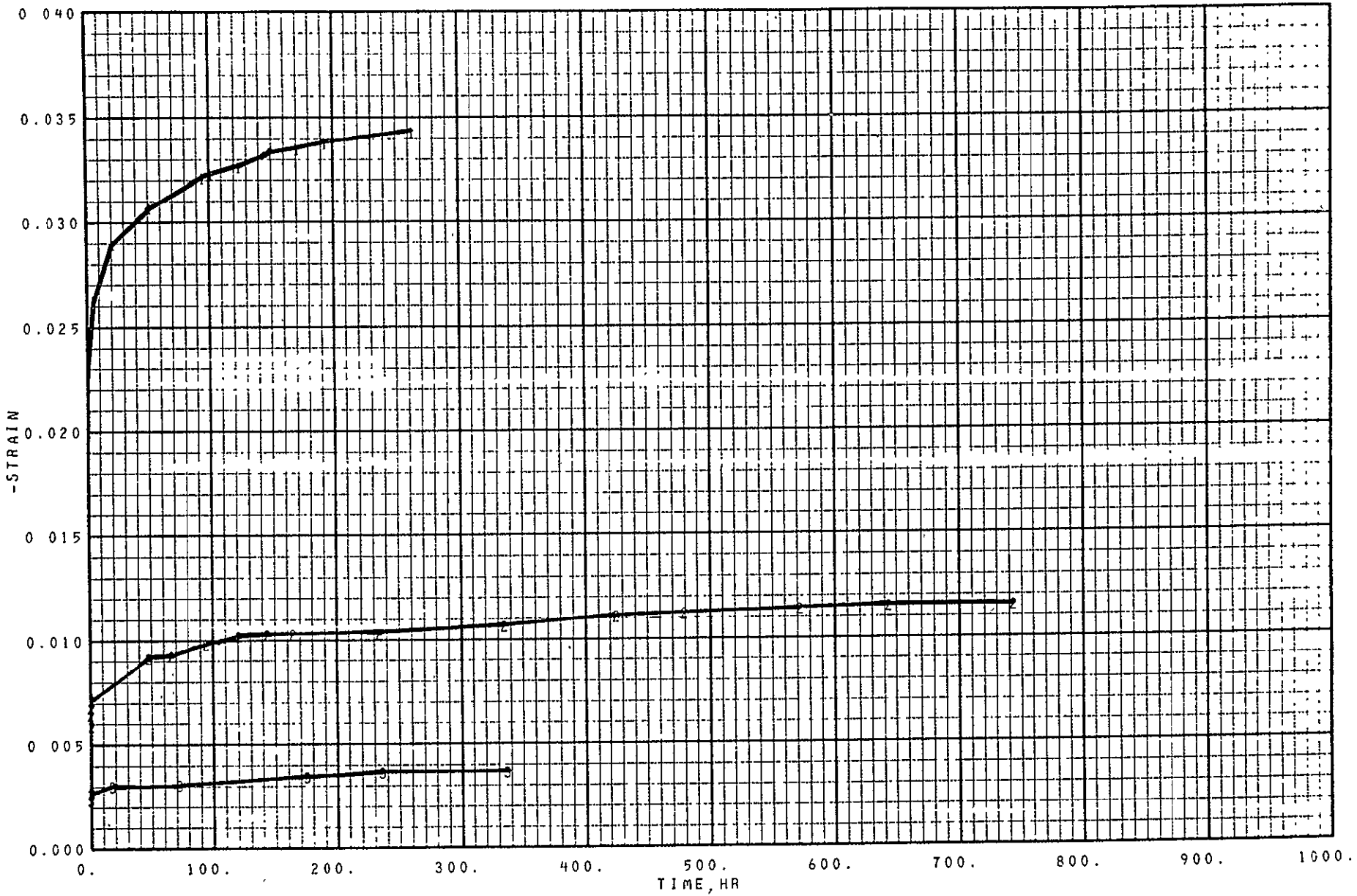

FIGURE 12. STRAIN DEPENDENCE OF HALON® G-700 AS A FUNCTION OF TIME AND STRESS AT 73 F

(1) Stress = 1200 psi
(2) Stress = 600 psi
(3) Stress = 300 psi

significantly different from those at temperatures just above or below the transition temperature. The data presented in these references show that the initial strains follow a consistent temperature dependence (i.e., the initial strain increases with increasing temperature). The data obtained in the present study do not follow this trend. While a room-temperature transition might account for some of the unusual behavior, it appears that other factors may also be involved. The unusual behavior at room temperature might have been caused by a shock during loading of the sample, differences in the machining conditions, etc. It is important for future tests that care be taken to give all the samples the same history.

The data presented in Figure 12 show that the strain does not increase in direct proportion to the applied stress. For example, increasing the stress from 300 to 1200 psi (2.1 to 8.4 MN/m^2 – a factor of 4) increases the strain from $\approx$ -0.0032 to -0.0322 at 100 hours (a factor of $\approx$ 10). This indicates that the strain is not linearly proportional to the applied stress. At the stresses used in this study, the material does not behave like a linear viscoelastic fluid and the material properties are stress-dependent. Any life test methodology must consider this stress dependence.

Creep Compliance: Time-Temperature and Time-Stress Superposition. The material property associated with the cold flow of polymer materials is the creep compliance D(t). The compliance, calculated from Equation (3), reflects the total deformation of the sample at any time. Figure 13 shows the compliance behavior at several temperatures. The data show that as the temperature increases, the compliance increases (i.e., the material becomes more deformable). Also, the curves at different temperatures appear very similar in shape but displaced on the time axis. The amount of horizontal shift required is termed the "shift factor", α_T. The shift factors which depend on the temperature have been determined for the data at 85, 100, and 125 F,* and are given in Table 9.

TABLE 9. SHIFT FACTORS FOR HALON® G-700

Temperature		α_T(a)
F	C	
85	29.4	1.0
100	37.8	6.75×10^{-2}
125	51.7	7.95×10^{-4}

(a) Data at 73 F excluded.

*29.4, 37.8, and 51.7 C.

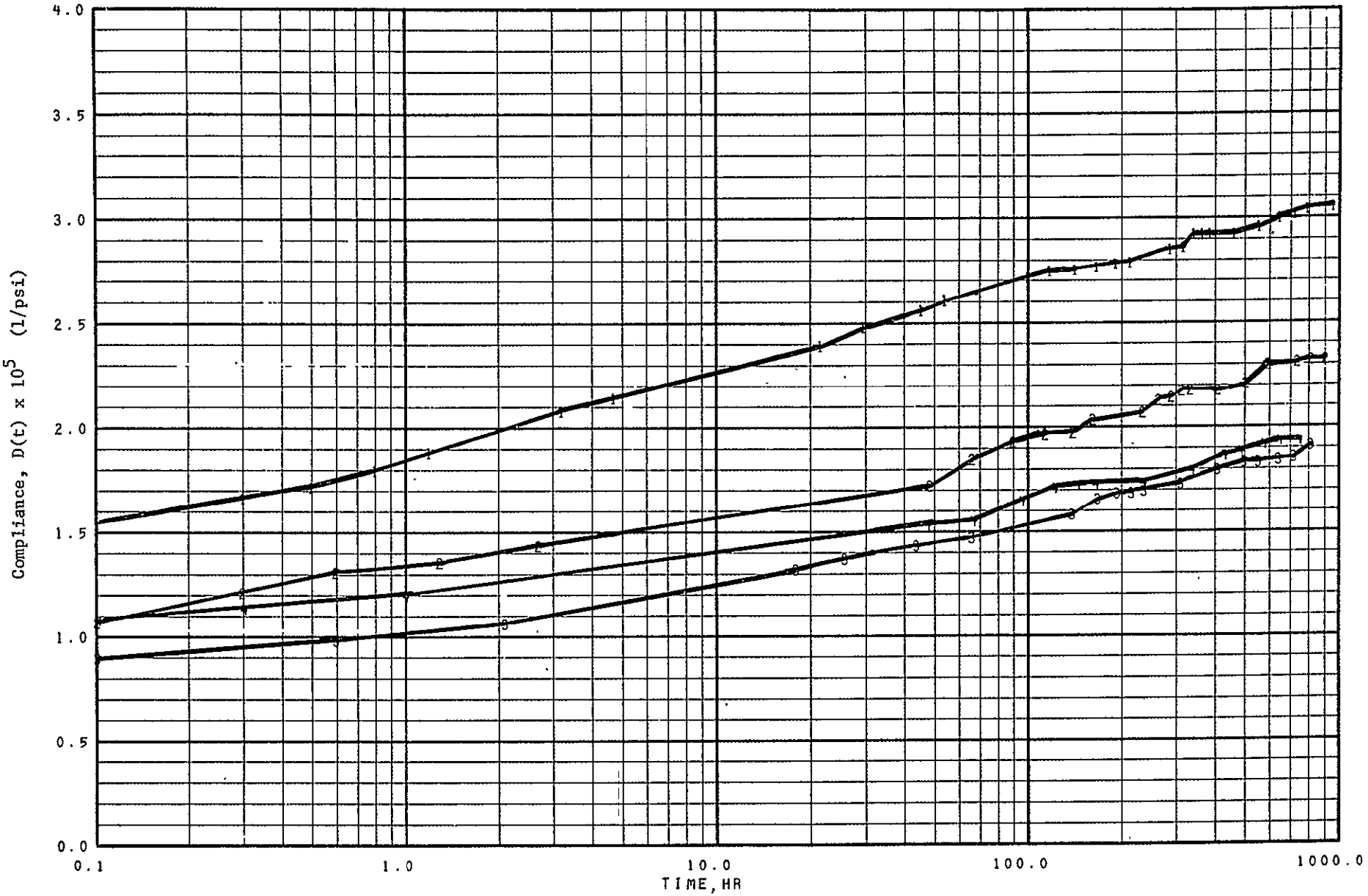

FIGURE 13. CREEP COMPLIANCE OF HALON® G-700 AT 600 PSI

(1) Temp = 125 F
(2) Temp = 100 F
(3) Temp = 85 F
(4) Temp = 73 F

A composite curve of compliance versus time at 85 F (29.4 C) can be constructed using the following coordinates:

$$D^*(t) = D(t)\left[\frac{T + 460}{85 + 460}\right] \tag{7}$$

$$t^* = t/\alpha_T \quad , \tag{8}$$

and such a curve is presented in Figure 14. The data, when superimposed, cover a larger range of times than the originally measured data.

The composite curve given in Figure 14 and the shift factors in Table 9 can be useful in several ways. If, for example, the valves containing elements made from Halon® G-700 are stored under a load of 600 psi at a temperature of 85 F for 2 years, the strain in the Halon® components can be determined from the composite curve directly. The compliance is taken from the curve at t = 2 years (1.75×10^4 hours), and the strain is determined via Equation (3). The strain determined using Figure 14 includes recoverable and nonrecoverable portions.

The shift factors can be useful in determining accelerated test procedures. For the example described above, the 2-year storage can be simulated by accelerated testing at higher temperatures if the length of time at the higher temperature equivalent to 2 years at 85 F is known. The equivalent time at the higher temperature can be determined from the shift factors and Equation (8). The equivalent time at 125 F is given by

$$t_{85} = \frac{t_{125}}{7.95 \times 10^{-4}}$$

$$\therefore\ t_{125} = t_{85} \times 7.95 \times 10^{-4} = 13.4 \text{ hours} \quad .$$

The 2-year storage condition at 85 F (29.4 C) can be simulated by testing for 13.4 hours at 125 F (51.7 C). The equivalent time at 100 F (37.8 C) is 1180 hours. It can be seen, therefore, that accelerated test conditions can be derived from the time-temperature shift factors.

Figure 15 shows the effect of stress on the creep compliance. As the stress increases, the compliance also increases. The compliance curves are similar in general shape but displaced on the time axis. Urzhumtsev and Maksimov[27] have presented a time-stress superposition theory similar to the widely used time-temperature superposition principle described above. The data in Figure 15 were shifted horizontally only to form the composite curve given in Figure 16 and the time-stress shift factors α_σ are given in Table 10.

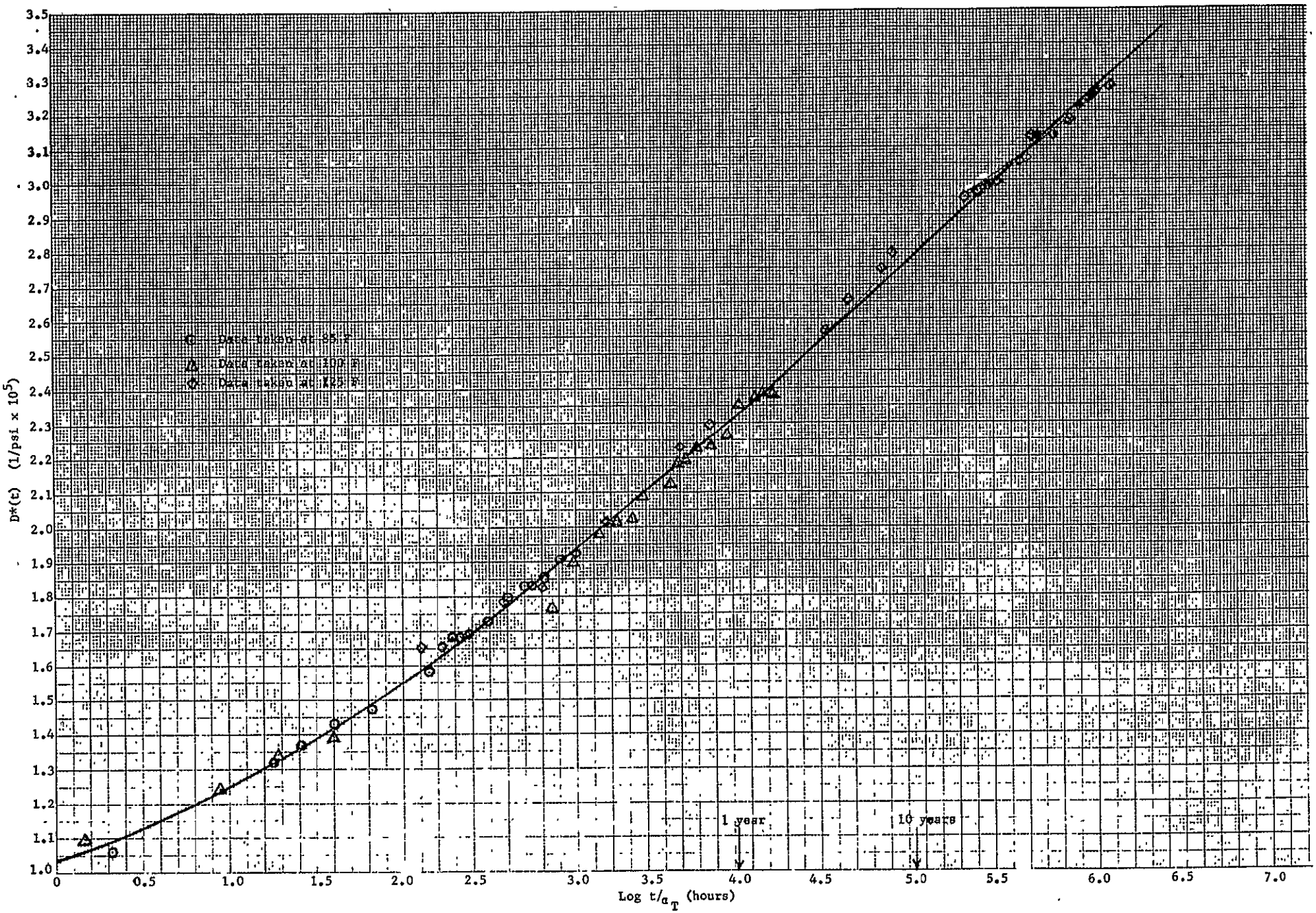

FIGURE 14. CREEP COMPLIANCE AT 85 F (600 psi)

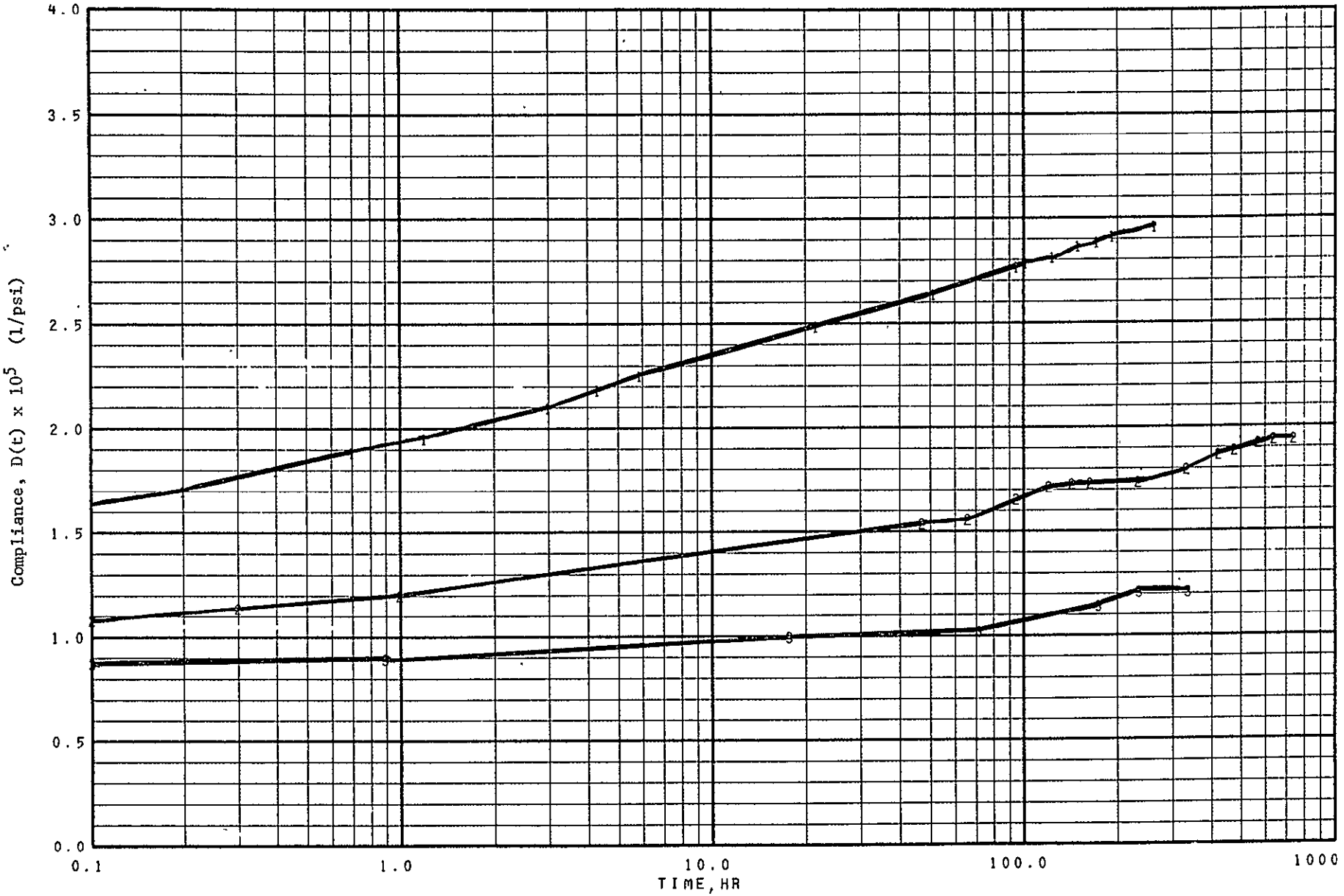

FIGURE 15. CREEP COMPLIANCE OF HALON^R G-700 AT 73 F

(1) Stress = 1200 psi (3) Stress = 300 psi
(2) Stress = 600 psi

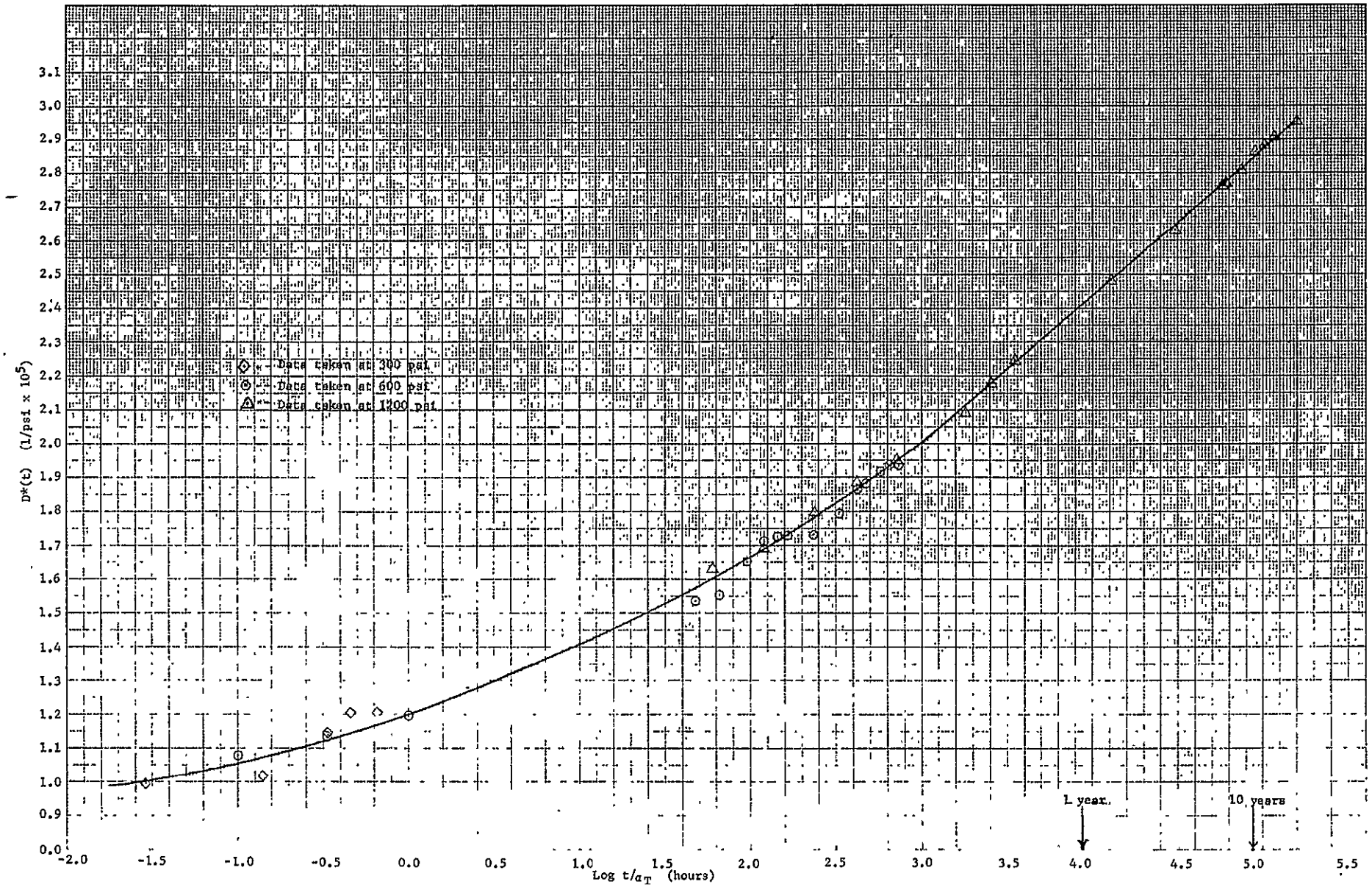

FIGURE 16. CREEP COMPLIANCE AT 600 PSI (73 F)

TABLE 10. TIME-STRESS SHIFT FACTOR

Stress	Shift Factor
300	5.14×10^{2}
600	1.0
1200	1.66×10^{-3}

The results presented in Table 10 can be used to predict long-term deformation at room-temperature conditions or to devise other accelerated test procedures. For example, if a test procedure designed to simulate 4 years under 600 psi (4.14 MN/m^2) stress is desired, the time-stress shift factor a_σ at 1200 psi is 1.66×10^{-3}. The required test time at 1200 psi (8.4 MN/m^2) is 4 years times 1.66×10^{-3}, or 58 hours. It should be noted that these results give the total deformation at any time, and that the permanent set will be some fraction of that amount.

There have been other time-stress superposition theories discussed in the literature, such as those by Brody[28], Bergan and Wolsternholme[29], and Cessna[30]. No generally accepted method has been developed for time-stress superposition. The method outlined above, of only a horizontal shift, may be less accurate for other materials or different stresses or stress ranges, especially if severe nonlinear effects come into play. If a valid time-stress superposition method is determined for a material under consideration, a second independent accelerated test procedure can be devised to complement a time-temperature devised procedure and possibly increase the reliability of the life tests.

Permanent Set During the Cold Flow of Polymers. In the cold flow or creep of polymers, the deformation is the sum of three terms: (a) the initial elastic deformation; (b) the time-dependent recoverable deformation; and (c) the nonrecoverable deformation or permanent set (P.S.). The time-temperature and time-stress superpositions discussed previously were presented for the total creep compliance D(t), and could have been equally well discussed for the time-dependent recoverable compliance $\Psi(t)$. The permanent set, however, may be determined directly from strain versus time data via the viscosity for purely viscoelastic materials.

The viscosity of the polymer may be determined in either of two ways. First, by Equation (6),

$$\epsilon(t) = \epsilon_0 + \epsilon_{VE}(t) + \sigma t/\eta \tag{6}$$

when the slope of the strain-time curve becomes constant, the slope is equal to the stress divided by the viscosity. This method requires fairly accurate strain-time

data with a minimum of scatter for accurate determination of the slope of the line. This method was not used in this study due to the scatter in the data (see Figures 14 and 13).

The second method utilizes the data obtained after the stress is removed. The nonrecoverable strain can be related to the viscosity via Equation (4)

$$\epsilon_{NR} = \sigma t_1/\eta \quad . \tag{4}$$

The viscosities were calculated using Equation (4) and are presented in Table 11. The strain was measured during the 24 hours after the stress was removed. The ultimate nonrecoverable deformation was determined by extrapolation to infinite time.

Except for the data point at 73 F (22.8 C), the viscosity increases as the temperature decreases. The low viscosity at 73 F probably is the result of the unusually high strain as discussed previously. The effect of stress is unusual in that the viscosity is more sensitive to changes in stress than to changes in temperature. The unusual stress dependence may be due to either or both of two factors: First, if insufficient time was allowed for complete recovery, the extrapolation would lead to erroneous results. Second, and probably more important, the assumption of a purely viscoelastic fluid may not be valid. This could come about if the material exhibits a plastic yield at relatively low strains. If this is the case, the nonrecoverable deformation will be the sum of the plastic yield and the viscous flow.

TABLE 11. VISCOSITY OF HALON® G-700

Temperature, F	Stress, psi	Viscosity[a] (poise) x 10^{16}
125	600	1.64
100	600	2.17
85	600	2.80
73	600	2.41
73	1200	0.84
73	300	5.71

(a) Viscosity calculated from Equation (4).

If the viscosity of the material is known under a variety of temperature and stress conditions, the permanent set can be calculated a priori. For the case of a constant temperature and applied stress, the permanent set (P.S.) for purely viscoelastic materials is given by Equation (5)

$$P.S. = \epsilon_{NR}(t) = \sigma t/\eta \quad . \tag{5}$$

In the more general case of time-dependent stress and temperature, and consequently time-dependent viscosity, the permanent set can be represented by

$$P.S. = \int_0^t \frac{\sigma(S)}{\eta(\sigma(S), T(S))}\, dS \tag{9}$$

where T is the temperature.

When the material exhibits plastic yield behavior, Equation (9) must be modified to incorporate the yield strains. Equation (9) would then become

$$P.S. = \Sigma\epsilon_y(\sigma, T) + \int_0^t \frac{\sigma(S)}{\eta(\sigma(S), T(S))}\, dS \tag{9a}$$

where ϵ_y is the yield strain, and $\Sigma\epsilon_y$ is the sum of the yield strain introduced over the time period $0 \rightarrow t$. Equations (9) and (9a) are essentially forms of Miner's Law of Linear Cumulative Damage[31] which states that the damage (or in this case permanent set) at any time t is the linear sum of the damage up to that time. An example of the use of Equation (9) is presented in Appendix D.

It can be seen that the problem of evaluating the permanent set in nonmetallic components can be approached via the deformation properties of the material. The viscosity of purely viscoelastic materials can be determined from relatively short-term creep experiments by the two calculation procedures described previously. The length of the creep tests required will be a function of the temperature, stress, accuracy of the measuring equipment, and extent of extrapolation required to predict service life. Where materials have plastic yield behavior, more extensive tests must be carried out to separate the yield and viscous behavior, since both contribute to the permanent set in different manners. The exact test procedure used to evaluate the permanent set needs to be tailored to the material. A procedure that will work for one material may not work for another. Further work is needed to refine the method of viscosity determination and to elucidate the plastic yield behavior of valve component materials at low strains.

Microhardness Tests. When a steel ball is placed on a viscoelastic surface, and a load is applied, the ball indents the surface and the indentation will increase with time. The progressive indentation with time is similar to the increase in strain with time in a creep measurement. Figures 17 and 18 present the indentation versus time data for the standard and modified ball indentors, respectively, and show several interesting points:

(1) As the load increases, the indentation increases. The increase in indentation is expected; however, the rate of increase is different for the standard and modified indentors. For the standard indentor, penetration increases approximately

FIGURE 17. EFFECT OF TIME AND LOAD ON INDENTATION

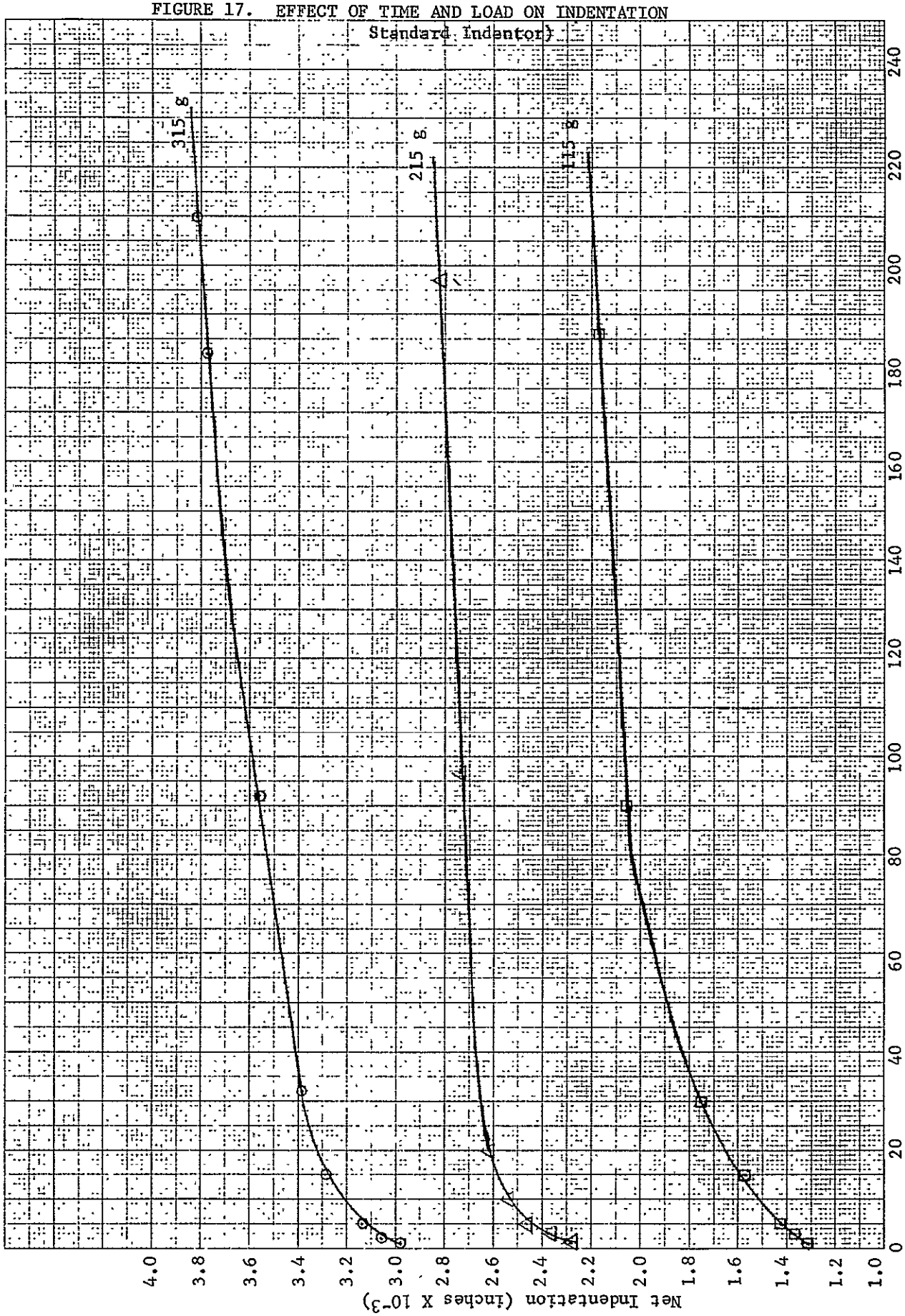

FIGURE 18. EFFECT OF TIME AND LOAD ON INDENTATION
(Modified Indentor)

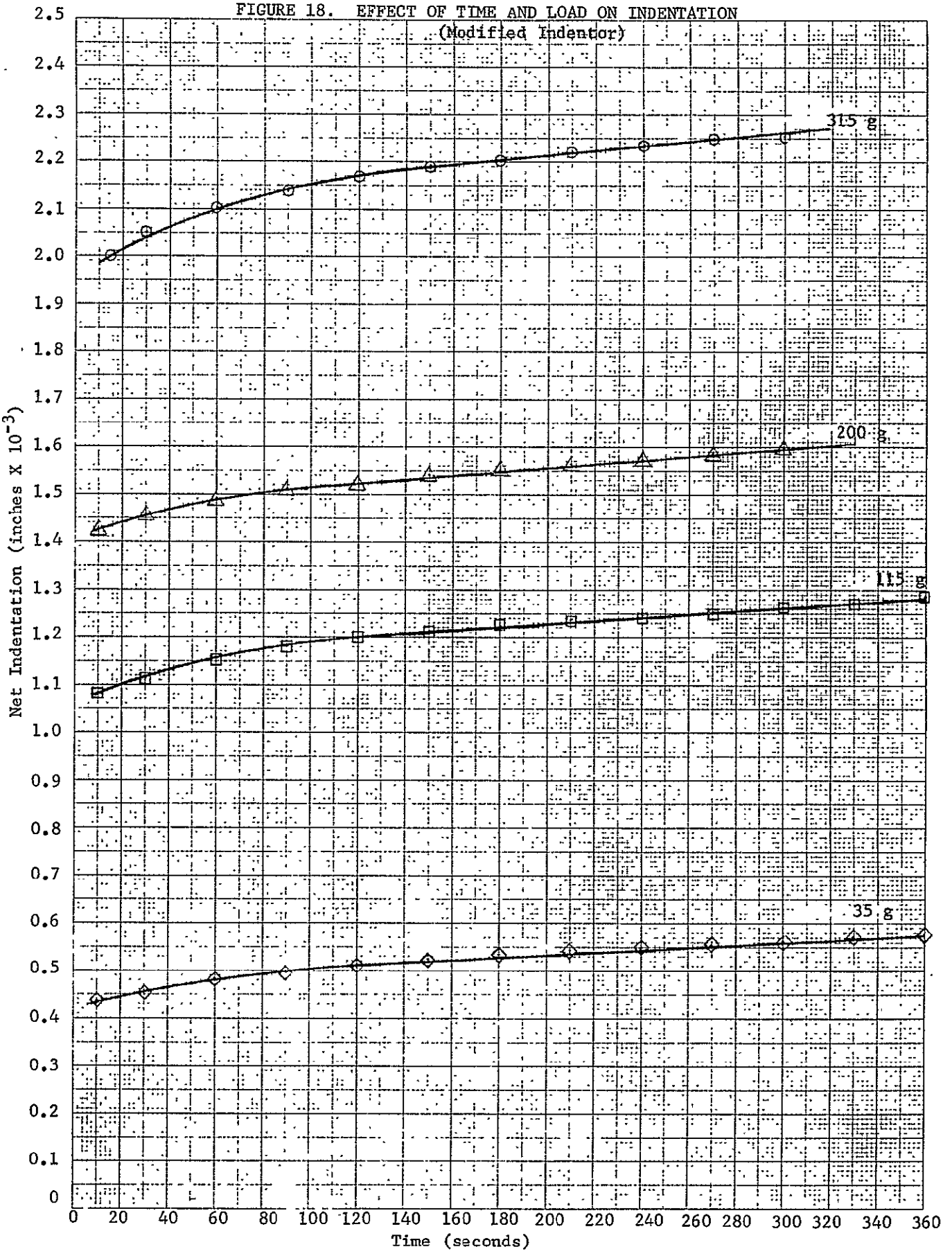

linearly with increasing load. For the modified indentor, penetration also increases with load but at a slower rate. This is probably related to the difference in geometry of the two indentors.

(2) The indentation is greater for the standard indentor than for the modified one. By effectively increasing the radius of the indentor, the penetration decreases, as expected. At the same load and penetration for the two indentors, the load is distributed over a larger area for the larger radius. Therefore, the stress is lower for the larger radius indentor.

Several workers[32, 33] have studied the problem of surface indentation of a viscoelastic material and, using a simple linear viscoelastic model, derived the following relationship:

$$J_c(t) = 16 \sqrt{R}\ (\alpha(t))^{3/2}/3P_0 \qquad (10)$$

where $J_c(t)$ is the shear creep compliance, R is the radius of the indenting ball, $\alpha(t)$ is the indentation depth, and P_0 is the applied load. The compressive creep compliance, D(t), can be roughly approximated from the shear compliance by

$$D(t) \approx J_c(t)/3 \quad . \qquad (11)$$

This is an approximation, and is valid only if bulk deformation is neglected.

The compressive creep compliance was calculated from the indentation data and Equations (10) and (11), and the results are presented in Figure 19 for the standard indentor. It is seen that the calculated creep compliances are somewhat lower than the measured ones. The stresses acting on the indentor, based on the projected area of the ball, range from approximately 1300 to 3600 psi (91 to 253 kg/cm^2) were considerably higher than the 600 psi (42 kg/cm^2) used in the creep tests. The published literature on creep of PTFE, and the results of the creep tests in the present study, show that the compliance should be higher at higher stresses. Also, the calculated compliances do not clearly increase with increasing load as would be expected from the actual creep tests. This may be due to the fact that the contact area changes as the indentation progresses and that the indentations are different for different loads. The actual stresses acting on the material may be much closer together than the applied loads indicate.

The calculated compliances for the modified indentor, while not present, show the same behavior as those for the standard indentor, indicating that increasing the indentor radius yields no measurable improvement in the calculated results. There does not appear to be a direct correlation between the results of the microhardness tests and those of the creep tests. If a more realistic viscoelastic model were used in the derivation of Equation (10), the results might be more directly related to creep tests. To derive a relationship similar to Equation (10) using a more complicated viscoelastic model is a formidable task and there may be no great improvement in the results. The microhardness test, therefore, does not appear suitable for predictions of long-term deformation of polymeric materials.

FIGURE 19. EFFECT OF LOAD ON CALCULATED CREEP COMPLIANCE

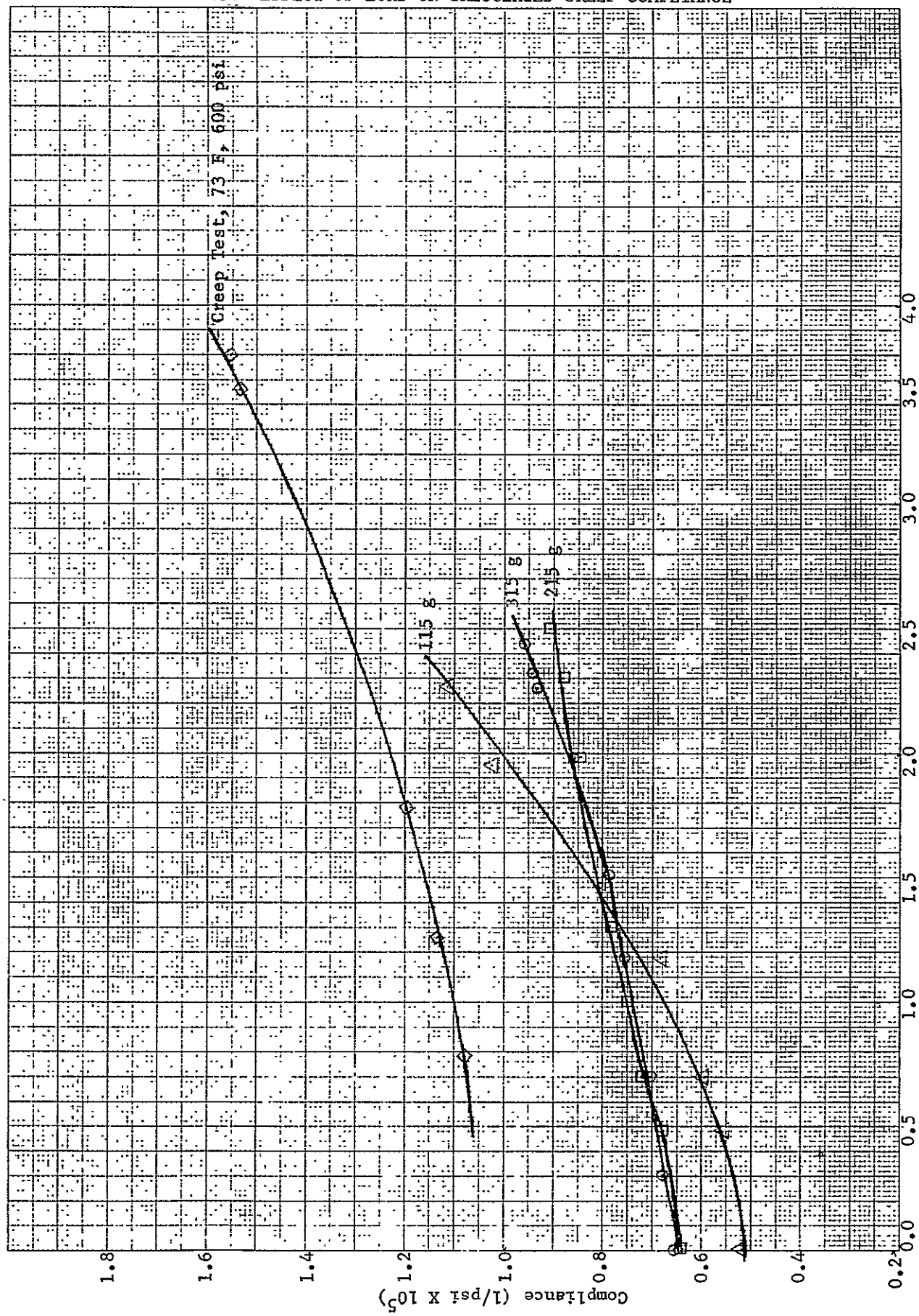

Conclusions

The following conclusions can be drawn from this study:

(1) The permanent set or nonrecoverable deformation of nonmetallic components can be determined from the viscosity and the plastic yield behavior of the material. A form of Miner's Law appears to be applicable for the evaluation of permanent set in cases of complex stress and/or temperature histories.

(2) The exact relationship and test procedures to be used in determining permanent set will depend on the type of material under consideration. If the plastic yield behavior is present, it must be subtracted from the permanent set before the viscosity can be determined.

(3) The viscosity of Halon® G-700, assuming the deformation to be pure viscoelastic, was evaluated from measurements of creep recovery. The length of time required for the creep measurements to accurately determine the viscosity will be a function of the temperature and stress applied and the measuring accuracy of the equipment.

(4) Unusual creep compliance behavior occurred at room temperature. The compliance of Halon® G-700 at room temperature was higher than that at 85 F (29.4 C). This behavior could be due to differences in machining or loading conditions. Care should be exercised to give all samples the same process and sample preparation history.

(5) Time-temperature and time-stress superpositions appear to be useful in predicting long-term behavior, and also in setting up accelerated test procedures. The data obtained in the present study may be useful in predicting behavior under storage conditions.

(6) Creep compliances calculated from microhardness test data did not conform to expected behavior based on the creep test results. As the load applied in the microhardness tests was increased, the compliance was erratic, contrary to anticipated results.

(7) The results of the microhardness tests do not appear directly relatable to the creep behavior of Halon® G-700. On this basis, the microhardness test does not appear suitable for service life determinations.

WEAR OF NONMETALLIC MATERIALS

Introduction

Wear is one of the principal modes of failure anticipated in the representative components analyzed during the first phase of this program. The critical areas of wear include nonmetallic sealing surfaces. These surfaces are subjected to sliding contact during closure of gate lip seals or sliding occasioned by oscillatory motion of actuator piston seals, etc. The wearing surfaces involve a metallic element sliding against a plastic or elastomer surface. Prediction of the service life of such a part depends on knowledge of the wear characteristics of the plastic or elastomer component. Development of a valid life test for these elements requires knowledge of the wear properties of nonmetallic materials under the following four operating conditions.

(1) Cryogenic temperatures

(2) Cycling from cryogenic temperatures to above room temperature and back again

(3) Aging

(4) Small-amplitude oscillatory motion.

There is little reliable information available which describes the effects on the wear characteristics of nonmetallic materials for the conditions described above.

The particular wear characteristics of concern for predicting the life of a seal or bearing are as follows.

(1) Linearity of wear as a function of time or number of cycles of operation

(2) Type of wear occurring

  (a) Release of loose wear debris

  (b) Localized transfer of surface material to contacting metal surface

  (c) Scoring, scratching, or galling.

If wear debris is released from the wear zone, it will be important to determine the particle sizes and distribution of the debris. This sort of information is important for evaluation of the probability of fouling by wear debris of close-clearance moving parts.

Localized transfer or scoring of the polymer in a sealing surface would increase leakage with a minimum amount of wear. In some seal applications where leakage is critical (such as the solenoid valve in the calibration gas supply module), such a material would be considered inappropriate for long-service-life applications. The wear test would serve to determine the length of time required to develop leakage producing surface damage.

The purpose of determining the above wear characteristics under the four operating conditions is to establish whether linear wear can be anticipated for most of the life of a component. If reasonable closeness of fit to the expression for wear is determined, then a life test can be designed for estimating the wear coefficient, K, from the following equations.

Mild wear, in which frictional heating is minimal and surfaces are dry can be expressed as

$$V = \frac{KNL}{P_m} \quad , \tag{12}$$

where

V = wear volume

N = load

L = total sliding distance

P_m = flow pressure of the plastic material at operating temperature

K = wear coeficient.

Since wear of seals and bearings is analyzed in terms of dimensional loss or inches penetration – rather than volume loss, Equation (1) can be modified as follows:

$$h = \frac{KP_b vt}{P_m} \quad , \tag{13}$$

where

h = reduction in thickness of polymer component

P_b = apparent bearing pressure = L/A (A = contact area)

v = sliding velocity

t = bearing life.

Wear coefficients for plastics, e.g., Teflon, have been derived from wear tests. Values of K ranging from 2.5×10^{-5} to 2.9×10^{5} have been obtained for Teflon. If it could be assumed that this material showed no anomalies in wear behavior at temperatures below its glass-transition point, then an established wear coefficient (such as the one described above) could be used in estimating wear life with Equation (2) by inserting the flow or indentation pressure

(determined from Brinell hardness or Durometer measurements) for the operating temperature in question.

Another test technique that has been used to predict the long-term wear life of polymeric materials is to accelerate the wear tests.

An accelerated test is a test in which the time frame is effectively compressed without changing the failure mechanism. In addition, a quantitative relationship between real time and accelerated "time" must exist. The accelerated testing of friction interfaces is extremely difficult due to the inherent mutually interactive nature of the system. For example, increases in speed can cause increases in temperature and can alter failure mechanisms. In order to accelerate wear tests, one must consider carefully the materials comprising the interface and determine the failure mechanism(s), and the effect on the failure mechanisms of the operating parameters such as load, speed, temperature, and environment. Ideally, an accelerated test is one in which a parameter related to time by a well-understood relationship (such as speed) can be increased without altering the failure mechanism being studied. With these basic requirements in mind, it is necessary to carefully study the system under investigation: in this case polymeric materials rubbing against steel at cryogenic and ambient temperatures.

Three possible performance parameters that appear to be most suitable for the acceleration of tests are the speed, the temperature, and the load. The speed is the parameter most used for accelerated bearing tests. One reason for accelerating the speed parameter is that there is a fairly clear-cut relationship between speed and time in terms of the number of cycles, or the number of times a given point on a friction surface is subjected to a tribological stress. The degree of acceleration available by increasing the speed in these tests is limited chiefly by thermal considerations. Especially important is the temperature at the polymer-steel interface (as opposed to the ambient temperature, which may be much colder. This method of acceleration is valid and rigorous provided that the temperature level, both transient and steady state, remains within a margin such that the wear mechanism is unaffected – and most important, that the wear rate varies linearly with rubbing speed.

Acceleration by increasing the temperature has been employed for chemical processes whose mechanisms are well understood. For uncharacterized wear mechanisms involving materials whose tribological/mechanical properties vary with temperature in a relatively unknown manner, temperature acceleration is not desirable (in contrast to creep, whose temperature acceleration is rigorous).

Load acceleration is theoretically valid within the constraints of the failure mechanism. The major drawbacks to this method are the difficulty in controlling the rubbing load for the critical ball/retainer interfaces, and the fact that no well-defined relationship between load and life exists for this bearing/lubricant system.

Thus, the most promising method of test acceleration for this system appears to involve increasing the speed of the bearing, or shortening the dwell periods. For systems operating in an intermittent fashion, such as that

characteristic of steppers, decreased dwell times (or increased duty cycles) offer the possibility of a rigorous accelerated test. This method, which yields accelerated data easily related to real time, is limited only by questions concerning thermal similitude, e.g., does the decreased dwell period between steps bring about an increase in running temperature due to motor heating or to friction heating? The degree of acceleration that can be produced faithfully by increasing the speed is likewise constrained by thermal effects. Such a method can be applied only if the higher accelerated rate used does not cause an increase in temperature at the friction interfaces that would result in a change in the wear/transfer mechanism.

Several models for the determination of the limiting temperature of a polymeric material in a rubbing interface have been proposed. Lancaster[34] has used Jaeger's analysis[35] as the basis for a determination of the flash (or transient) temperatures in sliding interfaces. This model assumes plastic rather than elasto-plastic deformation and, therefore, allows the calculation of the real area of contact (asperity tips) based on the flow pressure of the polymer.

For steel sliding at low speeds on a polymer

$$\theta = 1.10 \times 10^{-2} \mu \rho_m{}^{1/2} W^{1/2} V \quad , \qquad (14)$$

where

θ = flash temperature (C)

ρ_m = flow pressure ($\cong$ indentation hardness) (N/m^2)

μ = coefficient of friction

W = load (kg)

V = linear velocity (m/sec).

In the form given in Equation (14), the flow pressure is assumed to be independent of temperature. This assumption, valid for only very small values of θ, can be eliminated where hardness-versus-temperature data are available. This model has shown reasonably good correlation with wear data for polytetrafluoroethylene (PTFE, e.g., Teflon, Halon), polypropylene, polyacetal (Delrin), and polyamide (Nylon) materials.

Wear Tests

Introduction

Wear evaluations were carried out in order to determine the mechanisms of wear of nonmetallic materials at cryogenic and ambient temperatures, and to determine the nature of the wear process as a function of time. This information is necessary for the design of valid accelerated tests for nonmetallic components.

Wear tests have been carried out on all of the candidate nonmetallic materials found in the valves: PTFE (e.g., Teflon), virgin and glass-filled, KEL-F and Mylar. These tests have been carried out under conditions resembling the actual use conditions of the various valve components.

The wear evaluations made use of the cryogenic wear apparatus described in detail in Appendix E. The apparatus makes use of a three-rider configuration with the three riders in a triangular or milking-stool orientation. The hemispherical riders, consisting of three precision balls locked in place, slide on a flat disk of Teflon ~3 mm thick. A real-time wear measurement is made by means of a parallel-plate capacitor, the spacing of which is proportional to the wear. Torque and temperature are also measured.

The wear evaluations are carried out at liquid-nitrogen temperature and at room temperature on specimens of virgin Teflon. In both cases, the wear (capacities) and the friction (torque) were measured continuously for 6 hours of running at equilibrium temperatures. The rotational rate of 6 rpm was chosen to minimize friction heating. The specimen load was 0.303 kg/ball (0.667 lb), producing a mean Hertzian contact stress of 34.4×10^6 N/m^2 (4987 psi).

In addition, a series of short term, speed-accelerated tests were conducted at speeds up to 600 rpm at 77 K. The specimen load was identical to that of the long-term tests – 0.303 kg/ball (34.4×10^6 N/m^2) mean Hertzian contact stress.

Long Term Tests

Virgin Teflon. The capacitance/wear results are shown graphically in Figure 20. The upper curve is for an experiment carried out at 77 K; note that some anomalous behavior is indicated for the first 30 minutes of the test and after approximately 4 hours the wear rate has apparently stabilized. Results for the second experiment, carried out at room temperature, are plotted in the lower curve. The trends indicated are similar to the preceding; however, the total amount (depth) of wear indicated is over three times greater.

Talysurf profile traces of the wear depth present on the Teflon specimens are reproduced in Figure 21. Although the specimen surfaces are considerably deformed in the unworn surface areas, thereby making the reference surface rather uncertain, it is apparent that the wear path produced at room temperatures is several times deeper than that produced at 77 K.

Friction force, measured by application of an instrumented strain beam, as described in Appendix E, was monitored throughout each of the Teflon wear experiments. Coefficients of friction computed for the low-temperature experiments were significantly less than those computed for the room-temperature experiments.

The wear tracks produced on the Teflon specimens were examined microscopically to determine whether differences in wear mechanisms could be detected.

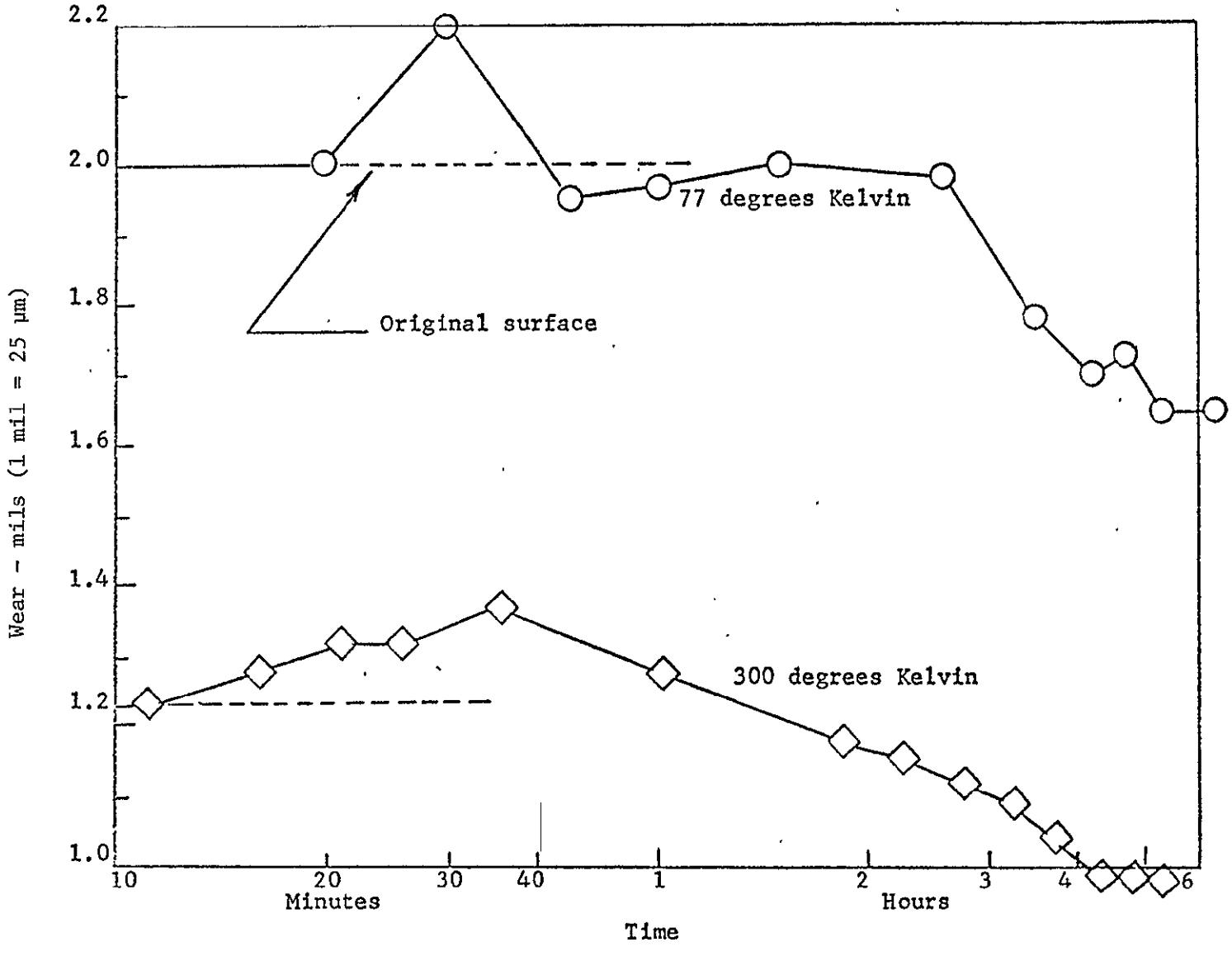

FIGURE 20. EXPERIMENTAL WEAR RESULTS FOR TEFLON

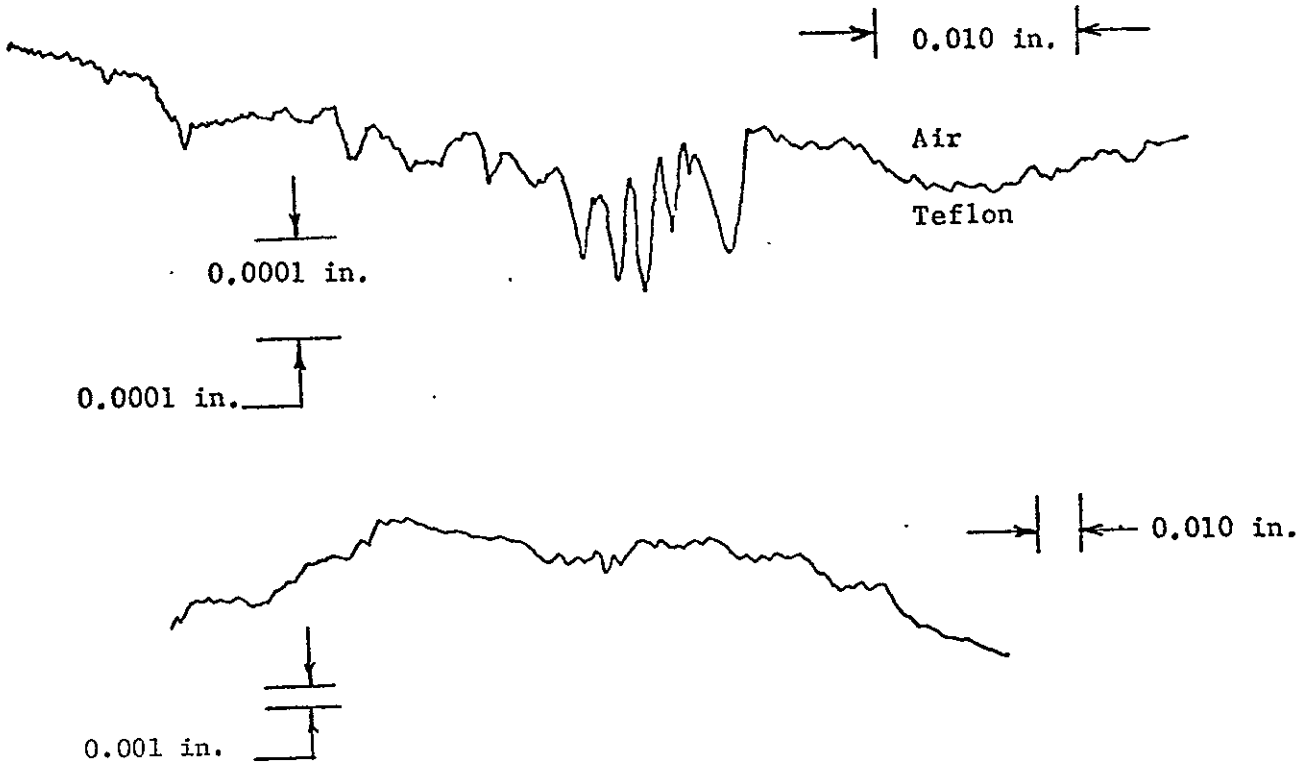

FIGURE 21. TALYSURF PROFILE SECTIONS ACROSS BALL TRACKS FROM ∿ 6-HOUR WEAR RUNS

One specimen was taken from a room-temperature wear evaluation and the other specimen was taken from the cryogenic run.

There were obvious differences to the naked eye in the appearances of the wear tracks. The wear track developed at 77 K was very shallow and consisted of several circumferential furrows. The wear track developed during room-temperature evaluation was a semicircular groove, conforming to the contacting ball profile. The surface of this track was very smooth and shiny.

Examination of the wear tracks by SEM (scanning electron microscopy) revealed significant fine details. The results are shown in the photomicrographs presented in Figures 22 through 25.

Figure 23 shows scratches in the wear track of the specimen operated at 77 K. The single scratch running from upper left to lower right is a groove made by the Talysurf stylus. The wear scratches are fairly wide and straightened, indicating they were made by blunted particles that are a little harder than is the surrounding. It appears that most of the scratches are indentations, i. e., they were not formed by machining away Teflon. This is evidenced by the original finishing marks that can be seen (faintly) crossing the wear scratches and appearing in the bottom of the scratches. The deepest scratch did not show any original finishing marks.

The wear track made at room temperature also contained circumferential scratches; however, there was no evidence of residual finishing marks. A detail of the wear track is shown in Figure 22.

At higher magnification, the wear process prevailing at 77 K can be observed. The scratch grooves tend to throw up an extruded lip of Teflon along their top edges and the lip is pulled off or rolled up as wear debris. Evidence of this mechanism is shown in Figure 25.

The high-magnification microscopy of the wear track generated at room temperature shows a much different surface texture when compared with that generated at 77 K. No evidence of sharp-sided scratches with extrusions could be found. Instead, a very fine "fish-scale" pattern was observed. This pattern can be seen in Figure 24. A surface replica was made and examined by transmission electron microscopy (TEM) at magnifications to 80,000X. A TEM micrograph at 30,000X is shown in Figure 26. Evidence of heavy plastic flow of the surface was found at this magnification. The wavy lines are typical of flow patterns produced in high viscosity semifluid materials (like taffy). Evidence of drawn-out tendrils can be seen. These are characteristic of a Teflon-transfer film structure.

High-magnification TEM analysis of the specimen evaluated at 77 K revealed no evidence of surface flow.

The wear debris, in both cases, adhered to the balls. Figure 27 shows a micrograph of the debris from the 298 K evaluation. It has the ribbon-like character normally associated with the wear of Teflon. The ribbons are the result of

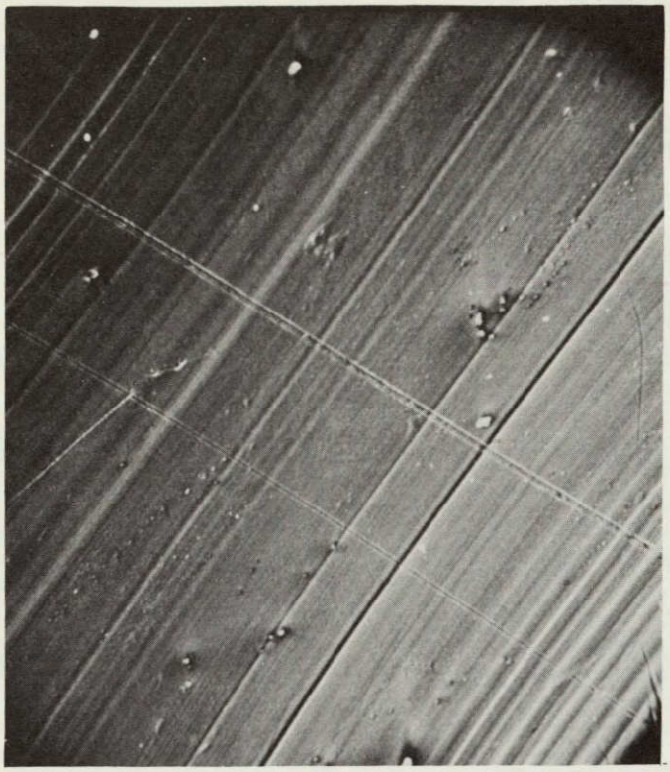

FIGURE 22. 100X SCANNING ELECTRON MICROSCOPE PHOTOMICROGRAPH OF A TEFLON WEAR TRACK PRODUCED BY A SPHERICAL STEEL RIDER AT 298 K

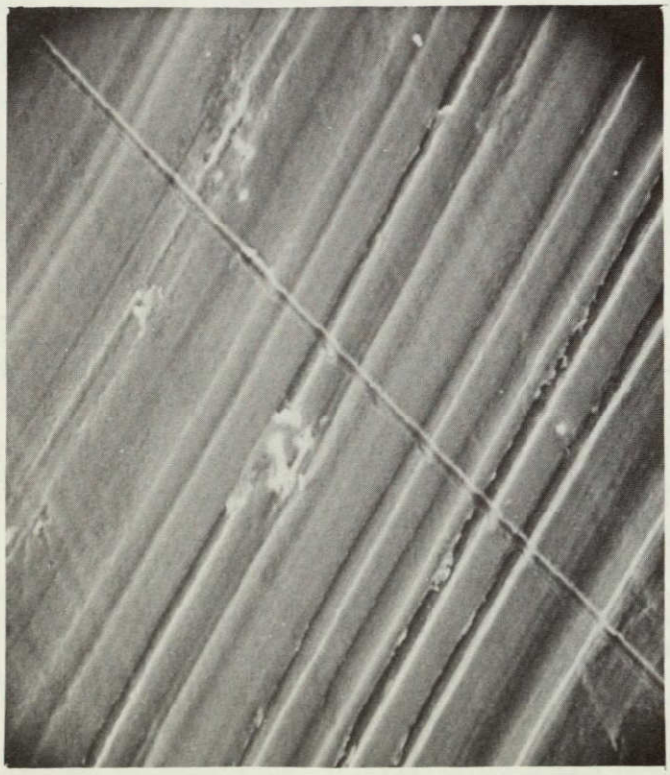

FIGURE 23. 200X SCANNING ELECTRON PHOTOMICROGRAPH OF A TEFLON WEAR TRACK PRODUCED BY A SPHERICAL STEEL RIDER AT 77 K

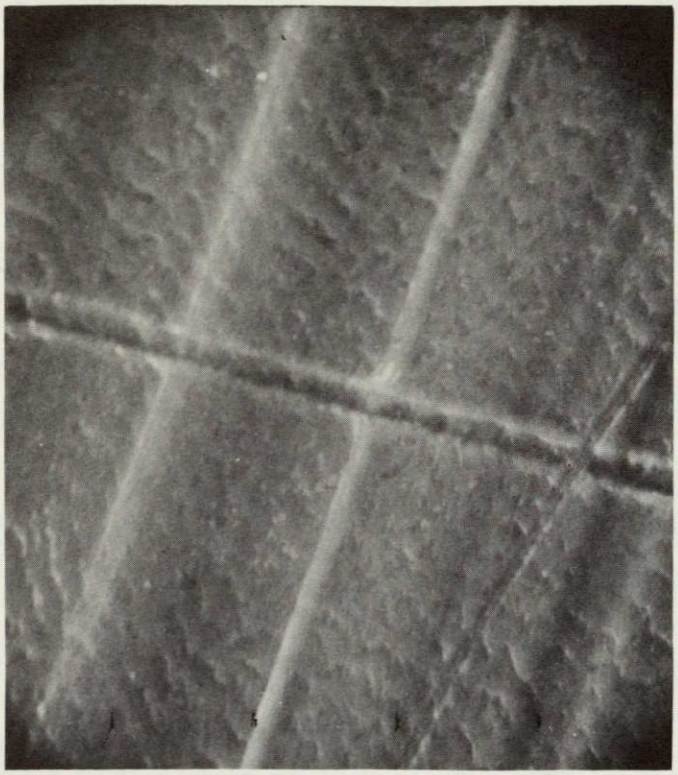

FIGURE 24. 1000X SCANNING ELECTRON PHOTOMICROGRAPH OF A TEFLON WEAR TRACK GENERATED AT 298 K

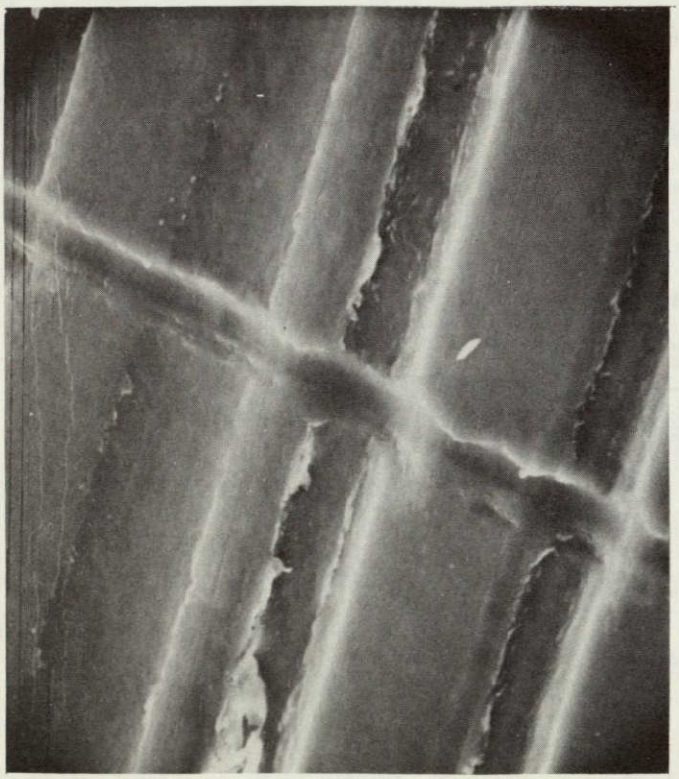

FIGURE 25. 1000X SCANNING ELECTRON PHOTOMICROGRAPH OF A TEFLON WEAR TRACK GENERATED AT 77 K

FIGURE 26. 30,000X TRANSMISSION ELECTRON PHOTOMICROGRAPH OF A TEFLON WEAR TRACK GENERATED AT 273 K

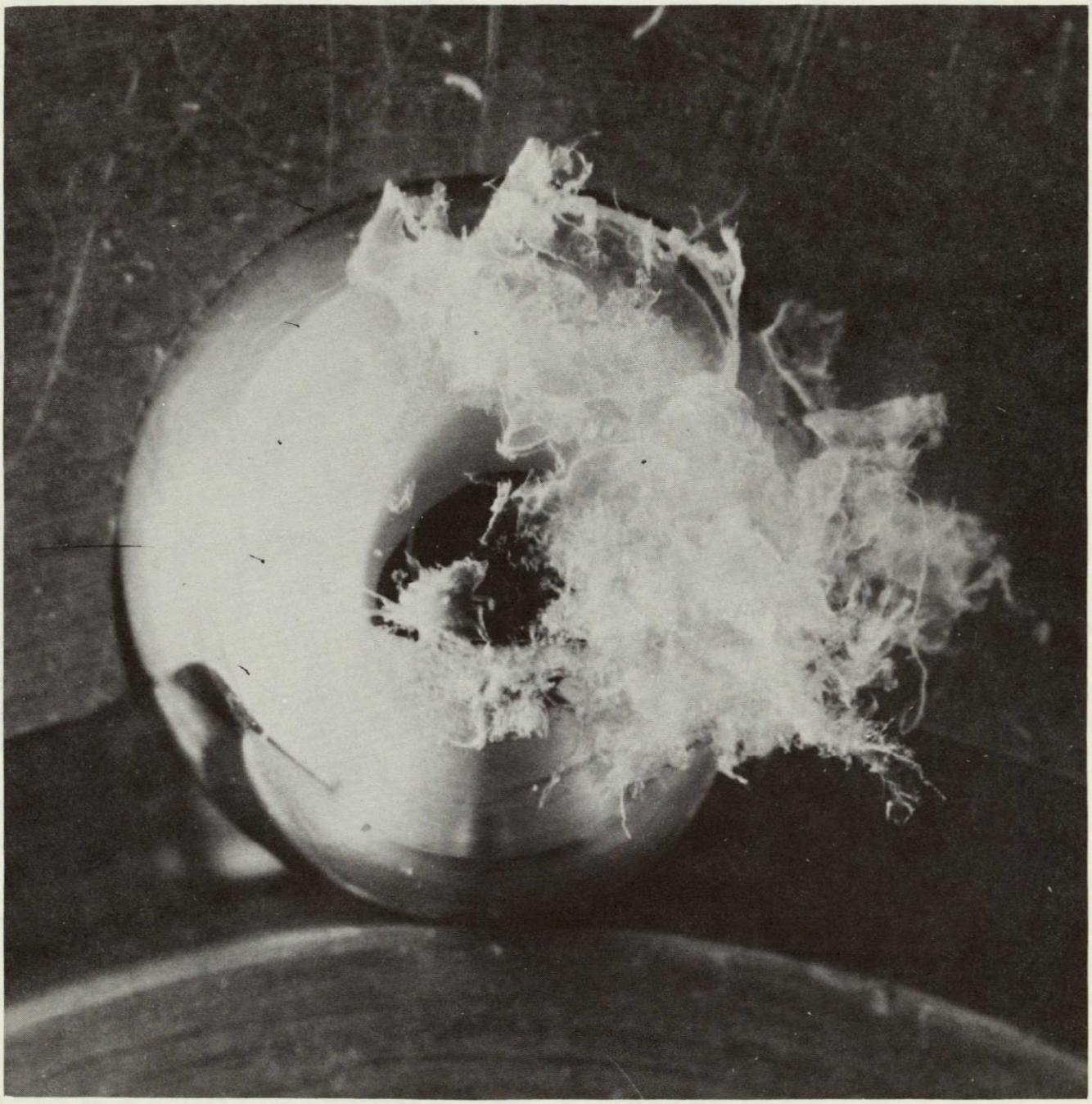

FIGURE 27. TEFLON WEAR DEBRIS GENERATED AT 298 K. THE CONTACT POINT BETWEEN THE STEEL BALL AND THE TEFLON SPECIMEN IS IN THE CENTER OF THE BALL SURFACE. THE DEBRIS IS ON THE TRAILING EDGE

an extrusion-machining process in which a thin "chip" is formed at the ball-Teflon interface and is separated from the Teflon surface by a shearing process. These ribbons can either adhere and burnish into a transfer film or be released as debris.

Wear debris generated at 77 K has a more particulate appearance, as shown in Figures 28 and 29. This is presumably the type of debris seen in the process of formation along the abrasion scratches seen in Figure 25.

The SEM and surface profilometry results are corroborated by the weight-loss measurements. The specimen run at room temperature lost ~3.6 mg of mass, while the specimen run at 77 K lost ~0.3 mg. Observations of the balls and the debris indicate that at 77 K less debris and less transfer film are formed.

From these examinations it was concluded that the principal wear mechanism at 77 K is abrasive wear – much like the abrasive wear characteristic of metals. The wear mechanism at room temperature can be described as a combined heavy plastic-deformation and adhesive-wear process. During the process, it is possible that thin fibers of Teflon transfer back and forth. Presumably, wear at room temperature involves a significant creep factor; therefore, creep would have to be accounted for in predicting wear life. The experiments have shown that, at least for virgin Teflon, accelerated life testing for cryogenic applications cannot be performed at room temperature, since the mechanisms of wear are different than they are at cryogenic temperatures.

Glass-Filled PTFE. Figure 30 shows the wear as a function of time for glass-filled PTFE at 298 K and 77 K. Note that, in contrast to virgin PTFE, the wear of the filled materials shows a behavior that might lend itself better to extrapolation. The gross "wear" of the 298 K specimen is greater than the 77 K specimen, as might be expected. It is noteworthy, however, that most of this "wear" takes place in the first few hours. There is ample evidence that the steep initial portion of the 298 K curve is due to creep.

Figures 31-34 show the condition of both halves of the friction couple after long-term rubbing at each temperature level. At 298 K, the ball surfaces showed large amounts of ribbon-like wear debris, but no evidence of glass particles. The contact area was indeed free from any transfer film and showed evidence of abrasive wear, Figure 31. The fringes at the contact area had gradually thickening patches of transfer film. The flat specimen from the 300 K tests, Figure 32, showed a well-defined wear track, in which was imbedded the short glass fibers that comprise the filler in this material. The track was rather deep but displayed less evidence of plastic flow than that produced in the virgin PTFE.

Figures 33 and 34 show the appearance of wear surfaces resulting from the 77 K test. The wear debris is very fine and is dispersed evenly around the wear area on the balls, Figure 33. A finely-worn surface was present on the ball contact areas after 25 hours of operation (9000 cycles); however, this was completely covered by a thin transfer film after 77 hours of operation (28,000 cycles). This change is illustrated in the 100X micrographs of Figure 34. It is also noteworthy

FIGURE 28. TEFLON WEAR DEBRIS GENERATED AT 77 K. THE TRAILING EDGE OF THE CONTACT PATCH IS TOWARD THE TOP OF THE PHOTOGRAPH

FIGURE 29. VIEW OF THE CONTACT PATCH GENERATED AT 77 K SHOWING WEAR DEBRIS AROUND THE PERHIPHERY AND EVIDENCE OF A NONUNIFORM TRANSFER FILM IN THE PATCH ITSELF

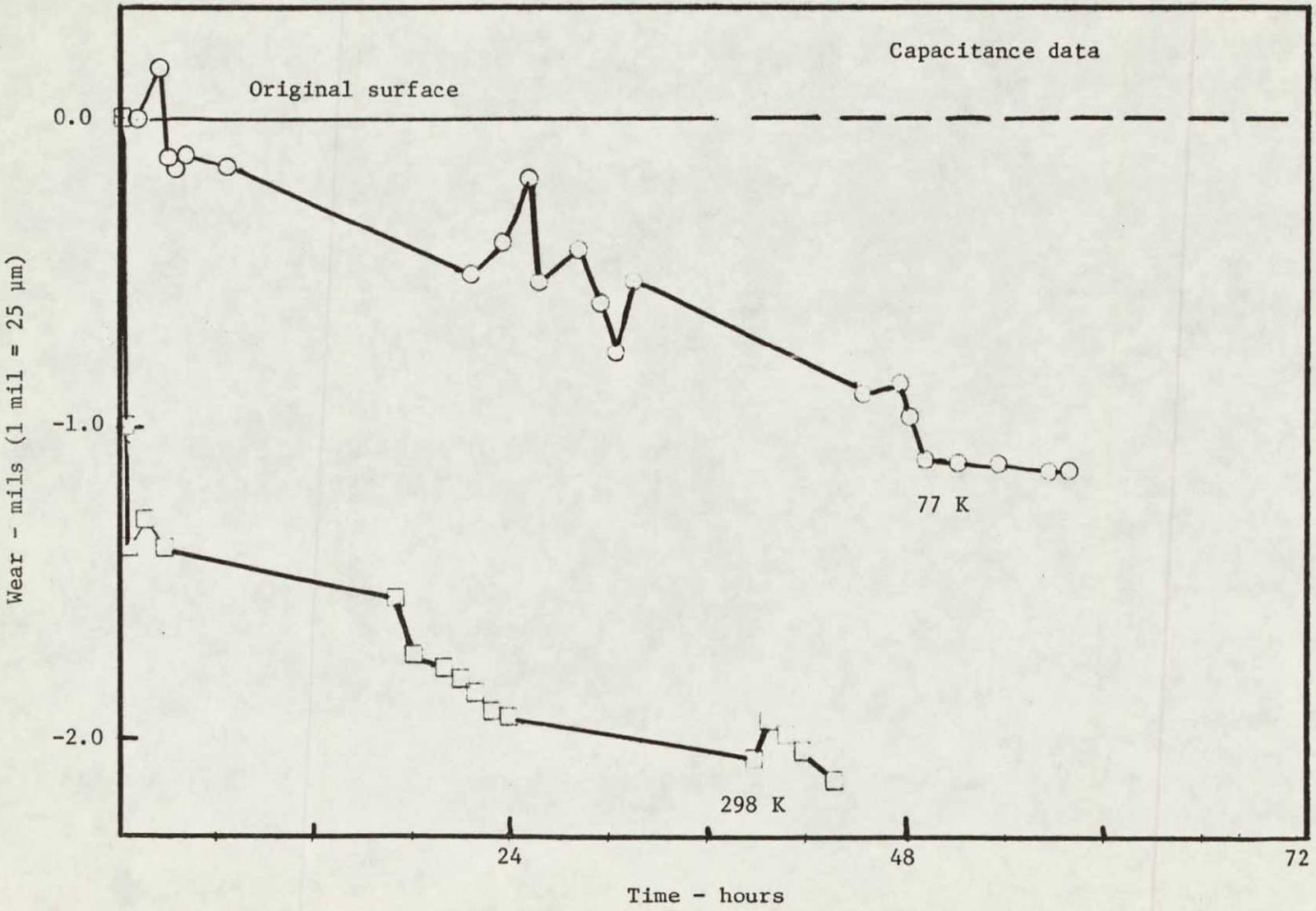

FIGURE 30. FILLED TEFLON 298 K AND 77 K

200X

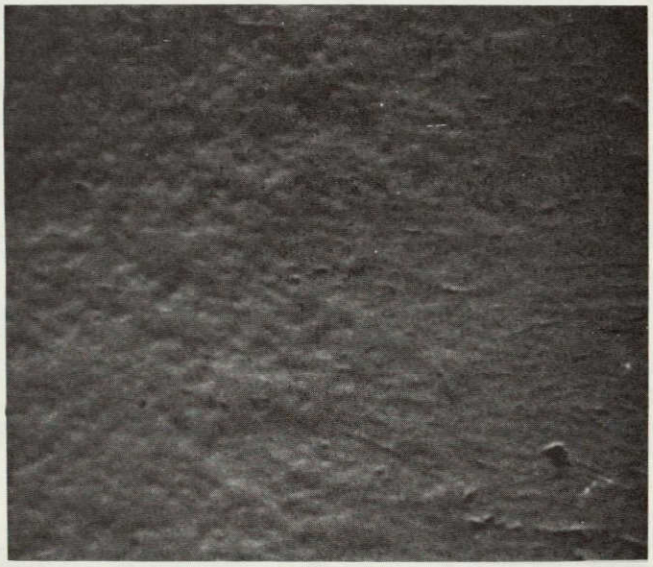

1000X

FIGURE 31. SEM PHOTOGRAPHS OF A BALL WEAR SCAR RESULTING FROM 16,550 RUBBING CYCLES AGAINST GLASS-FILLED PTFE - 6 RPM, 300 K

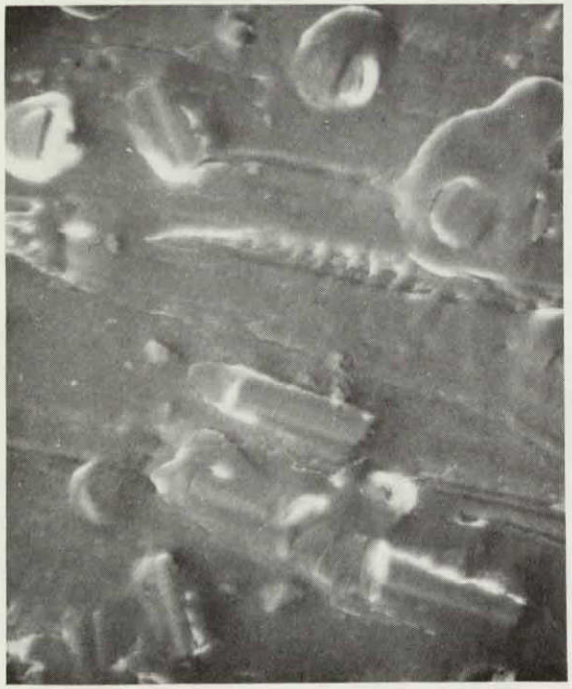

500X

Wear Track

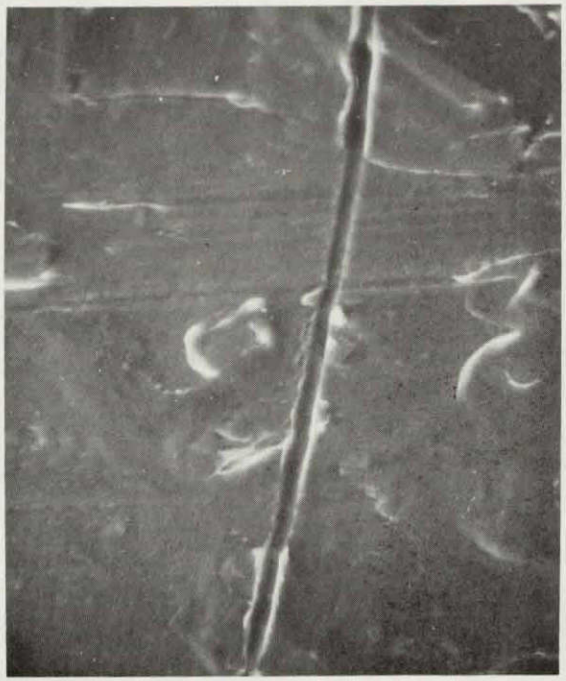

500X

Wear Track
(Vertical Score is Talysurf Scar)

500X

Unworn Surface

FIGURE 32. SEM PHOTOGRAPHS OF GLASS-FILLED TEFLON FLAT SPECIMENS AFTER 16,550 CYCLES AT 6 RPM AND 300 K

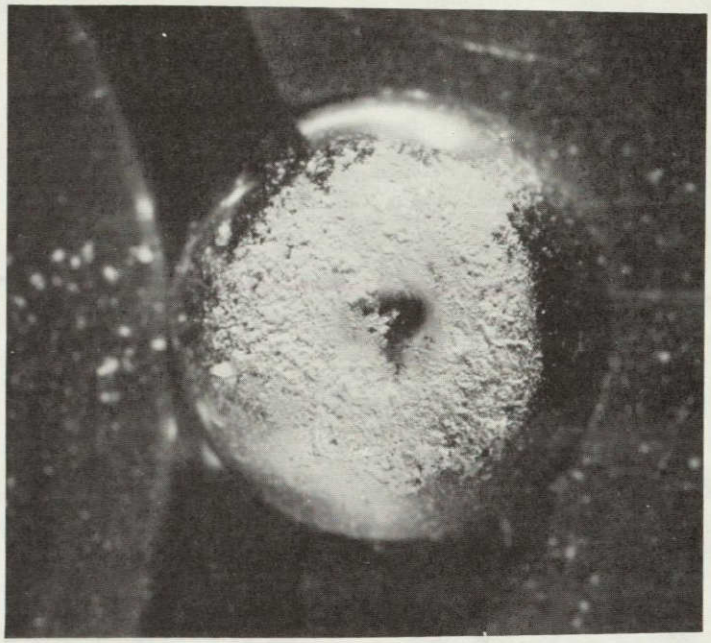

10X

Ball (440 SS)

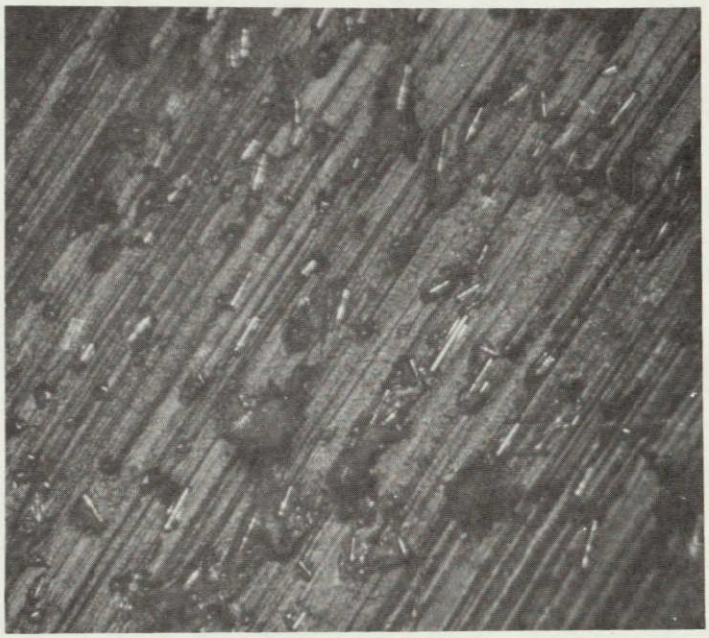

100X

Filled TFE Flat

FIGURE 33. GLASS-FILLED TEFLON EXPERIMENT 77 K - 6 RPM - 27,700 CYCLES

100X

9000 Cycles

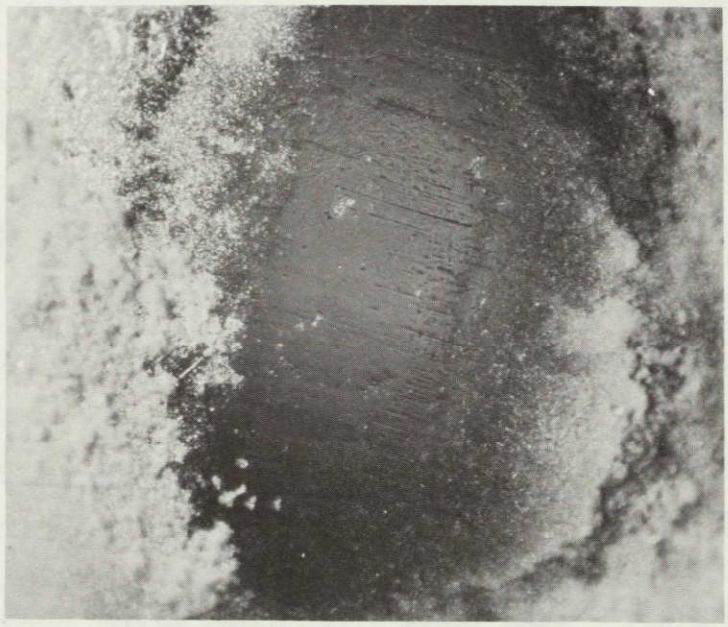

100X

27,000 Cycles

FIGURE 34. BALL WEAR SCARS FROM GLASS-FILLED TEFLON(77 K - 6 RPM) EXPERIMENT

100X

7400 Cycles

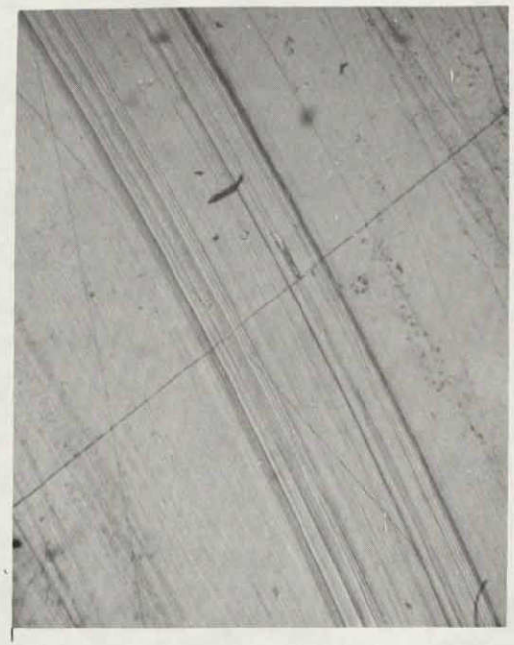

100X

17,850 Cycles

100X

26,300 Cycles

FIGURE 36. WEAR TRACK ON KEL-F FLAT SPECIMENS: 77 K - 6 RPM EXPERIMENT

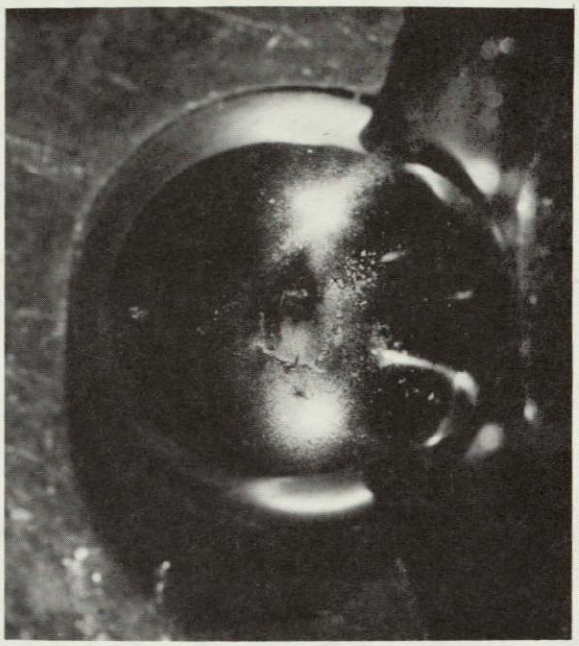

10X

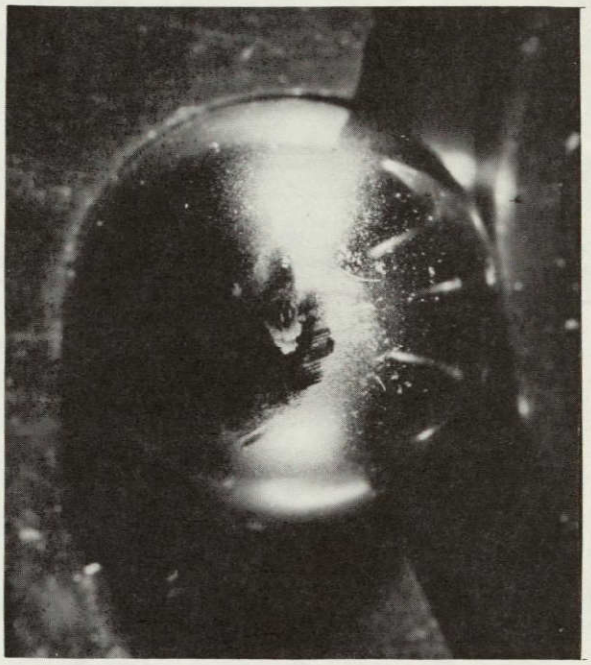

10X

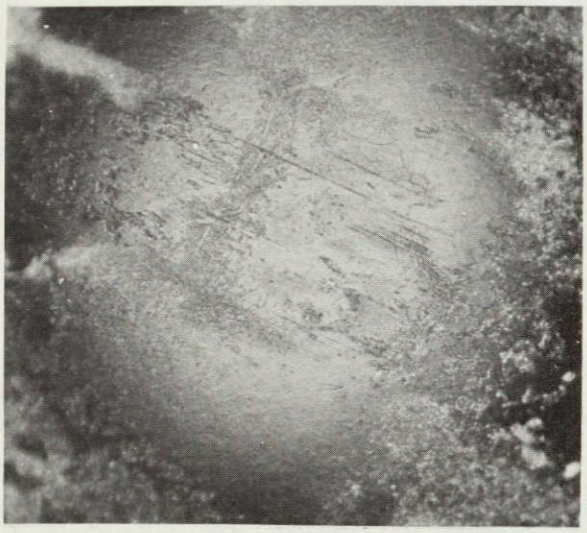

100X

17,850 Cycles

100X

26,300 Cycles

FIGURE 37. WEAR DEBRIS ON BALL SPECIMENS KEL-F, 77 K, 6 RPM EXPERIMENTS

100X

Ball Scar

100X

KEL-F Wear Track

FIGURE 38. SEM PHOTOGRAPHS OF WEAR AREAS ON KEL-F PLASTIC FROM 298 K - 6 RPM - 26,000 CYCLE EXPERIMENT

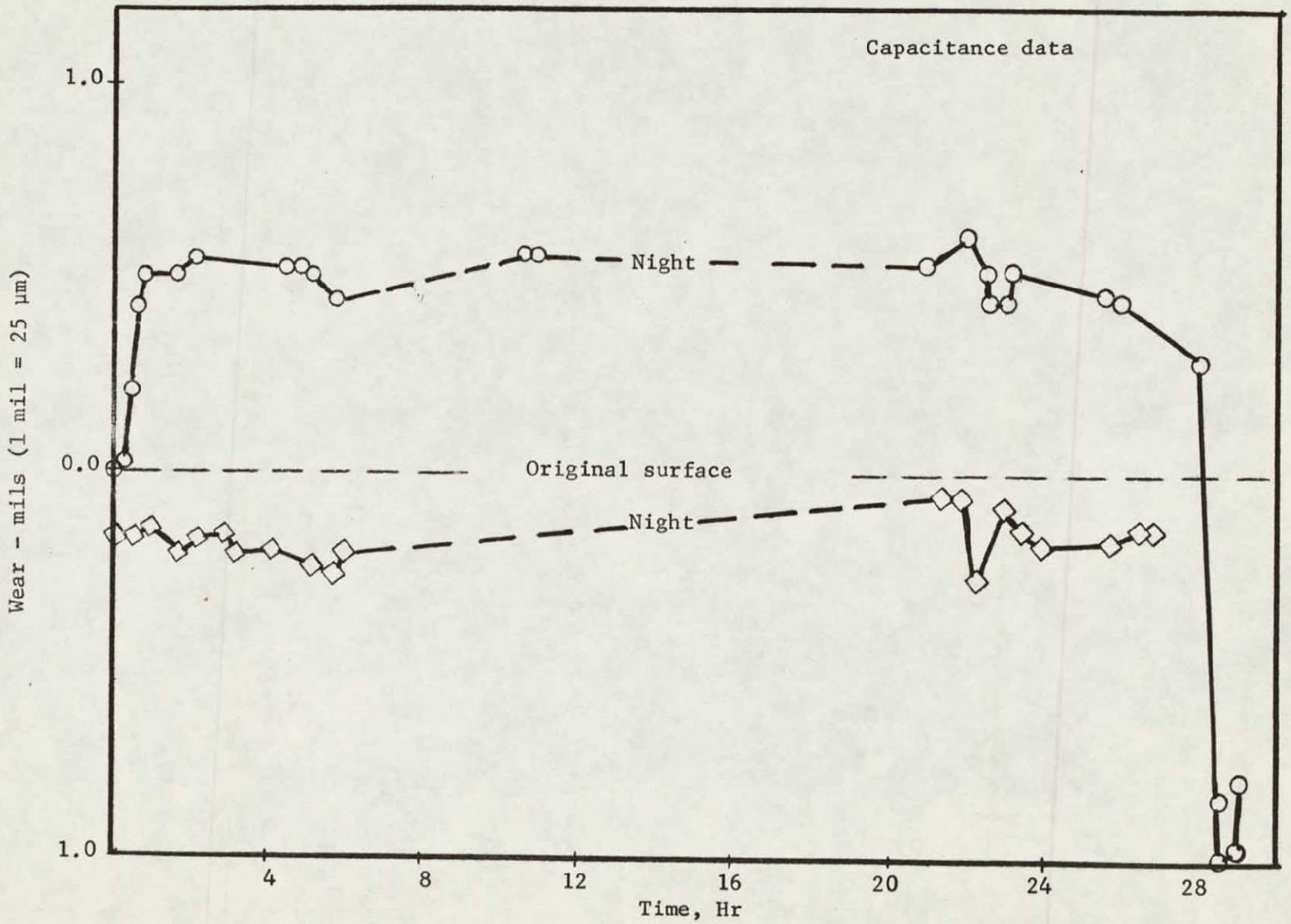

FIGURE 39. WEAR OF MYLAR AT 298 K AND 77 K

10X

SS Ball

100X

Ball Scar

200X

Mylar Flat
-Wear Track
-Unworn Area

FIGURE 40. WEAR AREAS ON SPECIMENS FROM 300 K - 6 RPM - 9,700 CYCLE MYLAR EXPERIMENT

10X

SS Ball

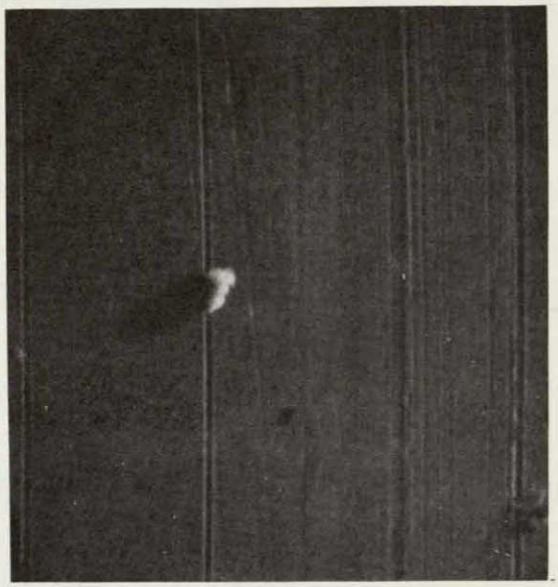

500X

Ball Contact

100X

Ball Contact
(Light Micrographs)

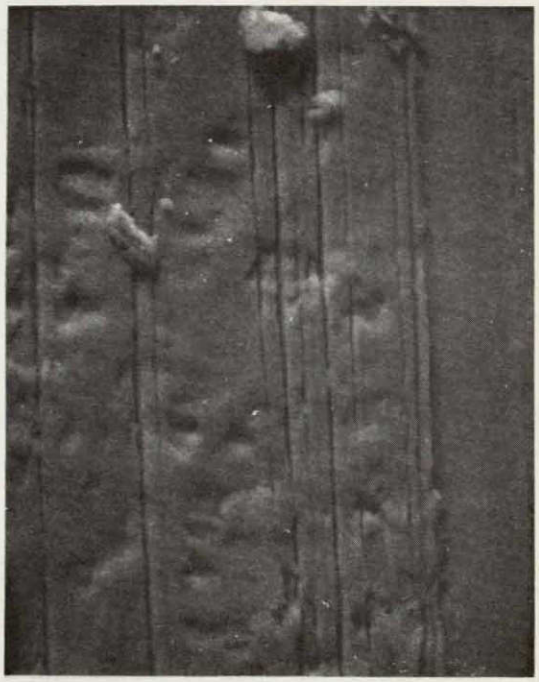

500X

Wear Track - Flat
(SEM Micrographs)

FIGURE 41. WEAR AREAS ON SPECIMENS FROM 77 K - 6 RPM - 10,250 CYCLE MYLAR EXPERIMENT

the long filaments are absent. The contact area contains a transfer film sufficiently thick to exhibit numerous parallel scratches caused during sliding. Original surface texture scratches appear faintly through the transfer film, and very fine wear particles are thinly dispersed over all exposed ball surfaces.

The Mylar plastic specimen exhibits a characteristic dendritic surface structure – a sort of reticulation pattern in bass relief (Ref. Figure 40). This appears smoothed by plastic flow in the ball-track area exactly like the room temperature result described above. The wear track is additionally characterized by parallel scratches which denote the sliding direction, and by numerous shallow pockets or depressions. These are similar in size to individual debris particles.

Accelerated Rate Tests

A second method of predicting the long-term wear life of polymeric materials is to conduct wear tests at speeds higher than normal such that the specimen is subjected to the real-time number of cycles in a shortened time span. The success of such an approach, as previously discussed, is somewhat dependent upon the temperature of the friction interface. Since most of the materials of interest show a different wear mechanism at 298 K than at 77 K, it was assumed that the wear process might be expected to be strongly influenced by the increased temperatures produced by friction.

To investigate this, wear experiments using filled PTFE were carried out at speeds from 60 to 600 rpm (a factor of 10 to 100 times the 6 rpm rate used in the long-term tests). These experiments were run at a specimen temperature of 77 K and under a specimen load of 0.303 Kg per ball. Each test was run for an identical number of cycles, 27,700 – equivalent to 77 hours at 6 rpm; and wear was determined by Talysurf depth measurements of the resulting wear tracks.

In order to determine the effects of creep acting in concert with wear, two series of experiments were carried out. In the first series, the wear tests were conducted in the same manner employed for the previous long-term experiments and the usual high initial "wear" rates resulted. The upper family of curves in Figure 42 summarizes the results of these tests. The wear curves diverge, and the appearance of the specimens suggested a change in wear mechanism at the higher speeds. This is apparent from the photomicrographs reproduced in Figures 43 and 44. In particular, the 600 rpm wear track showed a discoloration that is now attributed to oxidation wear of the steel debris. Further inspection revealed this phenomenon in all of the tests, and thus the discoloration is not an *a priori* indication of mechanistic changes due to friction heating.

In the second series of experiments, an effort was made to factor out the effects of creep at the PTFE by performing an initial conditioning operation on the specimen. This preconditioning was performed by operating the wear rig for 1 hour at room temperature and at 6 rpm (for minimum wear). After this each test, at a higher rotational speed, was carried out in exactly the same manner as before. The results of this series of experiments is shown in the lower family of

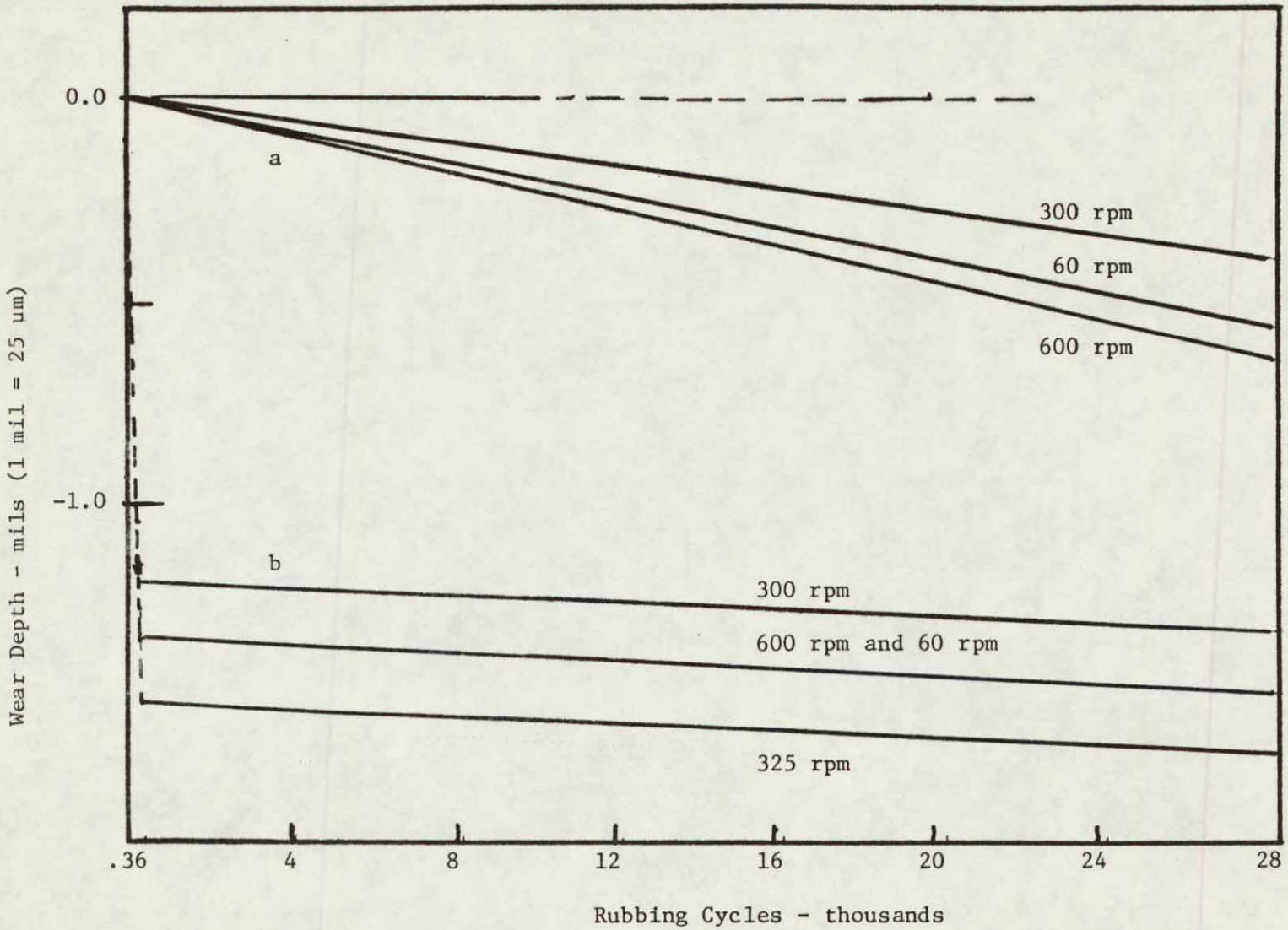

FIGURE 42. WEAR RESULTS (TALYSURF MEASUREMENTS) FOR EXPERIMENTS PERFORMED AT 77 K WITH GLASS-FILLED PTFE

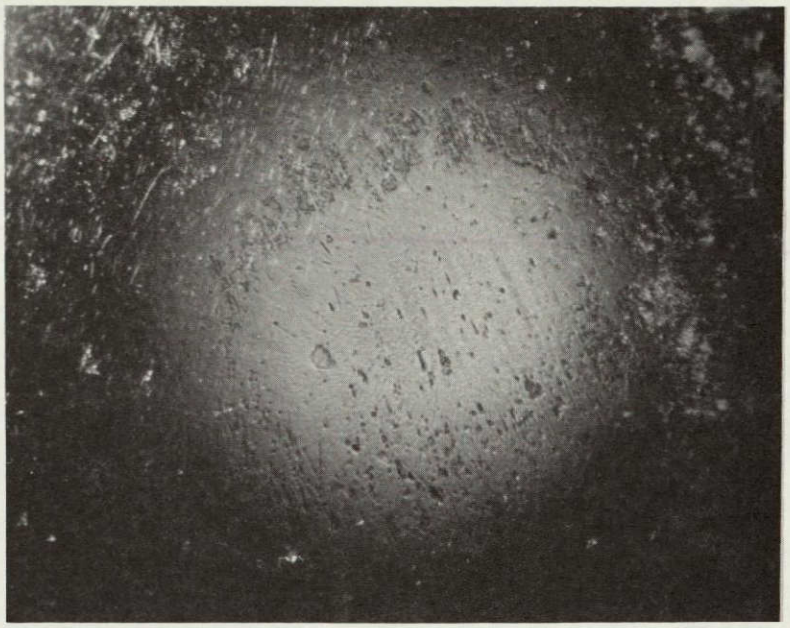

100X

Ball Scar

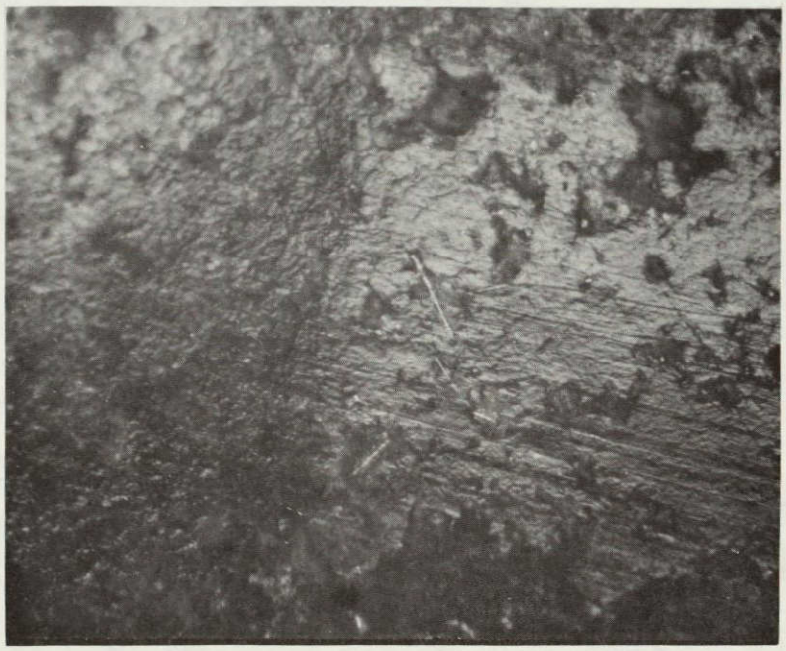

100X

Flat Scar

FIGURE 43. WEAR SCARS FROM FILLED TFE EXPERIMENT 77 K - 60 RPM

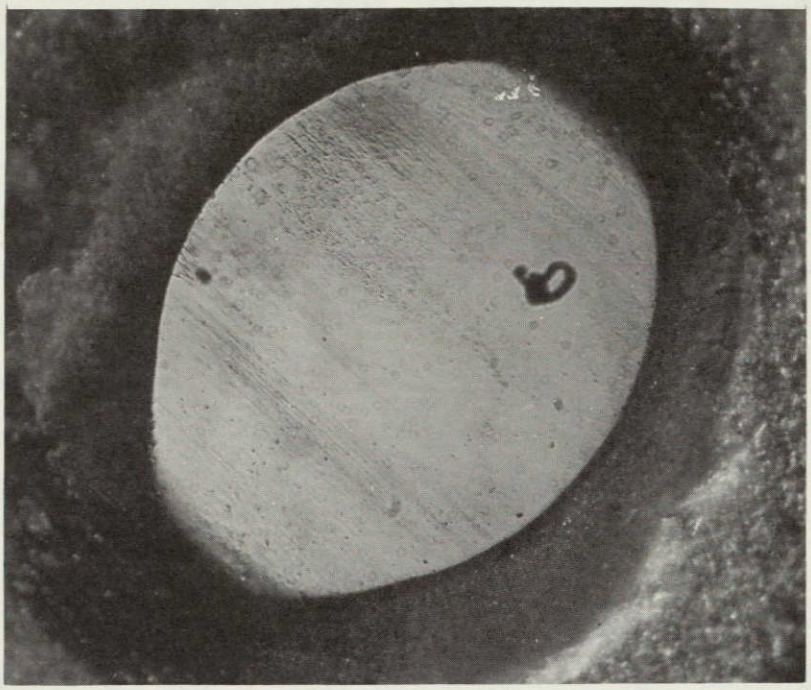

100X

Ball Scar

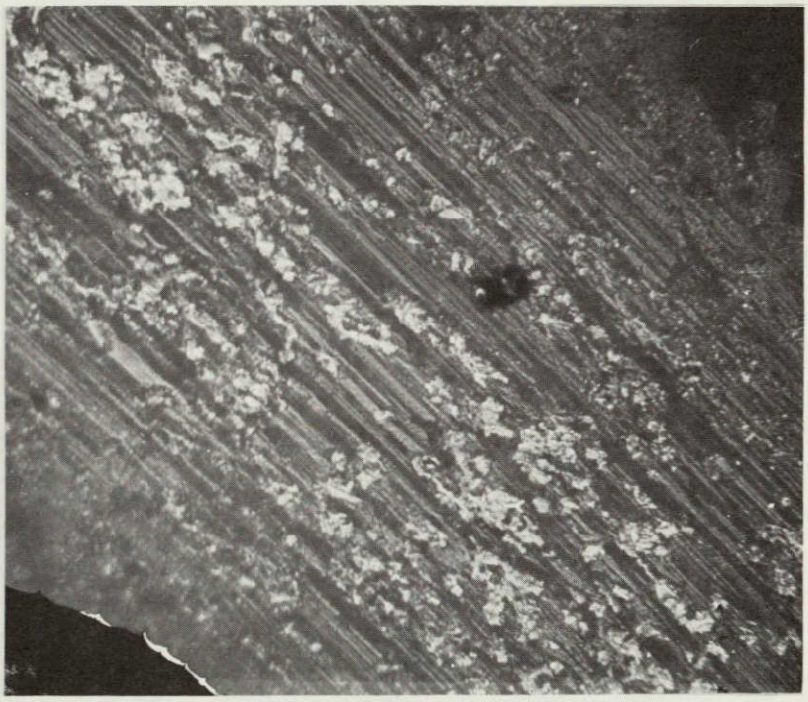

100X

Flat Scar

FIGURE 44. WEAR SCARS FROM FILLED TFE EXPERIMENT 77 K - 600 RPM

curves in Figure 42. This illustrates the family of parallel curves obtained for speeds ranging from 5 rpm (from a long-term test) to 600 rpm, a factor of 100 in speed. Thus, the wear rate, expressed in mils per cycle, appears constant over this speed range, in spite of observed differences in specimen appearances as illustrated in Figures 45 and 46.

Conclusions

The long-term wear experiments indicate that it is possible to perform a valid short-term accelerated wear life test using speed as the accelerating factor. For applications in which increase in clearance is the dominant failure mode, gross wear can be measured. For applications in which leakage is the critical failure mode, one might wish to measure the wear area profilometrically, and plot groove or score depth, or area density. The experiments have suggested that a realistic upper limit on speed for such accelerated tests at 77 K is about 50 cm/sec surface speed for filled and virgin PTFE. Further experiments are required to determine similar limits for Mylar and KEL-F.

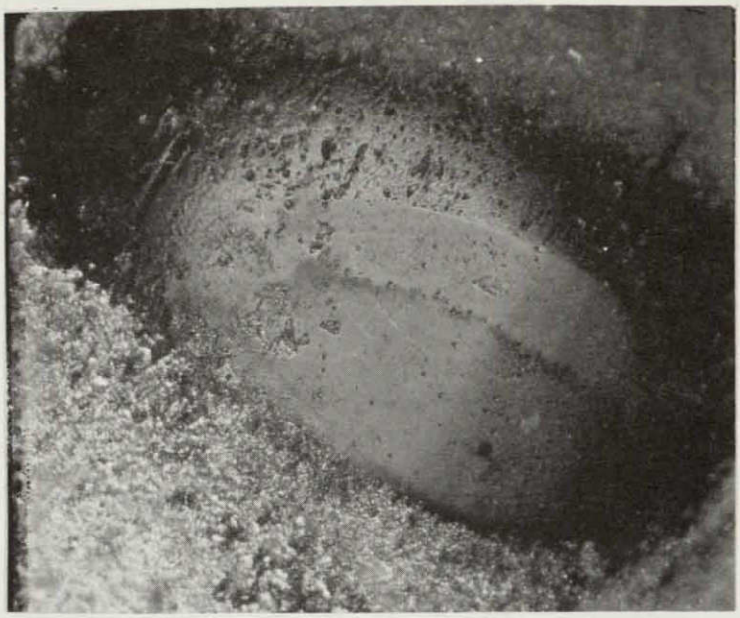

100X

Ball Scar

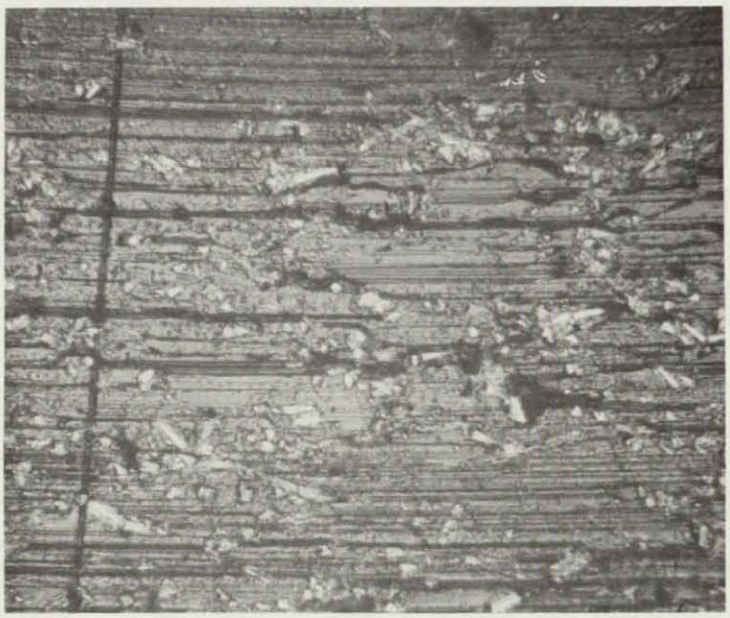

100X

Flat Scar

FIGURE 45. WEAR SCARS FROM FILLED TFE EXPERIMENT WITH PRE-CONDITIONING 77 K - 300 RPM

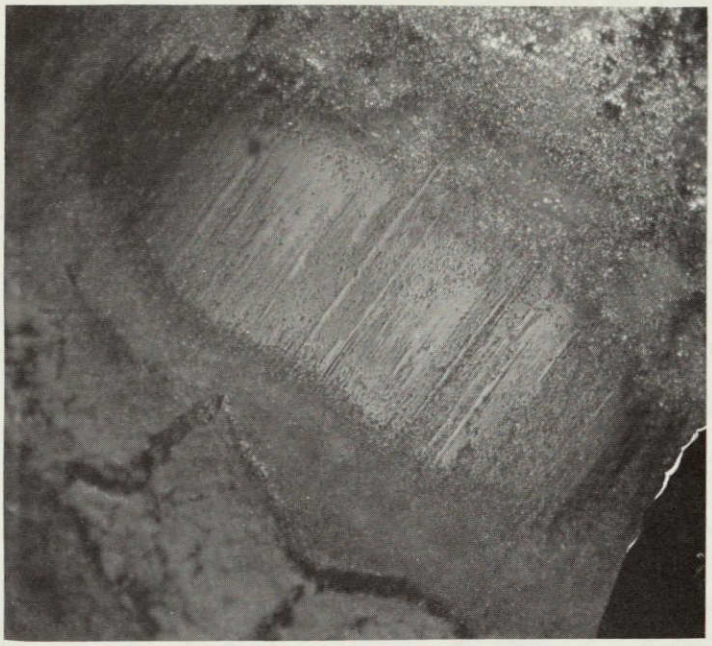

100X

Ball Scar

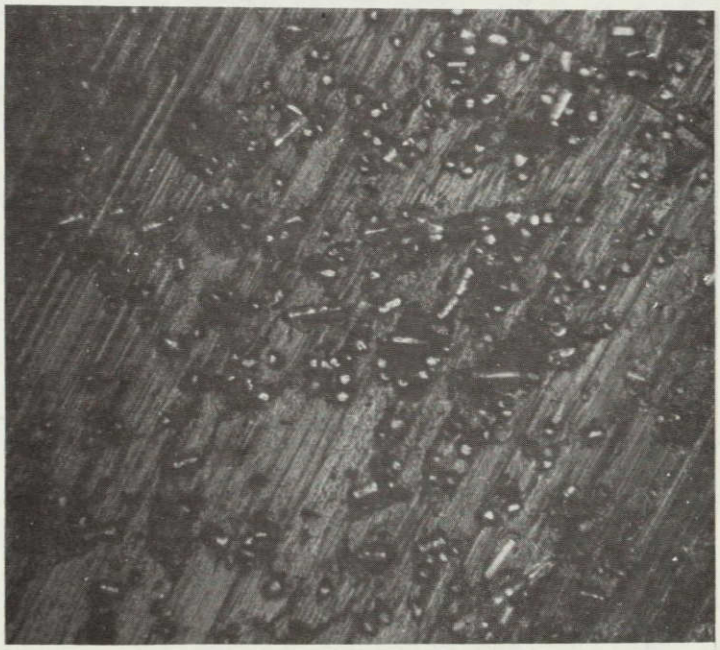

100X

Flat Scar

FIGURE 46. WEAR SCARS FROM FILLED TFE EXPERIMENT WITH PRE-CONDITIONING 77 K - 600 RPM

(18) Armeniades, C. D., and Baer, E., J. Polymer Sci., A-2, 9, 1345 (1971).

(19) Huang, Y. S., and Koenig, J. L., J. Appl. Polymer Sci., 15, 1237 (1971).

(20) Illers, K. H., and Breuer, H., J. Colloid Sci., 18, 1 (1963).

(21) Tajiri, K., Fujii, Y., Aida, M., and Kawai, H., J. Macromolecular Sci. – Physics, B4, 1 (1970).

(22) Kawaguchi, T., J. Polymer Sci., 32, 417 (1958).

(23) Thompson, A. B., and Woods, D. W., Trans. Faraday Society, 52, 1383 (1956).

(24) Hoffman, J. D., Williams, G., and Passaglia, E., J. Polymer Sci., C, 14, 173 (1966).

(25) Crissman, J. M., and Passaglia, E., J. Polymer Sci., C, 14, 237 (1966).

(26) Nagamatsu, K., Yoshitomi, T., and Takameto, T., J. Colloid Sci., 13, 257 (1958).

(27) Urzhumtsev, Yu. S., and Maksimov, R. D., "Time-Stress Superposition in Nonlinear Viscoelasticity", Mekhanika Polimerov, 4, 379-381 (1968).

(28) Brody, H., Plastics & Polymers, 37, 21 (1969).

(29) Bergan, R. L., and Wolsternholme, W. E., SPE Journal, 16, 1235 (1960).

(30) Cessna, L. C., Jr., "Stress-Time Superposition of Creep Data for Polypropylene and Coupled Glass-Reinforced Polypropylene", Polym. Eng. and Sci., 11, 211-219 (1971).

(31) Miner, M. A., J. Applied Mechanics, A12, 159 (1945).

(32) Lee, E. H., and Radok, J. R. M., "The Contact Problem for Viscoelastic Bodies", Trans. ASME, Ser. E, 27, 438-444 (1960).

(33) Ojema, T., Nishimura, M., Ino, M., and Ito, K., Trans. Soc. Rheol., 10, 99-132 (1966).

(34) Lancaster, J. K., "Estimation of the Limiting PV Relationships for Thermoplastic Bearing Materials", Tribology, p 82 (May, 1971).

(35) Jeager, J. C., "Moving Sources of Heat and the Temperature at Sliding Contacts", Proc. Royal Soc. of New South Wales, 76 (203) (1942).

APPENDIX A

CHARACTERIZATION OF DEGRADATION IN NON-METALLIC MATERIALS

APPENDIX

CHARACTERIZATION OF DEGRADATION IN NON-METALLIC MATERIALS

In previous sections, the fact that degradation of nonmetallic materials is frequently the result of several possible deteriorative mechanisms operating simultaneously and synergistically was discussed. Thus, acceleration of one degradative mechanism may substantially modify the effect of another mechanism. In many cases, the synergistic relationships among material deteriorative mechanisms are not sufficiently well understood to permit the development of accurate and quantitative accelerated tests. In these cases, life testing may be performed by exposing the material for a short time to a deleterious environment, then using a very sensitive technique, measure the extent of deterioration. Life-time evaluations could then be predicted by extrapolation of results from the short-term test.

This section discusses the selection of techniques which can be used to observe and quantify material deterioration.

Visual Examination

The visual examination of nonmetallic material surfaces can give very good indications of chemical and physical changes that are occurring within the bulk of the material being exposed. Under certain conditions, it can also give some indication of chemical changes provided a color change is involved. For example, a change in volume due to loss of volatile fragments or recrystallization or phase changes can result in the generation of very small cracks on the surface of the material. These cracks can be observed as a loss of gloss or a loss of shine or brilliance or even a color change such as a development of a whitish haze or film over the surface. It is possible by the establishment of comparison standards to assign numbers to the degree of change based on experience and careful observation.

Light Microscope

Observation of the surface of a material after exposure, using a light microscope with either transmitted or reflected illumination, can extend visual examination results due to its increased sensitivity over the visual technique. Due to the limiting factor of the wavelength of light, the degree of magnification is ultimately limited. Observations using optical microscopy can be used to evaluate cracking, formation of chalky surfaces, growth of mildew, biological attack, change in dimensions, changes in opacity, and even color changes. Here again, a numberical designation for the degree of change entails the use of secondary standards which are established on the basis of experience with the particular material involved.

Electron Microscope

Two types of electron microscopy are available for the study of deteriorating materials. The older and more common transmission electron microscopy detects changes in the opacity of materials to an electron beam. These changes are usually the result of crystal changes or changes in density or other changes that involve the electron absorption. Most electrically insulated materials are somewhat difficult to observe using the transmission electron microscope since the beam of electrons tends to generate an electron charge which then repels the electron beam and results in deterioration of ultimate resolution. The scanning electron microscope tends to overcome the problems of transmission electron microscopy. The operating principle involves use of an electron beam to scan the surface of the object. This scanning produces a reflection which can be manipulated to give a range of magnification from 20 to 50,000 diameters. The ultimate resolution of the scanning electron microscope is 300 angstroms. The depth of focus is exceptionally large, being of the order of several millimeters at lower magnifications. If the surface can be coated with a conductive metal layer and the specimen can stand high vacuum and electron bombardment without deterioration, no replica is necessary.

The scanning electron microscope has been used in several studies involving the deterioration of nonmetallic materials. The scanning electron microscope can be expected to produce micrographs of exceptional clarity and much better definition, high magnification, and greater depth of focus than either the light microscope or the transmission electron microscope. The scanning electron microscope should prove valuable in detecting small amounts of wear on, for example, valve seats.

Phase Microscope

The phase microscope is a specific adaptation of the optical microscope using specialized lighting, usually polarized light, in order to detect phase changes. This instrument has the same limitations as the normal optical microscope as to the degree of magnification. However, it is an extremely valuable tool in detecting changes in crystal structure. Some nonmetallic materials, particularly certain types of polymers, undergo crystal changes under the influence of temperature, ultraviolet radiation, or other deteriorative forces, which results in loss of flexibility, change in volume, etc. The phase microscope can be expected to detect such changes early in the deteriorative process before they result in such obvious failures as cracking or color changes.

Electron Probe Microanalysis

The electron probe scans a sample under observation with a finely focused beam of electrons. The impingement of these electrons causes a reflection of secondary electrons, a generation of X-rays characteristic of the bonbarded element, and photoluminescence. Small areas from a few microns to several hundred microns in diamter can be scanned in several modes to establish distribution of any elements from atomic number 5 (boron) through 92 (uranium). The readout can be by strip

chart, oscilloscope, or Polaroid photographs. Simultaneously, the topography of the sample can be photographed to help relate the probe information to light microscopy examinations. Alternatively, a specific area can be analyzed qualitatively and quantitatively for each element sequentially. Dispersed elements can be detected at levels as low as 100 parts per million, while isolated particles of an element can be identified if as little as 10^{-14} grams is present in a cubic micron.

Being nondestructive, the microprobe is well suited for analyzing materials which may require subsequent analysis by other techniques. For example, solid-state devices can be analyzed for elemental composition and distribution while being operated in either normal or unusual electrical conditions. Essentially any material stable in a moderate vacuum can be analyzed. A vacuum evaporator is used to coat nonconducting samples with carbon or some other conductor. A sample mounting press and metallographic polisher enable odd-shaped or tiny sampes to be examined in any desired area or in cross section. Electron probe analysis has been used to study the changes occurring in plastic materials. Results of these studies are summarized by the conclusion that "the ability of the electron probe to combine rapid elemental analysis with determination of film thickness and identification of coats (paint) offers a useful method for studying applied surface coatings, particularly for faultfinding and conformation or otherwise for adherence to specification".

This procedure can be used to detect changes in the surface chemistry of polymeric surfaces. These changes can then probably be correlated with failure patterns. It can also be used to detect and estimate the degree of wear, or loss, by abrasion on either of two contacting surfaces.

Cathodoluminescence

The impingement of electrons on certain materials causes generation of a characteristic cathodoluminescence. This effect is readily apparent in visually observing the sample during electron probe scanning. The glow is due to the presence of oxygen-containing materials, such as oxides, peroxides, etc. Analysis of the emittted light can yield valuable data on the composition of the source. The introduction of oxygen into a compound or a change in the oxygen content of the irradiated material can be expected to cause a change in the luminescence. This again leads to the establishment of a mathematical relationship between a failure mechanism and a failure mode. The technique is still in the development stage, and consequently its full capabilities and limitations are, for the most part, still unknown. Work is being done constantly with this technique with the expectation that it will become a very valuable tool for following chemical reactions in the near future.

Chemiluminescence

Because the measurement of light intensity is practicable down to extremely low intensities, light emission accompanying a chemical reaction (chemiluminescence)

allows a very sensitive measure of reaction rates for those reactions where light emission is a factor. Such reactions as peroxide decompositions and hydrocarbon oxidations produce weak chemiluminescence. This light emission is due to the formation of electronically excited products in the termination step of free radical chain reactions. Oxidized organic materials, such as paint films, plastics, polymers, rubbers, elastomers, etc., would be expected to contain significant amounts of peroxides. These peroxides on warming decompose to form free radicals. These in turn induce further oxidation by the free radical mechanism. The susceptibility of nonmetallic material to oxidation might be measured, using chemiluminescence emission, by two possible methods; (1) if the technique proves sufficiently sensitive, the course of the oxidation could be followed as the reaction proceeds under ambient or near ambient conditions. For many liquid hydrocarbons and some plastics, this has proved practical; (2) if the above method is not sufficiently sensitive, a measure of peroxide content after a period of exposure to oxidizing conditions might be made by heating the sample until the peroxides become thermally unstable. This should result in a momentary high concentration of free radicals and a correspondingly higher light emission.

The photooxidation of hydrocarbons might produce peroxides through the free radical mechanism or through the formation of singlet electronically excited oxygen. Singlet oxygen can react with unsaturated systems to produce hydroperoxides (if allylic hydrogens are present) or dioxetones (by adding across a double bond, a process enhanced by certain activating groups, such as alkoxy attached to the double-bonded carbon). Both of these products can give rise to chemiluminescence on heating due to their thermal decomposition. Thus photooxidative degradation of paint films might also be studied by the chemiluminescent method. Similarly, surface deterioration of elastomers and plastic materials might also be a candidate for this type of reaction.

Ellipsometry

The ellipsometer is a precision optical instrument for accurately measuring the refractive index of materials. It has been used to advantage in following the progress of a chemical reaction where the products of reaction have different refractive indices from those of the reactants. It should therefore be possible to follow surface changes in polymers, elastomers, and paint films such as occur in chalking, ultraviolet decomposition, or oxidation. Furthermore, it is felt that the early chemical changes in the resin as it undergoes oxidation or degradation can be followed provided the products have refractive indices sufficiently different from those of the original resin to permit these changes to be detected. Since the refractive index is a numerical designation, it adapts itself very well to the establishment of a mathematical relationship which could be extrapolated to a failure mode for a failure degree and consequently an expected service life.

Raman Spectroscopy

When a substance is illuminated by a monochromatic light, a large portion is reflected by an irradiated surface. A small portion of the light is adsorbed and reradiated at the same frequency as the original light. A still smaller fraction is adsorbed and reradiated at a frequency different from that of the original light. Spectroanalysis of the reradiated light shows the frequency differences to be quite definite and to be characteristic of bonds existing within the molecule. It is possible, therefore, to establish resonance relationships with certain linkages such as is done in infrared spectroscopy.

Although Raman spectra have been known since 1928, practical utilization has not been possible due to the very low level of energy in each band and the lack of suitably high energy monochromatic light source. The development of the laser as a high-energy, monochromatic light source has opened up this new field.

Raman spectral analysis is now considered as having good potential for an extension of and supplement to infrared spectral analysis. Work is currently under wat at Battelle's Columbus Laboratories and Case Western Reserve University on using a laser-illuminated Raman spectral analysis. However, this work has not proceeded to the point where the full possibilities and limitations have been established. It can be expected that when the full capabilities of this procedure are known, it will establish it as a primary method for studying changes occurring within polymeric materials exposed to ultraviolet and other irradiation environment.

Electron Spectrometry

Irradiation of a surface with either ultraviolet light or X-rays causes that surface to emit secondary electrons. The energy level of the emitted electrons is specific for each element of the periodic chart except for hydrogen and helium. In addition, there is a shift of energy depending on the environment of the atom analogous to the NMR (nuclear magnetic resonance) chemical shift. However, it is not limited by solubility such as with NMR. It is, therefore, applicable to the study of solid surfaces regardless of their solubility. This technique is so new that its sensitivity and limitations have not been well established. It should, provided the sensitivity is adequate, detect changes in the chemical makeup of the surfaces of nonmetallic materials, and the changes in chemical identity that are precursors of changes in mechanical properties and the loss of volatile materials all of which lead to changes in the four basic properties of a product under use.

It is easy to see that this technique, provided it has suitable sensitivity, is amenable to the establishment of a numerical change that can be extrapolated to future, more widespread, changes leading to the prediction of a usable service life.

Relaxation Time

Several years ago, research studies at Battelle's Columbus Laboratories showed that the electrical losses in a metal paint film system could be correlated with the development of corrosion products as as metal oxides and hydrated oxides at the metal-film interface. Since the time that this work was performed, considerable exploration of the use of elctrical measurements has occurred which permit following the changes in paint films. Some recent studies have shown that the dielectric constant changes observed during the curing process can be a measure of the mobility of polar groups and thus a measure of the degree of crosslinking in a resin. Similarly, changes in dielectric loss have been shown to be due to ionic conductance. This conductance can be, and usually is, due to the presence of such impurities as water or ionizable electrolites.

Changes in dielectric constant have been correlated with viscoelastic properties associated with the degree of crosslinking with an interesting degree of success. The frequency used to measure the electrical properties can reveal further information regarding molecular geometry.

Electrical measurements have been used to follow the curing process of polyester and epoxy resins with good success. However, to our knowledge, no attempt has been made to follow the reverse (degradation or depolymerization) process.

It is interesting to conjecture that electrical methods should furnish a key to the electrical performance of an insulation material. Therefore, it would seem highly desirable to make an exhaustive study of early electrical changes as related to the electrical performance of insulation materials over a long-life history.

Viscoelastic Behavior

Experience with the aging of thin coating films has shown that the film is an elastic body; that is, it experiences a change in volume or shape or both when a deforming force acts upon it and resumes (at least partially) its original dimensions when the force is removed, provided the elastic limit has not been exceeded. Several basic laws of physics apply to such a material as will be discussed later. Our experience also shows that the elasticity of a film usually undergoes marked changes during aging. These changes are usually noted as increases in hardness, loss of flexibility, failure by cracking, checking, and so forth. It has been shown by some workers that stress-strain relationships (Young's modulus) have a relationship to failure mechanisms. Work with the torsional pendulum has also shown some promise for following loss of mechanical properties of a film. However, both studies were made on free films, rather than films attached to a substrate such as the case with paint films. It is felt by many workers that the deteriorating mechanisms in free films differ from those of films attached to substrates. These changes are thought to be due to different degrees of orientation, in the fact that both sides of the film are free to be attacked by the failure force, and by the fact that the physical

structure of free films are felt to be different from those of attached films.

The viscoelastic properties of films as revealed by various moduli can be measured through the influence they exert on a vibrating body. Both low-frequency (sonic) and high-frequency (electrical) vibrations might be used to study paint films applied to certain substrates. Several techniques are being considered for application to this problem. The use of a rheogoniometer to study various moduli has some potential. The geometry of the sample might be metal foil which could be studied under torsional distrubance or as a vibrating reed or as a coil spring. Techniques have not been completely worked out; however, the method does appear to have considerable promise, and we feel it merits more intensive secondary consideration.

Thermal Diffusivity

It has occurred to us that a unique possibility exists for evaluating chemical and physical changes occurring through deterioration in a nonmetallic material by thermal examination. The basic physical phenomenon would be the manner in which heat is transferred from a generating source through the material being studied to a thermal detector. The temperature rise under these conditions would be dependent upon several factors related to degradation. Surface characteristics, roughness, the bonding of a film to a base material, differences in moisture content, differences in density, etc., should be detectable as differences in the rate of heat transfer from the source to the detector. The technique employed here would be to establish a fixed geometry and to follow the changes in thermal diffusivity which could be traceable to changes occurring through exposure to a deteriorative force such as heat, ultraviolet light, etc. Reference standards might be evolved for typical materials thus giving rise to a numerical designation which could be extrapolatable to future behavior. Another technique might be the comparison between an exposed spot and a protected spot on the same material to detect changes.

Infrared Microscope

The infrared emission of a material specimen when heated uniformly may be indicative of material deterioration, especially near the surface. A sensitive infrared microscope, perhaps incorporated into an automatic scanner, might be useful in the technique described above, or could be used to provide information from larger components, such as valves during operation.

Thermogravimetric Analysis (TGA)

This technique consists of a sensitive microbalance incorporated in a vacuum chamber in which controlled temperatures are possible. TGA has proved invaluable in determining weight loss in vacuum for space components.

Techniques of Secondary Interest

Many methods have been used for examining nonmetallic materials and their properties in the past. Many of these methods have been used in probing the reactions occurring in a deteriorating film, in a deteriorating polymer material, and in a deteriorating rubber composition. Their capabilities and limitations have been well established through widespread use. References regarding their use and application can be found in the technical literature. Since these methods are for the most part relatively well known, they will be only very briefly described in this section of the report.

Infrared Spectroscopy

The absorption of infrared energy is a function of the bond structure in an organic compound. It is possible through the careful study of the complete infrared spectrum to determine the bond structure existing in the compound by the adsorption peaks in the infrared spectrum. Thus we have a key to the chemical structure of the compound being observed. Any changes in the chemical structure are reflected in a decrease in the adsorption peaks for certain bond designations and an increase in other peaks representing the formation of a new compound. It is thus possible to follow chemical changes as they occur in a compound or material that is being subjected to a deteriorative force.

Gas Chromotography

Gas chromotography makes use of the rate of adsorption of vapor molecules by certain specific materials to identify these volatile materials. It is particularly useful in identifying the generation of volatile fragments in the decomposition of organic materials, provided the gases can be trapped and analyzed.

Differential Thermal Analysis (DTA)

DTA uses the thermal adsorption during melting, vaporization, and thermal decomposition to characterize a chemical compound. If this DTA is used in conjunction with a mass spectrometer, it is possible to generate pyrolysis products and analyze these pyrolysis products which then gives a point of reference for the thermal behavior of the product being questioned. DTA has been used successfully to determine whether long-range chemical reactions will influence the life of space components.

Meseran

The Meseran is a relatively new instrument that studies changes in surface chemistry and geometry by determining the rate of evaporation of a radioactively

tagged volatile liquid from that surface. Physical changes and often corresponding chemical changes of the surface are reflected in variations in the rate of evaporation of a volatile liquid from that surface. This method can be used, therefore, to detect early changes in the surface geometry of a paint film which can then be identified and quantified by other techniques.

Contact Angle

Although the measurement of a contact angle between a liquid and a solid is an old and often used technique for measuring interfacial tension, new techniques and instrumentations have been developed that result in greatly improved accuracy. A newly developed contact angle goniometer includes environmental chambers, photographic attachments, lighting by reflected or transmitted light, double-rotating cross hairs, goniometric scales, and microscopic viewing. Changes in chemistry of a surface can be expected to result in changes in surface tension or wettability. These changes should be detectable as changes in contact angle. Although changes in surface tension or interfacial tension might be difficult to relate to specific chemical changes, the fact that a change is occurring might be expected to predict the onset of other physical changes such as chalking of surfaces, color changes, loss of gloss, etc.

Nuclear Magnetic Resonance

NMR is a well known and widely used tool for determining the structural chemistry of organic compounds. Its use is very limited since the materials being studied must be soluble in one of a few limited solvents whose NMR spectrum is well known and carefully established. This excludes the use of NMR for a large number of nonmetallic materials that would be of interest to this particular problem, such as elastomers, polymers, etc. However, it is possible to extract or collect fragments from the decomposition of larger molecules on the surface that would be soluble in the NMR solvents which might then be studied to identify their structure. If the structure of the fragments generated by decomposition can be established, this is a valuable aid to the delineation of the deteriorative process being studied. Although NMR is not expected to be a primary tool for the study of the decomposition of nonmetallic materials, it should not be overlooked as a possible instrument of secondary interest.

X-Ray Spectroscopy

Irradiation of nonmetallic materials by X-rays causes the generation of secondary X-rays whose wavelength is a function of reactions that are occurring on the surface. For example, if the irradiation of a surface by X-rays causes a valence changes in any atoms in that surface, a corresponding change in the spectrum of the secondary X-rays can be noted. Here again is a secondary tool that is expected to be valuable in exploring what is going on during a deterioration

process rather than the primary purpose of assigning numbers to the amount of deterioration caused by a fixed amount of deteriorative force.

Similarly, X-rays may be used to show changes in crystal structure through a change in the diffraction pattern. This can also be helpful in reaching an understanding of the process involved in a deterioration process.

Extended Time Experiments

It is apparent that for some components and materials, the deteriorative mechanisms are sufficiently numerous and complex that meaningful accelerated life tests cannot be performed. Instead, it may be necessary to perform short-term tests by extrapolation. As an example, life testing for wear at a bearing-shaft interface cannot, in general, be accelerated, since the relationship between wear and time is unknown. In this case the wear, after a short period, must be determined then predicted for the intended lifetime. This may result in a lifetime prediction much lower than the actual life, but the inaccuracy cannot be avoided until considerable experience is gained with the technique.

TABLE B-1. COMPRESSIVE CREEP COMPLIANCE MEASUREMENTS

INITIAL STRESS = -600.02 TEMPERATURE = 125 F

TIME (HOURS)	STRESS (PSI)	STRAIN	COMPLIANCE (1/PSI)
0.0	-600.02	-0.00755	1.258E-05
0.1	-594.56	-0.00915	1.539E-05
0.3	-594.11	-0.00990	1.666E-05
0.5	-593.93	-0.01020	1.718E-05
0.8	-593.65	-0.01068	1.798E-05
1.2	-593.36	-0.01117	1.883E-05
3.2	-592.67	-0.01233	2.080E-05
4.7	-592.46	-0.01269	2.142E-05
21.7	-591.59	-0.01415	2.392E-05
29.7	-591.29	-0.01467	2.481E-05
45.6	-591.01	-0.01513	2.561E-05
54.2	-590.86	-0.01540	2.606E-05
100.3	-590.48	-0.01603	2.714E-05
117.6	-590.38	-0.01621	2.746E-05
141.9	-590.35	-0.01625	2.753E-05
166.7	-590.30	-0.01633	2.767E-05
191.6	-590.26	-0.01641	2.781E-05
213.7	-590.23	-0.01645	2.788E-05
286.9	-590.02	-0.01682	2.851E-05
315.4	-589.99	-0.01687	2.860E-05
341.7	-589.77	-0.01724	2.923E-05
364.5	-589.77	-0.01724	2.923E-05
385.1	-589.77	-0.01724	2.923E-05
459.3	-589.77	-0.01724	2.923E-05
555.9	-589.64	-0.01745	2.960E-05
647.6	-589.51	-0.01769	3.000E-05
724.3	-589.45	-0.01779	3.018E-05
796.1	-589.37	-0.01792	3.040E-05
959.9	-589.33	-0.01799	3.053E-05

TABLE B-2. COMPRESSIVE CREEP COMPLIANCE MEASUREMENTS

INITIAL STRESS = -599.95 TEMPERATURE = 100 F

TIME (HOURS)	STRESS (PSI)	STRAIN	COMPLIANCE (1/PSI)
0.0	-599.95	-0.00539	8.992E-06
0.1	-596.14	-0.00637	1.069E-05
0.3	-595.64	-0.00722	1.211E-05
0.6	-595.30	-0.00779	1.309E-05
1.3	-595.13	-0.00806	1.355E-05
2.7	-594.86	-0.00853	1.433E-05
48.8	-593.85	-0.01022	1.721E-05
66.3	-593.41	-0.01096	1.847E-05
90.3	-593.13	-0.01144	1.928E-05
114.4	-593.00	-0.01165	1.964E-05
140.4	-592.98	-0.01169	1.971E-05
162.5	-592.76	-0.01206	2.035E-05
235.4	-592.64	-0.01225	2.068E-05
264.1	-592.43	-0.01261	2.128E-05
290.3	-592.39	-0.01268	2.140E-05
313.1	-592.28	-0.01286	2.172E-05
333.6	-592.27	-0.01288	2.175E-05
407.7	-592.27	-0.01288	2.175E-05
504.3	-592.16	-0.01306	2.206E-05
594.3	-591.85	-0.01359	2.297E-05
739.7	-591.81	-0.01366	2.309E-05
817.7	-591.77	-0.01372	2.319E-05
908.6	-591.77	-0.01372	2.319E-05

TABLE B-3. COMPRESSIVE CREEP COMPLIANCE MEASUREMENTS

INITIAL STRESS = -599.95 TEMPERATURE = 85 F

TIME (HOURS)	STRESS (PSI)	STRAIN	COMPLIANCE (1/PSI)
0.0	-599.95	-0.00506	8.439E-06
0.1	-596.75	-0.00535	8.972E-06
0.6	-596.45	-0.00586	9.820E-06
2.1	-596.17	-0.00633	1.062E-05
18.1	-595.26	-0.00785	1.319E-05
25.9	-595.08	-0.00815	1.370E-05
44.1	-594.86	-0.00853	1.433E-05
66.2	-594.73	-0.00875	1.471E-05
139.2	-594.34	-0.00940	1.582E-05
168.0	-594.08	-0.00984	1.656E-05
194.0	-593.98	-0.01000	1.684E-05
216.7	-593.98	-0.01000	1.684E-05
237.3	-593.94	-0.01007	1.696E-05
311.6	-593.83	-0.01026	1.728E-05
408.0	-593.59	-0.01067	1.797E-05
498.0	-593.47	-0.01087	1.831E-05
553.8	-593.47	-0.01087	1.831E-05
643.5	-593.42	-0.01094	1.843E-05
721.4	-593.39	-0.01100	1.854E-05
815.4	-593.20	-0.01132	1.909E-05

TABLE B-4. COMPRESSIVE CREEP COMPLIANCE MEASUREMENTS

INITIAL STRESS = -599.95 TEMPERATURE = 73 F

TIME (HOURS)	STRESS (PSI)	STRAIN	COMPLIANCE (i/PSI)
0.0	-599.95	-0.00590	9.830E-06
0.1	-596.11	-0.00643	1.079E-05
0.3	-595.91	-0.00676	1.135E-05
1.0	-595.69	-0.00714	1.198E-05
47.5	-594.50	-0.00913	1.536E-05
66.2	-594.44	-0.00923	1.553E-05
95.1	-594.10	-0.00981	1.651E-05
121.1	-593.88	-0.01017	1.713E-05
143.7	-593.84	-0.01024	1.725E-05
164.3	-593.82	-0.01027	1.730E-05
234.5	-593.80	-0.01030	1.735E-05
335.0	-593.60	-0.01065	1.794E-05
425.0	-593.35	-0.01107	1.866E-05
479.6	-593.29	-0.01117	1.883E-05
572.4	-593.17	-0.01137	1.918E-05
643.7	-593.11	-0.01148	1.935E-05
743.8	-593.11	-0.01148	1.935E-05

TABLE B-5. COMPRESSIVE CREEP COMPLIANCE MEASUREMENTS

INITIAL STRESS = -1200.05 TEMPERATURE = 73 F

TIME (HOURS)	STRESS (PSI)	STRAIN	COMPLIANCE (1/PSI)
0.0	-1200.05	-0.01623	1.353E-05
0.1	-1177.13	-0.01928	1.638E-05
0.2	-1176.29	-0.02000	1.700E-05
0.4	-1174.94	-0.02114	1.799E-05
0.7	-1173.77	-0.02214	1.887E-05
1.2	-1172.90	-0.02288	1.951E-05
3.0	-1170.98	-0.02452	2.094E-05
4.3	-1169.83	-0.02550	2.180E-05
5.9	-1168.92	-0.02628	2.248E-05
21.6	-1165.82	-0.02893	2.482E-05
51.5	-1163.81	-0.03067	2.635E-05
95.1	-1162.13	-0.03211	2.763E-05
101.6	-1161.89	-0.03232	2.781E-05
124.0	-1161.53	-0.03263	2.809E-05
149.5	-1160.81	-0.03325	2.864E-05
171.4	-1160.57	-0.03345	2.883E-05
193.4	-1160.21	-0.03376	2.910E-05
263.2	-1159.61	-0.03428	2.956E-05

TABLE B-6. COMPRESSIVE CREEP COMPLIANCE MEASUREMENTS

INITIAL STRESS = -300.10 TEMPERATURE = 73 F

TIME (HOURS)	STRESS (PSI)	STRAIN	COMPLIANCE (1/PSI)
0.0	-300.10	-0.00231	7.690E-06
0.1	-299.32	-0.00261	8.715E-06
0.9	-299.30	-0.00267	8.933E-06
17.8	-299.21	-0.00297	9.941E-06
72.4	-299.19	-0.00304	1.017E-05
175.3	-299.08	-0.00341	1.140E-05
236.4	-299.02	-0.00361	1.208E-05
337.3	-299.02	-0.00361	1.208E-05

APPENDIX C

MICROHARDNESS TEST DATA

TABLE C-1. MICROHARDNESS TEST DATA--
STANDARD INDENTOR[a]

Time, min	Indentation (inches x 10^{-3})		
	115 g	215 g	315 g
1	1.3	2.28	2.90
2	-	-	3.06
3	1.37	2.37	-
5	1.43	2.46	3.14
10	-	2.53	-
15	1.57	-	3.29
20	-	2.61	-
30	1.75	-	-
32	-	-	3.38
90	2.06	-	-
92	-	-	3.56
97	-	2.74	-
182	-	-	3.78
186	2.17	-	-
197	-	2.82	-
210	-	-	3.82
273	-	-	3.85
317	-	2.87	-

(a) Ball of 1/64-inch diameter.

TABLE C-2. MICROHARDNESS TEST DATA--
MODIFIED INDENTOR(a)

Time, min	Indentation (inches x 10^{-3})			
	3.5 g	115 g	200 g	315 g
15	0.43	1.08	1.43	2.00
30	0.45	1.12	1.46	2.05
60	0.48	1.16	1.49	2.11
90	0.50	1.18	1.51	2.14
120	0.51	1.20	1.53	2.17
150	0.52	1.21	1.54	2.19
180	0.54	1.23	1.55	2.20
210	0.54	1.24	1.56	2.22
240	0.55	1.25	1.58	2.24
270	0.55	1.26	1.59	2.25
300	0.56	1.26	1.60	2.25
330	0.57	1.27	-	-
360	0.58	1.29	-	-

(a) Indentor consists of 1/64-inch rod with ≈ 0.1 inch radius crown.

APPENDIX D

EXAMPLE OF THE CALCULATION OF PERMANENT SET

APPENDIX D

EXAMPLE OF THE CALCULATION OF PERMANENT SET

To demonstrate the usefulness of Equation (9) and (9a) (see text), consider the following simple example: A purely viscoelastic material is placed under stress. The stress varies sinusoidally with time and has an amplitude $\Delta\sigma$. The viscosity is proportional to $1/\sigma$. The stress and viscosity are given by:

$$\sigma(t) = \sigma_0 + \Delta\sigma \operatorname{Sin} \omega t \qquad \sigma = \text{the initially applied stress}$$

$$\eta(t) = R/\sigma(t)$$

The permanent set at any time t can be evaluated via Equation (9)

$$P.S. = \int_0^t \frac{\sigma(S)}{\eta(\sigma(S))} dS = \frac{1}{R} \int_0^t \left[\sigma_0 + \Delta\sigma \operatorname{Sin} \omega S\right]^2 dS$$

or

$$P.S. = (\sigma^2 + \Delta\alpha^2/2)t + 2\sigma\Delta\sigma(1 - \operatorname{Cos} \omega t)/\omega - \Delta\alpha^2(\operatorname{Sin} 2\omega t)/4.$$

The permanent set at any time can be calculated using this relationship. Alternatively, given the maximum allowable permanent set, the useful life of a component can also be determined.

The simple example above led to a complex permanent set function. An analytic treatment as shown above is probably not possible for very complex stress and/or temperature histories, and the permanent set must be evaluated numerically.

APPENDIX E

CRYOGENIC WEAR-TEST APPARATUS

APPENDIX

CRYOGENIC WEAR-TEST APPARATUS

Drive System

The wear test apparatus, illustrated in Figures E-1 and E-2, was designed around an air table support for the stationary nonmetallic specimens which permits accurate frictional force measurements. The rotating member is driven by a drill press whose feed mechanism offers a convenient means for applying the vertical load to the specimen. Successful operation as a wear-test fixture spindle required several modifications to the drill press. Reliable vertical loading was achieved by removal of the built-in pinion shaft and by milling a keyway parallel to the shaft axis in the vertically movable spindle housing. This eliminated any tendency for vertical motion sticking and prevented rotation of the housing. The weight of the shaft and its vertically adjustable housing were counterbalanced by a concentric coil spring installed about the drive pulley. Spring force was adjusted for zero load (within ± approximately 50 g) when the specimens were just touching. Subsequently, desired specimen loading was achieved by the addition of weights to a clamped-on bar as illustrated in Figure E-3. Thus, the specimen load is not dependent upon the mechanical advantage of the arm/rack and pinion assembly. The standard drill press drive motor is not used because of its high inherent vibration level. A smooth-running 1/8-hp gear motor, mounted on an adjacent concrete wall to isolate vibration is employed as a variable-speed drive system. Connection to the drill press drive pulley is by means of a rubber O-ring. The speed is varied with a matching electronic motor-speed controller.

Air Table

The air table employed to support the nonrotating specimen (3 balls) consists of two 6-inch (15.24 cm) diameter by 1-inch (2.54 cm) thick hardened and ground steel disks. The lower disk contains a central 1-inch diameter protruding pin, and the upper disk a mating, honed hole – the clearance being ~0.0003 inch (0.0076 mm). The supporting air, at ~2 to 4 psi* flows upward through center of the pin thence downward through two grooves on opposite sides of the pin to the annular space formed by a champfer at the hole edge. This permits uniform distribution of air flow between the disks' surfaces. A separation of 2 to 4 mils (0.051 to 0.102 mm) was found to give best control of the gap width plus minimum rotational restraint. A filter and two pressure regulators were connected in series to effect close pressure control from the 85 psi ± 10 (.59 ± .07 MN/m^2) laboratory air supply system.

* 0.014 to .028 MN/m^2.

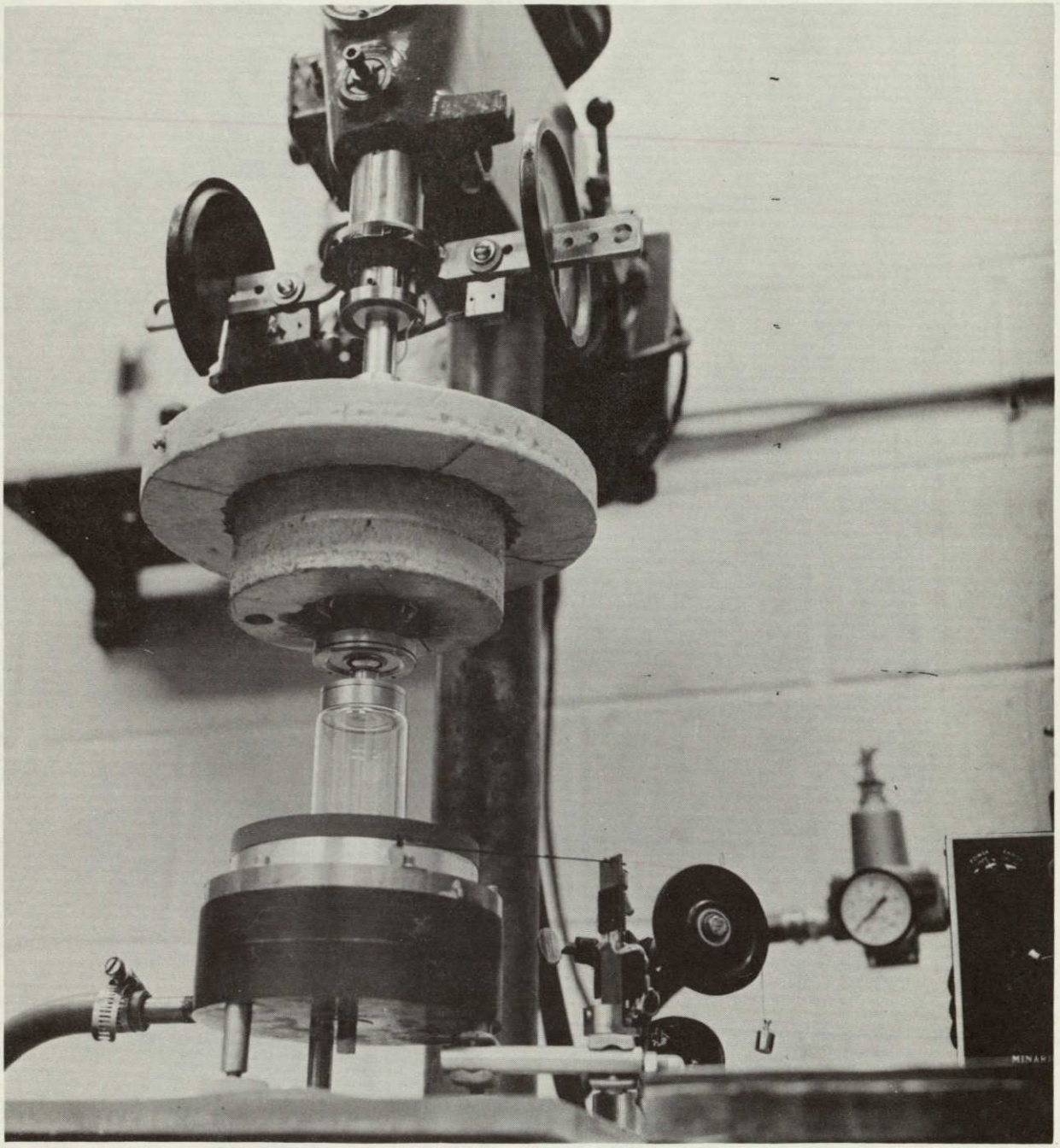

FIGURE E-1. OVERALL VIEW OF WEAR-TEST APPARATUS SHOWING (TOP-TO-BOTTOM) THE DRILL PRESS, LOADING SYSTEM, CRYOSTAT COVER, UPPER PLATE (SPECIMEN), LOWER PLATE (RIDERS), AIR BEARING, AND THE TORQUE-MEASUREMENT SYSTEM

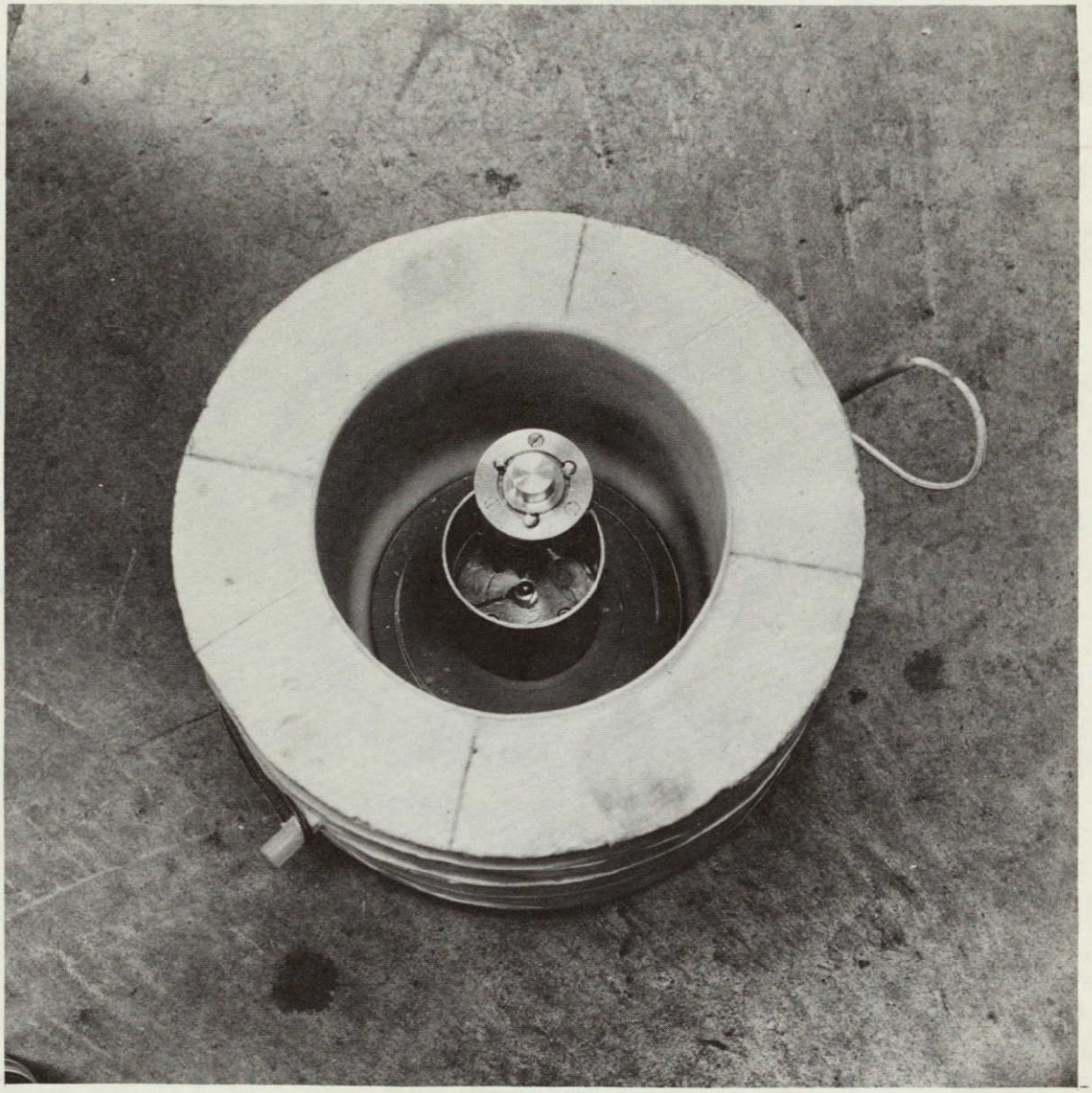

FIGURE E-2. VIEW LOOKING INSIDE CRYOSTAT SHOWING THE THREE-BALL RIDER CONFIGURATION. THE RIDER HOLDER NORMALLY RESTS ON THE BALL PIVOT SHOWN ON THE BOTTOM OF THE BRASS CHAMBER

Specimen Holders

The upper specimen is a washer-shaped sample of the plastic material under test. It is held by overlapping metal flanges on both ID and OD edges, and backed by a flat metal support which is attached rigidly to the drill press shaft for rotation and vertical loading.

The lower specimen consists of three nonrotating 1/4-inch (6.35 mm) hardened steel balls – bearing grade – rigidly clamped to the upper surface of a disk-shaped holder. The latter is supported and located by a single centrally located ball placed between opposed cone sockets. This arrangement is shown in the sketch shown in Figure E-3. It was anticipated that perfect rotational alignment through all phases of experimental use was an unrealistic objective; consequently, the self-aligning lower specimen-holder design was adopted. Rotation of the holder is prevented by a 1/8-inch (3.18 mm) diameter dowel pin, installed in the underside of the holder. The pin protrudes downward into an enlarged hole in the base of the brass cylinder which supports and surrounds the test specimen region. The liquid nitrogen coolant is contained outside the walls of this cylinder so that the experiment is carried out in an air environment at liquid-nitrogen temperatures – ~77 K.

Cryostat

The cryostat is built up from 1-inch (3.54 cm) thick washer-shaped disks of polystyrene foam. These are slipped tightly over a thin-walled polyethylene bottle which is subsequently cut off to form the open-top vessel shown. A tight-fitting lid, also cut from three polystyrene foam layers, is shaped to cover the vessel and protrude inside in order to seal the upper rim of the inner brass vessel. The bottom of the polyethylene bottle was removed and attached to a two-layer steel plate. This provides means for accurate alignment and firm support of the lower specimen holder on the air table. A 3/4-inch (19 mm) layer of red-fiber plastic is inserted between the air table and the bottom plate of the cryostat in order to reduce heat transfer from the table upward.

During initial use it was found that several layers of 4-mil-thick (0.102 mm) polyethylene sheeting also inserted between the air table and the cryostat base plate further reduced heat transfer and prevented ice-up of the air table. Liquid nitrogen was poured into the closed cryostat through a polyethylene, funnel-type orific inserted in the lid; an overflow tube inserted straight through the wall served to indicate the "full" condition. Sealing the 1-inch-diameter (tube) rotating shaft at the cryostat lid perforation presented a problem since friction at this point would not be separable from specimen friction which was to be measured. Effective sealing in combination with friction torques less than 1 gram was achieved by use of a stack of several washers cut from 4-mil polyethylene sheet and installed around the shaft. An additional aluminum collar, clamped to the shaft just above the washer stack contributed to the effectiveness of the seal by rpoviding support for the loose ice crystals which inevitably formed during low-temperature tests. This seal was

effective in eliminating condensation and frost on the wear specimens, even after several hours of cryogenic operation. A thermocouple was installed to touch the lower specimen holder; its lead wires were very small and were hung loosely outside the cryostat in order to minimize their influence on torque measurements.

INSTRUMENTATION

Friction Torque

Two types of instrumentation were installed on the experimental apparatus; a friction-force (torque) transducer and a capacitance probe for the measurement of wear.

Torque measurements were carried out by application of a force transducer for sensing the reaction force transmitted to the upper (floating) disk of the air table. This force results from the friction produced at the ball-plastic rubbing contact. The transducer consists of a 3 x 1 x 1/16-inch (76 x 25 x 1.6 mm) thick flat beam containing a 4-arm strain gage bridge. The gages are mounted in pairs on opposite sides and are oriented and connected for maximum sensitivity and temperature conpensation. The beam is supported from one end of the base of the air table and the other end is connected by means of a thread to the edge of the floating plate which holds the cryostat and lower specimen holder. The force transducer is operated by means of a Brush d.c. bridge amplifier, Model 13-4312, and its output is monitored by a Brush 220 recorder. Calibration of the transducer is effected by hanging balance weights on a thread draped over a low-friction pulley and connected to the strain beam in the same manner used for measuring the reaction torques.

Capacitance – Wear Measurement

The capacitance transducer consists of two 3/8-inch (15.9 mm) diameter brass plates which move toward each other as wear progresses at the plastic specimen surface. Both plates are concentric with the axis of the system. The lower flat plate is an integral part of the ball-specimen holder – it is stationary, and parallel to the plane formed by the highest point at each of the three balls. The upper plate, has a 174-degree concial tip, is attached to the upper specimen holder, and is expected to descend, i.e., move toward the lower plate, as wear in the plastic specimen proceeds. A rigid attachment to the upper capacitor plate is made above the drill press drive pulley by means of a long rod running through a concentric hole in the center of the spindle. In order to eliminate the capacitive pickup resulting from long leads, the adjusting rod has an insulating section just above the upper plate. At this point, a slip-ring is used to carry the signal to the capacitance bridge. The

upper end of the rod is held by a concentric coil spring acting against the spindle of a micrometer which rigidly is attached to the drillshaft quill (reference Figure E-2). Thus adjustments of the micrometer affect corresponding changes in the level of the upper capacitor plate. Since the air table is installed on leveling screws which are set into a thick plastic insulating plate, the lower capacitor plate is electrically isolated from the drill-press table which is connected electrically to the upper plate. Shielded leads are used to connect the lower plate and upper plates to a Boonton Model 75C capacitance bridge. This instrument permits balancing out the capacitive and resistive effects of the leads before measurement of the experimentally determined values for capacitance (wear).

Two methods were used for monitoring wear through use of the capacitance transducer. In the first, the transducer was employed as a sensitive contact probe: with rotation stopped the micrometer was used to advance the upper capacitor plate until it contacted the lower plate, then the upper plate was retracted exactly 5 mils and the wear tests was allowed to proceed for 30 to 60 minutes. Rotation was then stopped at the same angular position and the micrometer was advanced to get plate contact. The amount of advance needed would logically be less than 5 mils since the intervening wear should have narrowed the 5-mil gap. Since the actual wear produced for the chosen operating conditions was often less than 0.1 mil (0.003 mm), the method was not sufficiently sensitive to produce reliable results.

The second method for wear measurement was designed to make use of the great sensitivity inherent in the capacitance-bridge technique. Before beginning the wear evaluation, the specimens were brought together under light contact, then the micrometer was advanced to locate the capacitor-plate "touch" setting. The upper plate was then raised 2 mils (0.051 mm) and the bridge was rebalanced (nulled). During the wear evaluation, the rotation was periodically stopped and the bridge was nulled again. The successive bridge-balance readings are related to gap size, and hence wear, by means of a calibration curve. The accuracy of the results depends on the accuracy of the gap-versus-capacitance calibration curve, and on the ability to detect and correct for electrical and mechanical drift. Since the data needed to plot a calibration curve are produced fairly rapidly, it was feasible to obtain such data prior to each wear experiment and, in one case, again immediately following the experiment. Drift in the capacitance bridge and in the shielded (RG-57) leads connected to the apparatus was detected and compensated for by use of a standard 15 pf standard capacitor placed in parallel with the wear monitor capacitor. With the lower plate lead disconnected at the cryostat, the bridge was set at 15.00 pf and the compensation controls adjusted for bridge balance. Next, the lead was reconnected and the bridge rebalanced. This procedure was followed before every gap-reading if more than 2-3 minutes had elapsed since the previous reading.

PERFORMANCE

Performance of the fixutre was evaluated in terms of accuracy of specimen alignment, sensitivity and accuracy of the friction and wear measuring techniques, and ease of operation of the total apparatus.

Following the initial operation evaluation and modifications, the specimen-holder axes were aligned to within ~1.5 mils (0.038 mm) and the upper specimen runout was determined to be ~5 mils (0.127 mm). The latter figure reflects the diametral clearance of the shaft bearings magnified by the long shaft extension. The influence of runout and the inherent friction in the vertical (loading) shaft motion have already been described. The rotational drive system operated very smoothly, without transmitting vibrations to the specimens, and required no modifications. Likewise, the air table performed satisfactorily for extended operating periods once good alignment had been achieved. Also good performance was obtained from the torque transducer-amplifier-recorder system. The sensitivity of the force transducer was ~0.4 g which represents the reading accuracy on the recorder chart. Background noise is ~0.6 g at the sensitivities used. The force required to rotate the air bearing was considerably less than this, probably <0.02 g. Variations in torque reaction force which occurred during specimen rotation were typically 1 to 2 grams.

Because no prior experience was available, the performance of the capacitance-measuring technique received more intensive evaluation than did other features of the rig. To gain experience, capacitance-versus-gap data were obtained for a variety of conditions and procedures. During this phase, 12 calibration plots were made and each of these led to either an improved procedure or an apparatus modification. For example, Figure E-4 illustrates calibration data for (1) both capacitor plates flat, and (2) one plate with ~174-degree cone tip. Note the greater sensitivity for the (2) design. These curves also illustrate the nature of the capacitive phenomenon – the gap changes exponentially for monotonic capacitance changes. Expressed mathematically, the formula for the curve for the conical plate design is:

$$\ln G = 9.92 - 0.396\, C \quad ,$$

where G = gap in mils and C = capacitance in picofarads. The data also indicates that for gaps between 1 and 10 mils (0.025 and 0.25 mm), a straightline plot is obtained. Additional data (not shown here), indicate that nonlinearities are introduced when the gap is greater than ~13 mils (0.33 mm) or less than ~1 mil (0.025 mm).

As a result of experience gained during wear experiments it was determined that an optimum gap was 1-2 mils (25-50 μm) since this provided for maximum sensitivity with consistent and linear response. Minor changes were noted for calibrations carried out at ~77 K as compared with those performed at room temperature. Some drift at very small gaps was noted at 77 K and was attributed to thermal effects. Based on the calibration studies a given capacitance reading may be interpreted with a tolerance of ~ ± 10 μm. This will result in wear values of ± 10 % accuracy for wear in the 0.2 mm (0.008-inch) range. Only Teflon®-type specimens displayed wear of this magnitude during the abbreviated experiments used during this program.

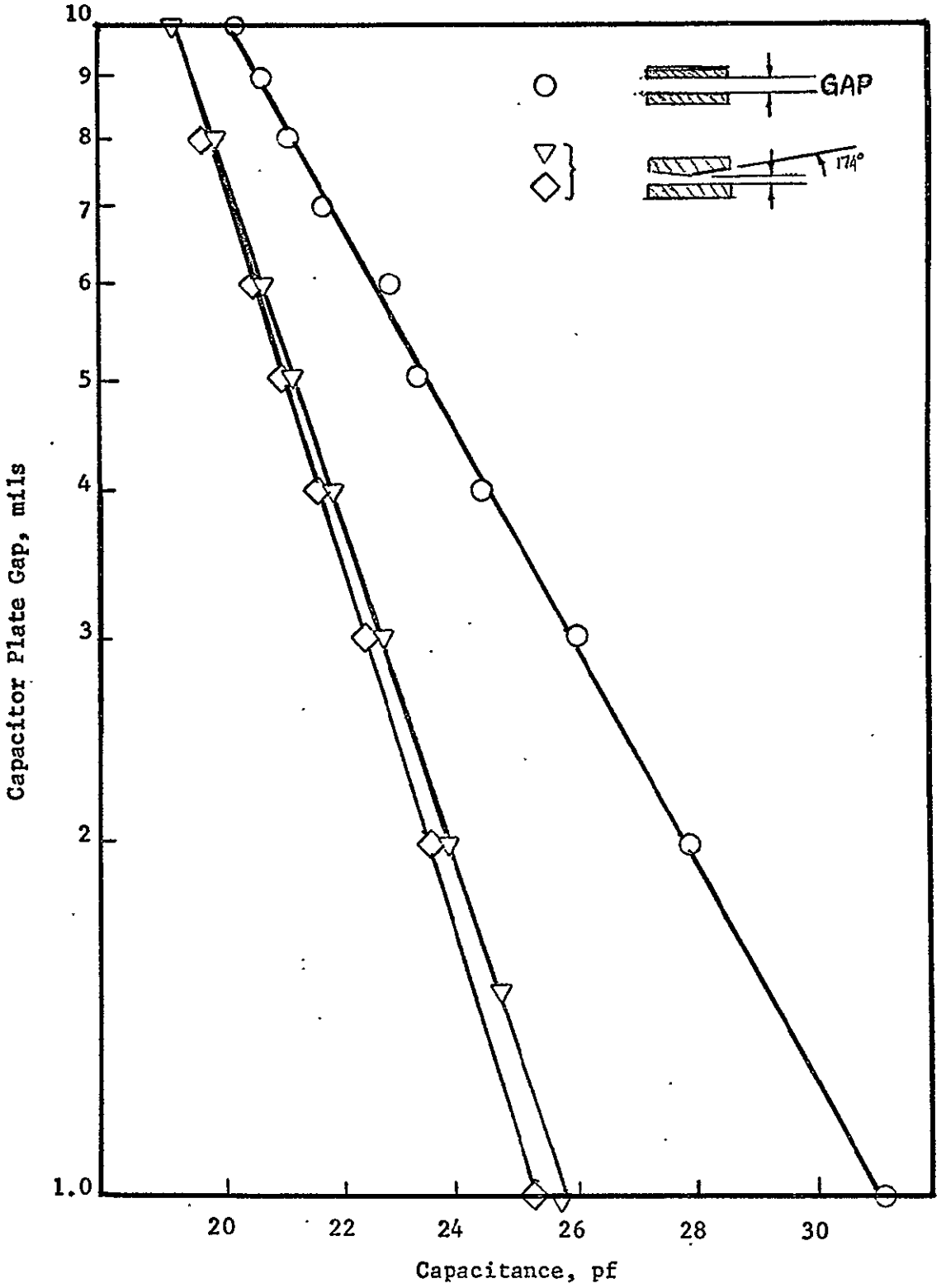

FIGURE E-4. CALIBRATION CURVES FOR WEAR-RATE MEASUREMENTS